Aus der

Abteilung für Klinische Pharmakologie

Klinikum der Ludwig-Maximilians-Universität München

Effect of Prior Flavivirus Immunity on the Adaptive Response to the Yellow Fever 17D Vaccine

Dissertation
zum Erwerb des Doctor of Philosophy (Ph.D.)
an der Medizinischen Fakultät der
Ludwig-Maximilians-Universität München

vorgelegt von
Antonio Santos del Peral

aus
Leganes, Madrid, Spanien

Jahr
2024

Mit Genehmigung der Medizinischen Fakultät der
Ludwig-Maximilians-Universität München

Erstes Gutachten:	Prof. Dr. Simon Rothenfußer
Zweites Gutachten:	Prof. Dr. Anne Krug
Drittes Gutachten:	Prof. Dr. Oliver T. Keppler
Viertes Gutachten:	Priv. Doz. Dr. Günter Fröschl

Dekan:	Prof. Dr. med. Thomas Gudermann

Tag der mündlichen Prüfung: 15.04.2024

Table of content

Disclaimers

1) The neutralizing antibody titer of the study participants (shown in Figure 3A) was determined by Lisa Lehmann as an integral component of her doctoral thesis. Including these data here is endorsed by Lisa Lehmann's authorization due to the significance of this dataset for formulating the hypothesis and defining the initial goals of the project that this dissertation aims to cover.

2) Fabian Luppa measured the anti-TBEV neutralizing antibody titer and cross-reactivity assays that are not shown as part of this dissertation but helped categorize the study cohort into TBEV-vaccinated and TBEV-unvaccinated groups.

3) This dissertation includes results used for publications:

a. Santos-Peral, A., Luppa, F., Goresch, S. et al. Prior flavivirus immunity skews the yellow fever vaccine response to cross-reactive antibodies with potential to enhance dengue virus infection. Nat Commun 15, 1696 (2024). https://doi.org/10.1038/s41467-024-45806-x. A first version of the manuscript has been uploaded as a preprint copy to Biorxiv, DOI: https://doi.org/10.1101/2023.05.07.539594. There is shared content between the manuscript and this dissertation in Figures 2, 3, 4, 5, 6, 7, and 8. Both documents contain data encompassing the cohort description and serology data (including IgG titer, designed antigen constructs, and epitope specificity analysis of the antibody response as well as IgM and antigen-specific IgG depletion followed by neutralization and quantification of dengue virus antibody-dependent enhancement). In the online article, it is credited that Antonio Santos-Peral wrote the manuscript and that the article is part of this dissertation.

b. Santos-Peral et al. Basal T-cell Activation Predicts Yellow Fever Vaccine Response Independently of Cytomegalovirus Infection and Sex-related Immune Variations. (submitted).

Note:

We use the consensus virus names instead of the notation updated by the ICTV in the 2022 release. Eg. Yellow fever virus instead of *Orthoflavivirus flavi*; Dengue virus for *Orthoflavivirus denguei*; Tick-borne encephalitis virus for *Orthoflavivirus encephalitidis* and Japanese encephalitis virus for *Orthoflavivirus japonicum*

Abstract*

The yellow fever 17D vaccine (YF17D) is the most effective of all flavivirus vaccines. Given the widespread prevalence of flaviviruses, YF17D is frequently administered to individuals with pre-existing cross-reactive immunity, potentially influencing immune responses. Here, I investigated the impact of pre-existing flavivirus immunity induced by the tick-borne encephalitis virus vaccine (TBEV) on the response to YF17D vaccination in 250 individuals up to 28 days post-vaccination (pv).

Previous TBEV vaccination did not influence the early neutralizing response to YF17D, predominantly driven by the IgM antibody fraction. TBEV pre-vaccinated individuals, however, developed high amounts of cross-reactive IgG antibodies with limited capacity to neutralize YF17D. In contrast, TBEV-unvaccinated individuals elicited a non-cross-reacting but efficiently neutralizing response. Utilizing recombinant YF17D envelope protein mutants displaying different epitopes, I identified quaternary dimeric epitopes as the main target of neutralizing antibodies and the fusion loop epitope (FLE) as the focus of cross-reactive antibodies. TBEV pre-vaccinated individuals expanded anti-FLE IgG antibodies that can cause antibody-mediated enhancement (ADE) of dengue virus infection in vitro.

Flow cytometric analysis consistently showed a greater expansion of antigen-specific memory B cells in TBEV-pre-vaccinated individuals following YF17D vaccination. Furthermore, TBEV pre-vaccinated individuals displayed a diverse antibody response, covering a wide range of specificities beyond cross-reactive epitopes shared by TBEV and YF17D. TBEV-induced antibodies enhanced YF17D vaccine immunogenicity, resulting in higher antibody titers and a more robust antigen-specific CD4 T cell response, measured in an ex vivo restimulation assay on day 28. In contrast to the significant differences in serum antibody titers, TBEV pre-vaccination had no impact on the longitudinal dynamics of bulk and tetramer-specific CD4 and bulk CD8 T cell responses, as assessed through multiparametric spectral flow cytometry. Genomic DNA bulk B cell receptor (BCR) sequencing indicated limited clonal expansion in the bulk repertoire and reduced diversity by days 7 and 14 post-vaccination, consistent with the B cell population kinetics observed through flow cytometry.

In conclusion, the YF17D vaccine elicits both humoral and cellular immune responses that culminate in the generation of protective immunity. Pre-existing TBEV immunity does not impact the timing of the cellular immune response, but it significantly boosts YF17D immunogenicity and modifies the immunodominance of YF17D epitopes. This shift redirects the response in TBEV-pre-vaccinated individuals from a finely tuned, non-cross-reactive neutralizing response to a cross-reactive response focused on the FLE, with the potential to enhance dengue virus infection.

List of figures

List of tables

List of abbreviations

ADCC: Antibody-dependent cellular cytotoxicity

ADCP: Antibody-dependent cellular phagocytosis

ADE: Antibody-dependent Enhancement

AF: Alexa Fluor

AIM: Activation-Induced Marker

APC: Allophycocyanin

AU: Arbitrary Units

BCR: B Cell Receptor

BFA: Brefeldin-A

BSA: Bovine Serum Albumin

BV: Brilliant Violet

CCR: Chemokine (C-C) Receptor

CD: Cluster of differentiation

CDR: Complementary Determining Region

COMPASS: Combinatorial Polyfunctionality Analysis of Single Cells

cTfh: Circulating follicular helper T cells

CTL: Cytotoxic T Lymphocytes

CXCR: Chemokine (C-X-C) Receptor

Cy: Cyanin dye

DC: Dendritic Cell

DENV: Dengue Virus

DI-II: Domain I and II

DIII: Domain III

DMSO: Dimethyl Sulfoxide

DN: Double Negative (CD27-IgD-)

DNA: Deoxyribonucleic acid

E protein: Envelope protein

EDE: Envelope Dimer Epitope

EDTA: Ethylenediaminetetraacetic acid

ELISA: Enzyme-linked immunosorbent assay

EMA: European Medicines Agency

Fab: Fragment antigen-binding region

FBS: Fetal Bovine Serum

FC: Constant Fragment (antibody)

FCS: Fetal Calf Serum

FCyR: FC gamma Receptor

FDA: Food and Drug Administration

FITC: Fluorescein IsoTioCyanate

FLE: Fusion Loop Epitope

FluoRNT: Fluorescence Focus Reduction Neutralization Test

FR: Framework Region

FRNT: Focus Reduction Neutralization Test

FS: Functional Score

GC: Germinal Center

gDNA: Genomic DNA

HLA: Human Leukocyte Antigen

HRP: Horseradish peroxidase

ICS: Intracellular Cytokine Staining

ICTV: International Committee on Taxonomy of Viruses

IFN-y: Interferon gamma

IgA: Immunogloulin A

IgD: Immunoglobulin D

IgG: Immunoglobulin G

IgM: Immunoglobulin M

IL: Interleukin

JEV: Japanese Encephalitis Virus

KFDV: Kyasanur Forest Disease Virus

L/D: Live Dead

LAIV: Live Attenuated Influenza Vaccine

mAb: Monoclonal Antibody

MBC: Memory B cell

MHC: Major Histocompatibility Complex

MOI: Multiplicity of Infection

NK: Natural Killer

NS1: Non-Structural Protein 1

OAS: Original Antigenic Sin

PBMC: Peripheral Blood Mononuclear Cell

PBS: Phosphate-Buffered Saline

PD1: Programmed cell death protein 1

PE: Phycoerythrin

PerCP: Peridinin Chlorophyll Protein Complex

PFS: Polyfunctional Score.
PIE: Probability of Interspecies Encounter
PrM: Pre-Membrane protein
PRNT: Plaque Reduction Neutralization Test
RU: Relative Unit
SD: Standard Deviation
SDS PAGE: Sodium dodecyl-sulfate polyacrylamide gel electrophoresis
sE: Soluble Envelope protein
SHM: Somatic Hypermutation
SLEV: St. Louis Encephalitis Virus
TBEV: Tick-Borne Encephalitis Virus
T-CM: Central Memory T cell

TCR: T cell receptor
T-EM: Effector Memory T cell
T-EMRA: Late effector memory T cell
TF: Transcription Factor
Tfh: T follicular-helper cell
Th: T helper
TNF-α: Tumour Necrosis Factor α
T-RM: Resident Memory T cell
Tscm: Stem-cell memory T cell
VLP: Viral-like Particle
WB: Western Blot
WHO: World Health Organization
WNV: West Nile Virus
YF17D: Yellow Fever 17-D strain
YFV: Yellow Fever Virus
ZIKV: Zika Virus

1. Introduction

1.1 Human flaviviruses: epidemiology, medical importance, and vaccines*

The genus *Orthoflavivirus* (hereinafter referred to as flaviviruses, family *Flaviviridae*), currently includes 53 species as per the latest ICTV release (Walker et al., 2022). While some flaviviruses lack a known vector and a minority have birds, rodents, or bats as hosts, the majority are dual-host viruses. These dual-host viruses can be categorized into tick/vertebrate viruses, such as tick-borne encephalitis virus (TBEV), Langat virus, and Powassan virus, or mosquito/vertebrate viruses, including yellow fever (YFV), dengue (DENV), Zika (ZIKV), West Nile (WNV), and Japanese encephalitis virus (JEV) (Blitvich & Firth, 2015; Gould & Solomon, 2008).

Over thirty flaviviruses with human pathogenic potential have been identified, making them a leading cause of morbidity and mortality worldwide (Gould & Solomon, 2008). In the case of DENV, it infects up to 400 million people annually, while ZIKV infects approximately 40,000 people each year (Guo et al., 2022). WNV has infected approximately 2-4 million people in the United States alone since 1999 (Pierson & Diamond, 2020). Flaviviruses are distributed globally but not uniformly. TBEV is present in Europe and Central and Eastern Asia. In tropical and subtropical regions of Africa and the Americas, YFV cocirculates with ZIKV and DENV. DENV is also found in Southeast Asia, while JEV is restricted to Eastern Asia and Australia (Pierson & Diamond, 2020). Flaviviruses and their arthropod vectors are found on all continents and they are rapidly spreading due to international trade, travel, poorly planned urbanization, and ecological and climate changes. Consequently, there has been a recent expansion of dengue-endemic areas and a broader intercontinental distribution of other flaviviruses such as WNV and TBEV (Kraemer et al., 2015; Vasilakis et al., 2011). Recently, increasing numbers of autochthonous cases of dengue have been detected in France (Cochet et al., 2022) and of WNV in Italy (Riccardo et al., 2022; Riccò et al., 2021) and Spain (García San Miguel Rodríguez-Alarcón et al., 2021). Additionally, dengue has become one of the most important emerging diseases among European travelers (Gossner et al., 2022) with an increasing incidence in recent years, reaching over 4000 cases in Germany in 2019 (Allwinn, 2011; ECDC, 2022).

There are currently no specific antiviral therapies to treat flavivirus infections, and vaccination is the most effective instrument for combating their spread. Formalin-inactivated vaccines are available for TBEV, JEV, and Kyasanur forest disease virus (KFDV). The life-attenuated yellow fever vaccine (YF17D) was empirically developed (Theiler & Smith, 1937) and achieved an optimal balance between immunogenicity and attenuation. It is estimated that YF17D vaccination has adverted 2 million deaths in the period 2000-2019 and is expected to prevent 5.6 million deaths between 2000-2030 worldwide (X. Li et al., 2021). Although some studies have addressed the reasons for the outstanding performance of the YF17D vaccine (Barba-Spaeth et al., 2005; Davis et al., 2022; Fernandez-Garcia et al., 2016), the immunological basis for its effectiveness remains poorly defined. Additionally, YF17D vector vaccines have been developed for JEV, and DENV. As of 2023, a new live-attenuated tetravalent dengue vaccine based on

*With modifications from Santos-Peral et al. 2023 (see Disclaimers on page 8)

the DENV2 genetic backbone has been approved for use by the European Medicines Agency and in four other endemic countries (Rivera et al., 2022)

Flavivirus global distribution, high prevalence, and increasing vaccination coverage result in a rising number of individuals with immune experience to flaviviruses. Since all flaviviruses are serologically related, previous cross-reactive immunity may likely exist at the time of vaccination or natural infection with another member of the *Flaviviridae* family.

1.2   Flavivirus biology: mode of cell entry, life cycle, and virion structure*

All different flaviviruses share common features in their structural organization, mode of cell entry, life-cycle biology, maturation mechanisms, and assembly processes. Flaviviruses are spherical enveloped viruses with an approximate diameter of 50 nm. They contain a single-stranded, positive-sense RNA genome of approximately 11,000 nucleotides. This genome encodes for a polyprotein that is post-translationally cleaved into three structural proteins: capsid, pre-membrane (PrM), and envelope (E). Additionally, it encodes seven non-structural proteins (NS1, NS2A, NS2B, NS3, NS4A, NS4B, NS5). In mature virions, the structural E and the Pr-cleaved M proteins are embedded in the host-derived lipid bilayer in an icosahedral architecture. This structure consists of 180 units of the E protein, organized in 90 head-to-tail homodimers forming 30 rafts, which cover the surface of the virion (Figure 1). Flaviviruses enter host cells through receptor-mediated endocytosis, with the E protein performing both receptor binding and fusion functions. The exposed fraction of the E protein consists of three ectodomains (DI, DII, and DIII), connected to two transmembrane domains by three stem helices. The central DI connects the dimerization domain, DII, with DIII. DIII mediates cell binding and executes the physical force in the structural rearrangement necessary for viral fusion. DII contains the highly conserved hydrophobic fusion loop (FL). Endocytosis is initiated when the E protein-DIII binds to probably different receptors, which are not well-characterized and may differ among flaviviruses. Heparin, along with other glycosaminoglycans, integrins, lectins like DC-SIGN, and cellular lipid receptors such as TIM/TAM, have been suggested as receptors mediating cell entry (Mukhopadhyay et al., 2005; Stiasny et al., 2023). Upon entry, the acidification of the endosome triggers an irreversible conformational rearrangement of the E proteins from dimers to trimers that expose the FL, allowing it to insert into the endosomal membrane, ultimately leading to the fusion of the viral and endosomal membranes. Following fusion, and the release of genetic material into the cytoplasm, protein translation and virion assembly take place simultaneously while budding into the endoplasmic reticulum. The newly formed virions are then transported through the secretory pathway and released via exocytosis. During this process, the PrM protein serves as a chaperone for the proper folding of the E protein, to which it remains tightly bound in immature viral particles, covering the fusion loop and preventing premature fusion in the acidic environment in the trans-Golgi network. In this mildly acidic environment, furin processes the PrM protein into Pr peptides and M. The peripheral Pr peptide remains bound to the virus at low pH, inhibiting virus-membrane interaction. Upon exocytosis, the release of Pr at a neutral pH completes virus maturation into an

*With modifications from Santos-Peral et al. 2023 (see Disclaimers on page 8)

infectious particle. However, this process is often incomplete, resulting in the heterogeneous shedding of fully mature infectious particles together with immature, and chimeric uninfectious virions with uncleaved PrM proteins (Crampon et al., 2023; Mukhopadhyay et al., 2005; Slon Campos et al., 2018).

Since the E protein is exposed, covering the surface of the virion and participating in receptor binding and fusion-related conformational changes, it is the primary target of the neutralizing antibody response. Therefore, its structure and dynamics define the epitope landscape of the virus (Heinz & Stiasny, 2012; Stiasny et al., 2023)

1.3 Flaviviruses antigenic landscape*

The epitope accessibility determines the flavivirus antibody landscape and is influenced by the quaternary organization of the E protein in the mature viral particle, the structural oscillations of E, and the presence of immature particles.

Antibodies can target monomeric and domain-specific epitopes as well as quaternary epitopes within the dimeric structure of the E protein. A significant proportion of the humoral immune response generated after a flavivirus infection targets the fusion loop epitope (FLE), which is typically concealed within the dimeric arrangement of the E protein. Therefore, antibody binding to FLE requires dimer dissociation, which occurs only transiently for mature particles, in immature patches, and during fusion. FLE is highly immunodominant and anti-FLE antibodies are cross-reactive across all flaviviruses; however, due to its limited accessibility, FLE antibodies exhibit poor neutralization capacity (Cherrier et al., 2009; Sevvana & Kuhn, 2020). In effective anti-flaviviral immunity, a relevant fraction of the humoral response is directed against the dimeric arrangement of the E protein in mature viral particles. Antibodies can target inter- or intra-dimeric epitopes. The envelope dimer epitope (EDE) is a quaternary epitope that spans conserved regions in the DII of one protomer and DIII in the opposing protomer. Upon binding, EDE antibodies crosslink both dimer subunits, preventing the conformational changes required for fusion. EDE antibodies were first described in DENV and have been precisely mapped for DENV and ZIKV (Barba-Spaeth et al., 2016; Dejnirattisai et al., 2015). Nevertheless, envelope dimer epitopes are likely to exist in all other flaviviruses (Sevvana & Kuhn, 2020).

Virus breathing, defined as dynamic natural oscillations of the mature virions, adds complexity to the flavivirus epitope landscape facilitating the generation of antibodies and their binding to otherwise concealed epitopes (Dowd et al., 2011, 2014; Stiasny et al., 2022; Zhao et al., 2020). These small-scale oscillations vary considerably across flaviviruses, and a single amino acid change can lead to significant alterations in viral breathing, resulting in profound implications for antibody binding and antibody neutralizing potential (Austin et al., 2012; Goo et al., 2017; Zhao et al., 2020). Viral breathing modulates epitope accessibility in different E protein regions, like DIII lateral ridge, which is typically inaccessible in the interior of the virion (Zhao et al., 2020); the DII lateral hi loop, located close to the adjacent raft dimer unit (Fibriansah et al., 2021) and, importantly, the accessibility of the FLE (Dowd et al., 2011)

---

*With modifications from Santos-Peral et al. 2023 (see Disclaimers on page 8)
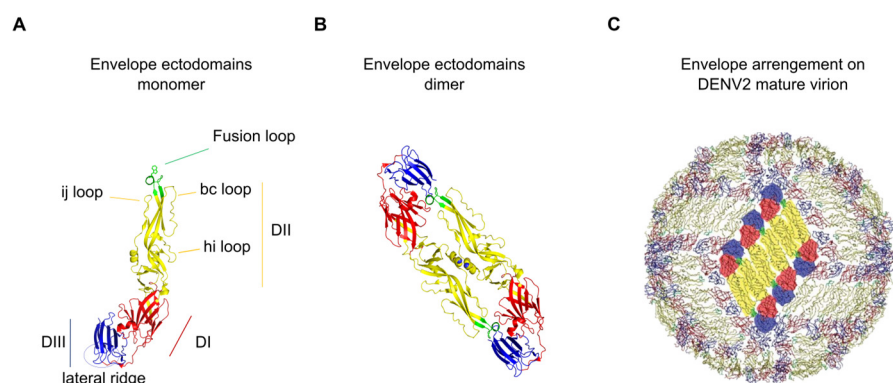
Figure 1. Flavivirus E protein structure and arrangement.

A) Illustration of the structure of the envelope protein ectodomains (sE). PDB: 6IW4 edited using Pymol.
B) Illustration of the structure of the envelope protein pre-fusion dimer conformation. PDB: 6IW4 edited using Pymol.
C) DENV2 viral particle. One raft, consisting of three dimers in parallel, is highlighted. Reproduced with permission from CellPress (Zhang et al., 2004) (license number: 5650100091768)
Domain I is depicted in red, Domain II in yellow, and Domain III in blue. The fusion loop is shown ingreen.

The occurrence of immature or chimeric viral particles during a natural infection or live-virus vaccination primes the generation of antibodies against the Pr peptide. Furthermore, the spiky-like structural arrangement of the E protein in these particles facilitates the production of FLE antibodies (Cherrier et al., 2009; Pierson & Diamond, 2012).

Finally, NS1 is another target of the antibody response. Monomeric NS1 plays an essential role in immune evasion and viral replication throughout the virus life cycle. NS1 is also exposed in hydrophobic dimers on the membranes of infected cells and is secreted in a hexameric form. Anti-NS1 antibodies may offer protection against severe disease through mechanisms unrelated to virus neutralization, such as neutralizing the extracellular functions of NS1 or via antibody-dependent cellular cytotoxicity (ADCC) and complement-mediated functions (Slon Campos et al., 2018).

1.3.1 Antibody-mediated neutralization

The neutralization of flaviviruses is most accurately described by a "multiple-hit" model, wherein neutralization occurs after multiple antibodies dock onto the virus exceeding a threshold for inactivation (Pierson et al., 2007). The number of antibody molecules required for neutralization is dependent on the interplay between antibody affinity and epitope accessibility. The arrangement of the E protein in the virion necessitates the independent blockade of all 30 rafts for effective neutralization (Dowd & Pierson, 2011).

Only antibodies that interfere with essential steps in the virus entry, such as receptor binding, fusion, and the conformational rearrangements necessary for fusion, can effectively neutralize the infection (Rey et al., 2018). For instance, antibodies specific to FLE could potentially disrupt the infection by preventing the insertion into membranes of the FL. In fact, FLE-specific antibodies with neutralizing potential have been identified

for ZIKV (Dai et al., 2016). However, the stoichiometry needed to block infection with a FL-directed antibody would require simultaneous binding to 60 trimers in the fusogenic conformation. This, along with the concealment of FLE in the mature virion, renders this subset of antibodies not effective at neutralization. Relevant neutralizing determinants have been discovered for different flaviviruses in DIII, responsible for receptor binding and dimer-to-trimer reorganization (Robbiani et al., 2017; Svoboda et al., 2023). For West Nile virus (WNV), the lowest occupancy required for neutralization was 30 antibody molecules for a highly accessible epitope in DIII (Pierson et al., 2007). Other monomeric neutralizing determinants have been found in the FL-proximal area, coinciding with the conserved Pr-binding site. Antibodies binding to the FL-proximal epitope replicate the Pr functions in the trans-Golgi network, preventing the E-dimer rearrangement and fusion (Y. Li et al., 2022; Lu et al., 2019)

The affinity and avidity of binding introduce an additional layer of complexity to the neutralizing potential of antibodies, aside from the epitope specificity. The antibody affinity for binding defines the fraction of epitopes bound by antibody molecules at any given concentration. Naturally, antibodies with high affinity tend to be more effective at neutralization. Mechanistically, neutralization sometimes relies on the avidity of antibody binding to the complex oligomeric structure of the virion. Recently, the neutralizing capacity of DENV and ZIKV of the cross-neutralizing antibody C10 was found to be highly reliant on the bivalent binding of the IgG isotype (Sharma et al., 2021). Similarly, despite the typically low binding affinity of IgM antibodies, the IgM-mediated neutralization mode benefits from multivalent binding to the virion's multimeric structure (Singh et al., 2022). IgM can simultaneously bind to 10 to 12 positions, effectively coating the virion and blocking virus entry and fusion. The multivalency of the IgM subtype and, to a lesser extent, IgGs, can mediate neutralization through cross-linking circulating virus particles with different Fab arms. This cross-linking facilitates virus clearance and reduces the number of available infectious virions for cell infection (Chan et al., 2011).

In summary, antibodies targeting crucial epitopes within the antigenic structure of flaviviruses can achieve neutralization when present at sufficient concentration.

1.3.2 Antibody-dependent enhancement and cross-reactivity as a challenge for anti-flavivirus vaccines

When antibodies are present at subneutralizing concentration, below the threshold for neutralization, or are non-neutralizing, they can instead promote virus phagocytosis by cells bearing Fc gamma receptors (FcγR). This, in turn, results in antibody-dependent enhancement (ADE) of infection in these cells. Thus, FcγR-expressing cells become susceptible to viral infection, even by immature or chimeric viral particles (Rodenhuis-Zybert et al., 2011).

Humoral cross-reactivity among flaviviruses has been thoroughly described for DENV and ZIKV (Priyamvada et al., 2017) and even among more distantly related flaviviruses (Rey et al., 2018). Flavivirus infections and contemporary vaccination practices frequently lead to the production of cross-reactive antibodies that exhibit limited or no

capacity for cross-neutralization against heterologous infections (Beltramello et al., 2010; Chih-Yun et al., 2008; Dejnirattisai et al., 2016; Malafa et al., 2020; Priyamvada et al., 2017). This humoral cross-reactivity is often expanded in heterologous infections or subsequent vaccinations (Malafa et al., 2020; Rogers et al., 2017). Frequently, the expansion of FLE antibodies is responsible for this cross-reactivity (Chih-Yun et al., 2008; Crill & Chang, 2004) and in the case of DENV, it also involves anti-Pr antibodies (de Alwis et al., 2014). Cross-reactive antibodies can have infection-enhancing potential via ADE. ADE has clinical implications, and it has been linked to an increased risk of severe dengue disease upon secondary heterotypic and heterologous DENV infections in humans (Anderson et al., 2011; Dejnirattisai et al., 2010, 2016; Katzelnick et al., 2017). Notably, ADE is the underlying cause of the suboptimal protection provided by the DENV vaccine, Dengvaxia, in children and seronegative individuals. For these individuals, the vaccine acts as a silent primary infection placing them at greater risk of severe disease (Ferguson et al., 2016).

Flavivirus cross-reactivity poses a major challenge for the development of new vaccines. Novel vaccine designs aim to minimize cross-reactivity while priming for effective neutralization (Slon-Campos et al., 2019). Among the existing flavivirus vaccines, the JEV vaccine has been associated with an elevated risk of dengue disease (Anderson et al., 2011) whereas the YF17D vaccine has not shown this association (Luppe et al., 2019). Understanding the immunodominance of epitopes in the YF17D vaccine within the context of flavivirus cross-reactivity and neutralization is crucial, especially considering the high prevalence of DENV in YFV endemic areas.

1.4   The YF17D vaccine

The YF17D vaccine, created in 1937, induces life-long protective immunity and is considered one of the most effective vaccines ever developed (Kling et al., 2022; Poland et al., 1981; Theiler & Smith, 1937). Even though the vaccine has been administered for over 80 years, YFV has reemerged strongly in the last two decades with 80,000 to 200,000 cases reported annually worldwide (Monath & Vasconcelos, 2015; Oyono et al., 2022). In addition, several recent outbreaks (Angola 2017, Brazil 2018, Nigeria 2019) have raised concerns about low vaccine supplies and our poor insight into viral biology and vaccine immunogenicity.

The YF17D vaccine has outstanding efficacy with up to 97% of vaccinees developing a long-lasting protective immunity mediated by neutralizing antibodies and T cells (Fuertes Marraco et al., 2015; Kling et al., 2022; Monath & Vasconcelos, 2015; Poland et al., 1981). These characteristics make YF17D the most successful of all vaccines and it is often used as a model to understand the molecular basis of long-lasting immune protection (Pulendran, 2009). Currently, the YF17D vaccine model has gained momentum in the efforts to understand how effective vaccines stimulate protective immune responses (Fourati et al., 2022; Hagan et al., 2022; Pulendran, 2009; Querec et al., 2009). Nevertheless, YF17D was developed empirically and the molecular determinants underlying the effectiveness of YF17D remain poorly understood. Surprisingly, only 32 mutations differentiate YF17D from the original infectious Asibi

strain (Hahn et al., 1987). It has been hypothesized that the YF17D virus induces a more robust cytokine response (Fernandez-Garcia et al., 2016). Additionally, YF17D can infect dendritic cells (DC) without affecting their activation and antigen presentation capacity (Barba-Spaeth et al., 2005). In conclusion, the YF17D vaccine features that lead to the development of protective immunity must be examined within the framework of flavivirus biology and antigenicity.

1.4.1 The antigen-specific CD4 and CD8 T cell response to YF17D vaccine

YF17D is known to induce a robust IFN-I signature shortly after immunization. Consequently, the robust activation of the innate immune system concurs with the efficient activation of DCs and other innate immune cellular effectors resulting in a cytokine milieu that preferentially primes for a CD4 T helper (Th) type 1 anti-viral response (Gaucher et al., 2008). This cascade of events ultimately leads to the generation of strongly-neutralizing antibodies, which are positively correlated with the magnitude of activated CD4+ T cells that likewise act as central regulators of pathogen-specific adaptive immunity (Kohler et al., 2012). Durable generation of neutralizing antibodies relies on B cell affinity maturation and isotype-switching, a fact that requires the involvement of antigen-specific T follicular helper (Tfh) cells in the germinal center (GC) reaction. Circulating Tfh (cTfh) cells can be found in peripheral blood and serve as a surrogate for the Tfh response within the GC (Morita et al., 2011). cTfh cells have been recognized to play a pivotal role in the generation of protective responses following YF17D vaccination (Huber et al., 2020; Sandberg et al., 2021).

An immunological advantage of live vaccines is their capacity to stimulate a T cell-specific response against both structural and non-structural viral proteins. YF17D-induced immunity includes the generation of polyfunctional long-lasting memory T cell responses that persist for up to 30 years pv. (Akondy et al., 2017; Fuertes Marraco et al., 2015; James et al., 2013; Slon Campos et al., 2018). Numerous studies have described in depth the characteristics and the dynamics of the T cell immune response elicited by YF17D vaccine (Akondy et al., 2009; Blom et al., 2013; Bovay et al., 2020; Gaucher et al., 2008; Hou et al., 2017; Huber et al., 2020; Miller et al., 2008; Sandberg et al., 2021). Importantly, T cells have been identified as mediators of viral clearance, constituting a significant component of vaccine-induced protection in animal models (Chen et al., 2020; Watson et al., 2016) and humans (Weiskopf et al., 2013).

Overall, T-cell responses are crucial for vaccine-induced protection and serve as a correlate of vaccine immunogenicity. A profound understanding of the T-cell response is essential for comprehending the proper generation of effective antiviral responses.

1.4.2 The B cell and antibody response to the YF17D vaccine

The neutralizing antibody titer is the gold standard correlate of vaccine-induced protection and can last over 30 years following a single vaccination dose (Poland et al., 1981). The B cell plasmablast response reaches its peak on day 14 post-vaccination but YF17D-specific B cells continue to mature for 6 to 9 months after vaccination, likely due to the persistence of antigens in the GC (Hägglöf et al., 2023; Wec et al., 2020).

The antigenic structure of YF17D replicates the principal characteristics of the flavivirus epitope landscape. The primary antigenic sites of YF17D have been previously investigated (Vratskikh et al., 2013). However, the analysis of antibody specificities in the polyclonal sera of YF17D vaccine recipients has been limited to the E monomer, ectodomains, and full virion particles. Consistent with other flaviviruses, antibodies in sera primarily bind to regions in DII. Interestingly, only a minor fraction of antibodies seem to target DIII (Vratskikh et al., 2013; Wec et al., 2020). The FL-proximal area was found to be an important determinant for YFV neutralization (Doyle et al., 2022; Haslwanter et al., 2022; Y. Li et al., 2022; Lu et al., 2019). The binding sites of the FL-proximal mAb 5A, identified by Daffis et al. (2005) have been structurally mapped in the FL and the adjacent b strand, bc loop, and ij loop on DII. This antibody mediates neutralization by directly preventing fusion or cell attachment in both pre and post-fusion conformations (Lu et al., 2019).

A comprehensive dissection of the antibody specificities elicited by YF17D vaccination, including quaternary epitopes, has not been conducted yet. While inter or intra-dimer epitopes compatible with the EDE have been mapped for other viruses like ZIKV, DENV, and WNV, this has not been done for YFV (Sevvana & Kuhn, 2020). Nevertheless, there is evidence indicating the significance of quaternary epitopes in YFV neutralization. For instance, reactivity against the isolated monomeric E protein accounts only for a small part of the neutralizing activity of the polyclonal sera which suggests that neutralizing antibodies target other complex oligomeric structures (Vratskikh et al., 2013). Daffis et al. generated escape variants in response to highly neutralizing monoclonal antibodies and identified escape mutations in DI and DII of opposing E protomers, indicating the potential presence of a highly neutralizing EDE-like epitope in YFV (Daffis et al., 2005). Other studies have found escape mutations that, with current knowledge, are consistent with an EDE-like epitope (Lobigs et al., 1987; Ryman et al., 1997).

Altogether, the YF17D vaccine confers lifelong immunity through the stimulation of antigen-specific CD4 and CD8 T cells, as well as the production of neutralizing antibodies. However, further efforts are required to elucidate the immune interactions in the response to vaccination that ultimately lead to the development of neutralizing immunity.

1.5 Immune responses to live vaccines and viral infections in the context of pre-existing immunity

The YF17D vaccine is often administered to individuals who possess pre-existing cross-reactive immunity acquired through vaccination or natural infection with another flavivirus. However, the effects of pre-existing immunity on vaccine immunogenicity and the accessibility of epitopes within the structure of the YF17D virus remain poorly understood. Pre-existing immunity can potentially impact the response to a live vaccine in several ways. Firstly, it may facilitate vaccine-virus neutralization and clearance. Secondly, pre-existing antibodies could mediate live-virus infection enhancement via ADE. Additionally, pre-existing immunity could result in epitope masking and trigger an antibody feedback mechanism. Lastly, vaccination may induce an anamnestic response

and pre-existing immune imprinting may contribute to what is known as "original antigenic sin" (OAS).

Firstly, if pre-existing immunity facilitates virus neutralization, reduces vaccine-virus replication, accelerates viral clearance, or engages inhibitory Fc receptors on B cells, it has the potential to hinder the optimal boosting of immunity. Vaccine virus neutralization is suspected to be an underlying factor contributing to the loss of efficacy observed with yearly subsequent immunizations of the live-attenuated influenza vaccine (LAIV). In fact, LAIV is only effective in children who lack prior anti-influenza immunity (Matrajt et al., 2019; Singanayagam et al., 2018).

Conversely, in flavivirus immunity, pre-existing cross-reactive antibodies have the potential to enhance the productive infection of antigen-presenting cells through ADE (Mok & Chan, 2020). Consequently, this leads to an increased viral burden and more effective bridging of the innate and adaptive immune systems, resulting in the induction of activation signals and improved antigen presentation. Chan et al. (2016) demonstrated this effect by showing that cross-reactive antibodies induced by the JEV vaccine enhanced the immunogenicity of the YF17D vaccine via ADE (Chan et al., 2016).

In addition to its impact on immunogenicity, previously acquired immunity can influence the immunodominance of vaccine epitopes. Cross-reactive antibodies can reconfigure the arrangement of epitopes within the viral particle and modulate the dynamic motion of the virus, resulting in the exposure of cryptic or less accessible epitopes (Lok et al., 2008). Notably, monoclonal FL-proximal antibodies were observed to disassemble TBEV-soluble E dimers in solution, resulting in the exposure of the FLE (Tsouchnikas et al., 2015). Pre-existing antibodies can also impact the development of memory B cells (MBC). When pre-existing antibodies bind strongly to dominant epitopes, they shield the accessibility of these epitopes presented by follicular dendritic cells in the GC reaction. Consequently, this antibody feedback leads to the diversification of the humoral response to other accessible epitopes (Schaefer-Babajew et al., 2023). This 'antibody feedback' mechanism effectively lowers the activation threshold for new B cells that are continuously entering the GC reaction, favoring the development of low-affinity B cell clones directed toward different epitopes. This process can persist for months following infection or immunization (Hägglöf et al., 2023; Muecksch et al., 2022; Schaefer-Babajew et al., 2023). This mechanism has contributed significantly to broadening vaccine-induced protection against emerging SARS-CoV-2 variants in subsequent mRNA vaccinations and has had a substantial impact on the vaccine response in patients who received antibody cocktail therapies before immunization (Schaefer-Babajew et al., 2023). It is plausible that a similar effect contributes to the diversification of the immune response to flaviviruses, either by epitope masking or dimer dissociation (Tsouchnikas et al., 2015).

Lastly, immune memory could result in an anamnestic response to a subsequent vaccination. An anamnestic response would be characterized by more rapid and stronger T and B cell responses, leading to higher amounts of antigen-specific T cells and plasmablasts. This was shown to be underlying the course of Sars-Cov-2 breakthrough

infections in vaccinated individuals (Painter et al., 2023). During an anamnestic response, pre-existing B cell clones may predominate over de novo cells undergoing GC reactions, thereby limiting the final diversity of the B cell response to the new challenge with an antigenically related pathogen (Wong et al., 2020). This phenomenon, often referred to as original antigenic sin or immune imprinting, results in an inaccurate response that is preferentially directed against previously seen epitopes to the detriment of new antigen-specific epitopes (Vatti et al., 2017).

1.5.1 Pre-existing immunity and subsequent flavivirus infections or vaccinations

The impact of prior flavivirus immunity on the outcome of YF17D vaccination remains poorly understood. Previous studies have noted that the YF17D vaccine enhances cross-reactive hemagglutination inhibition titers in individuals previously infected with St. Louis encephalitis virus (SLEV) and DENV, but not in those who have not been exposed to flaviviruses or individuals who have received double YF17D vaccinations (Pond et al., 1967). In general, sequential immunization with heterologous viruses appears to enhance cross-reactivity (Kayser et al., 1985). Subsequent exposures to both DENV and ZIKV lead to the expansion of cross-reactive, poorly neutralizing antibodies directed against the FLE, which have the potential to mediate ADE while ZIKV infection alone induces predominantly a de novo B cell response that is finely tuned and highly neutralizing (Rogers et al., 2017). Conversely, although subsequent infections with different serotypes of DENV preferentially increase the production of cross-reactive antibodies (Mathew et al., 2011), they also facilitate the development and expansion of cross-neutralizing antibodies that target EDE specificities (Dejnirattisai et al., 2015). This may be due to the refinement of the humoral response and antibody diversification in secondary DENV infections. However, when subsequent exposures involve phylogenetically distant viruses lacking cross-neutralizing determinants, other studies have reported a substantial increase in cross-reactive IgG antibodies in individuals who were previously vaccinated with YFV, TBEV, or both following primary ZIKV infection (Malafa et al., 2020). The YF17D-induced response was found to hinder the induction of neutralizing antibodies by the subsequent TBEV-inactivated vaccine which in turn induced lower IgG antibody titers but with increased cross-reactivity (Bradt et al., 2019).

The interplay between immune imprinting, the feedback of pre-existing antibodies, and ADE on immune responses to secondary flavivirus infections and, in particular, YF17D vaccination remains incompletely understood. YF17D vaccination is often given to individuals who may have previously encountered other flaviviruses. Consequently, investigating how the preceding immune priming impacts the immunodominance and immunogenicity of YF17D becomes a pertinent question. Moreover, YF17D vaccination is administered in regions where other flaviviruses are co-circulating, including both endemic regions and travelers to these areas. This highlights the significance of understanding how the immunity elicited by the YF17D vaccine could impact the course of subsequent natural flavivirus infections.

1.6   Study aims

In this dissertation, I investigated the immune response triggered by YF17D vaccination in a longitudinally sampled human cohort comprising 250 participants, more than half of whom have a history of prior TBEV vaccination. TBEV, although phylogenetically distinct, shares antigenic similarities with YF17D, presenting an excellent opportunity to contrast the responses to YF17D in individuals with no prior exposure to flaviviruses with the effect of prior immunity on vaccine responses.

With this cohort I address various fundamental questions in immunology and vaccinology: 1) How pre-existing immunity influences the immunodominance of YF17D epitopes and the humoral response. 2) What is the effect of pre-existing immunity to a related virus on the immunogenicity of a live vaccine and the kinetics of the immune response 3) What specific attributes of the YF17D vaccine lead to the establishment of lifelong protection. 4) What potential impact might the immune status conferred by YF17D vaccination have on the progression of a subsequent DENV infection in both TBEV-pre-vaccinated and unvaccinated individuals.

Specifically, this study provides a detailed examination of the neutralizing and cross-reactive determinants of YF17D and how they are primed after vaccination. Additionally, it offers a thorough characterization of the functionality of antigen-specific CD4 and CD8 T cells, which are essential components of vaccine-induced protective immunity. Furthermore, this research entails a longitudinal analysis of the kinetics of CD4, CD8, and B cells, including an in-depth exploration of B cell repertoire dynamics following vaccination. Altogether, this investigation aims to discern the disparities between a primary immune response and the effect of prior flavivirus immunity on the vaccine response to the highly effective YF17D vaccine.

2.   Material and Methods

REAGENT or RESOURCE	SOURCE	IDENTIFIER
Antibodies		
Hybridoma: D1-4G2-4-15	ATCC	Cat# HB-112
Hybridoma: 2D12	ATCC	Cat# CRL-1689
Anti-YFV 5A	Daffis et al. 2005. Produced by G. Barba-Spaeth	
Anti-human IgG HRP	Jackson ImmunoResearch	Cat# 109-035-088
Anti-human IgM HRP	ThermoFisher	Cat# 31415
Anti-human IgG	Sigma Aldrich	Cat# I2136
Fluorochrome-conjugated antibodies	Appendix A.	
Bacterial and Virus Strains		
YF17D Stamaril	Sanofi Pasteur, Lyon, France	
YF17D-Venus	Dr. Charles M. Rice (Rockefeller University, NY, USA).	
Biological Samples		
Sera, plasma and PBMC of YF17D vaccinees	This study	
Chemicals, Peptides, and Recombinant Proteins		
Recombinant TBEV domain III	Jena Bioscience	Cat# PR-1450-S
Recombinant YF17D domain III	Dr. G. Barba-Spaeth	
Recombinant YF17D domain I and II	Dr. G. Barba-Spaeth	
Recombinant YF17D soluble envelope	Dr. G. Barba-Spaeth	
Recombinant YF17D locked-dimer	This study	
Recombinant YF17D locked-dimer N71K	This study	
Recombinant YF17D locked-dimer N71K A240R	This study	
Recombinant YF17D breathing-dimer	This study	
Recombinant YF17D breathing-dimer W101H	This study	
DENV2 reporter virus replicon particles (VRP)	Dr. Beate Kümerer. Lücke, A.-C.et a. 2022	
Coelenterazine	Carl Roth	Cat# 4094.3
StrepTactin-HRP	Bio-Rad	Cat# 1610380
BD OptEIA TMB Substrate Reagent Set	BD	Cat# 555214
Polyethylene Glycol 8000	Carl Roth	Cat# 5322-68-3
TrueNuclear Perm Buffer	Biolegend	Cat# 424401
Foxp3/Transcription Factor Staining Buffer Set	Invitrogen	Cat# 00-5521-00
Zombie UV	BioLegend	Cat# 423108
Fixable Viability Dye eFluor 780	Thermo Fisher	Cat# 65-0865-14
Fixable Far Red Dead Cell Stain	Thermo Fisher	Cat# L10120
Paraformaldehyde	Sigma Aldrich	Cat# 8.18708
Effectene	Qiagen	Cat# 301425
BirA	MClab	Cat# BBLA-110
D-Biotin	EMD Millipore	Cat# 8.51209.0001
ATP	Thermo Fisher	Cat# R0441

Magnesium acetate	Sigma Aldrich	Cat# M5661
MHC tetramers	NIH Tetramer Facility, Emory University, Atlanta	
Brefeldin A	BioLegend	Cat# 420601
Phusion Hot Start II DNA-Polymerase	NEB	Cat# M0530S
Critical Commercial Assays		
Anti-human IgM agarose beads	Sigma	Cat# A9935
MagStrep XT beads	IBA	Cat# 2-4090-002
Pur-A-Lyzer™ Mini Dialysis Kit	Sigma Aldrich	Cat# PURN60100
GenElute miniprep kit	Sigma-Aldrich	Cat# G1N70
NucleoSpin Gel and PCR clean-up kit	Macherey-Nagel	Cat# 740609.250
QuantiFluor® dsDNA System	Promega	Cat# E2670
DNA D1000 ScreenTape	Agilent	Cat# 5067-5582
PhiX	Phix Control Kit V3	Cat# FC-110-3001
Miseq Reagent Kit v3 (600 cycle)	Illumina	Cat# MS-102-3003
Experimental Models: Cell Lines		
drosophila S2 cell lines	Thermo Fisher	Cat# R690-07
Vero B4	ATCC	Cat# CCL81
THP-1	ATCC	Cat# TIB-202
K562	ATCC	Cat# CCL-243
A549	ATCC	Cat# CCL-185
Oligonucleotides		
Primers	Metabion	Customised
Recombinant DNA		
pMT vector carrying E protein mutants	DuBois RM et al. 2013	
pCoPuro plasmid	Iwaki, T et al. 2003	
Software and Algorithms		
GraphPad Prism 8	GraphPad, La Jolla, CA, USA	https://www.graphpad.com/
FlowJo	FlowJo	https://www.flowjo.com/
R		https://www.r-project.org/
SnapGene	SnapGene	https://www.snapgene.com/
Devices		
FLUOstar Omega reader	BMG Labtech	https://www.bmglabtech.com
CytoFLEX LX	Beckman Coulter	sn: BE48044
LSR Fortessa II	BD	sn: H647794E6064
BD FACSCanto	BD	sn: V96300312
Cytek Aurora	Cytek	sn: U1086
4150 TapeStation System	Agilent	sn: G2992AA
MLS 50 Optima Max-XP Ultracentrifuge	Beckman Coulter	sn: CT312128
MiSeq	Illumina	AG Hornung lab

Table 1. Key materials

2.1   Cohort Samples*

250 healthy young adults, naive to natural flavivirus infection as well as a negative vaccination history to JEV and YFV, were recruited from 2015-2019 at the Division of Infectious Diseases and Tropical Medicine (DIDTM) as well as the Department of Clinical Pharmacology, University Hospital, LMU Munich, Germany. Permission by the institutional review board of the Medical Faculty of LMU had been granted before study initiation (IRB #86-16). The clinical study was retrospectively registered in the ISRCTN registry (ISRCTN17974967). Study participants were vaccinated subcutaneously with the YF17D vaccine (Stamaril; Sanofi Pasteur, Lyon, France) and samples were collected before vaccination and on days 3, 7, 14, and 28 post -vaccination. Serum and plasma samples were stored at -80°C. PBMC samples were isolated manually from buffy coat following Ficoll-Paque PLUS (GE Healthcare) density centrifugation and cryopreserved in heat-inactivated fetal calf serum (FCS) supplemented with 10% DMSO (Sigma-Aldrich) in liquid nitrogen. All assays started with the thawing of cryopreserved PBMC with an average recovery of 70 %. Briefly, the cryopreserved samples were quickly thawed in the water bath and transferred to a 15 ml Falcon tube with pre-warmed R10 medium (RPMI-1640 with 10% heat-inactivated FCS, streptomycin and penicillin 100 mg/ml). After 5 minutes of centrifugation at 400g, the cells were resuspended, counted, and plated as required.

2.2   YF17D and YF17D-Venus virus production*

The YF17D virus was directly obtained from a Stamaril vaccine dose. YF17D variant YF17D-Venus plasmid was generously provided by Charles M. Rice and Margaret MacDonald from The Rockefeller University in New York, USA. The production of the virus was conducted following a previously established protocol with some minor adjustments (Scheck et al., 2022; Tan & Lok, 2014). In brief, Vero B4 cells were cultured in DMEM with 10% heat-inactivated FCS, streptomycin and penicillin 100 mg/ml, and 5mM of glutamine at 37°C under 5% CO_2. These cells were expanded and then infected with the YF17D virus at a multiplicity of infection (MOI) of 0.1. Supernatants were harvested 3-4 days after infection when a cytopathic effect was visible, and cellular debris was homogenized using a douncer. Subsequently, the supernatants were mixed with polyethylene glycol (PEG 8000) at a concentration of 7% (w/v) and left to rotate slowly at 4°C overnight. The virus-PEG complexes were then subjected to centrifugation, and the resulting precipitate was homogenized in TNE buffer (comprising 20 mM Tris-HCl at pH 8, 150 mM NaCl, and 2 mM EDTA). Further purification and isolation of infectious virus particles were carried out through a sucrose cushion separation method, involving the use of 30% and 60% sucrose layers, followed by ultracentrifugation at 160,000 × g at 4°C for 2 hours using an MLS 50 rotor (Beckman). A distinct band of virus located between the two sucrose cushions was collected, diluted in TNE buffer, quantified using a plaque assay, and subsequently stored at -80°C until needed.

---

*With modifications from Santos-Peral et al. 2023 (see Disclaimers on page 8)

2.3   Serology*

YF17D virus neutralization and determination of neutralizing antibody titer*

The neutralizing antibody titer was determined by a Fluorescence Reduction Neutralization Test (FluoRNT) as previously described by Scheck et al, 2022 (Scheck et al., 2022). For the assay, YF17D-Venus virus was incubated with donor sera that were both inactivated and serially diluted, in equal quantities, for 1 hour at 37°C in serum-free DMEM. A viral concentration of 21,000 plaque-forming units (PFU) per well was utilized to achieve approximately 50% infection. Subsequently, this viral-serum mixture was introduced to Vero cells at a density of 25,000 cells per well in a 96-well plate and allowed to incubate for a period of 24 hours. Following incubation, the cells were trypsinized, subjected to APC viability staining (ThermoFischer), and fixed with 4% paraformaldehyde (PFA) before being analyzed in either the FACS Canto or CytoFLEX LX flow cytometry instruments. The frequency of infected cells in the absence of vaccinee serum was established as 100 %, and the reduction percentage was computed for each dilution step according to the formula:

$$100 - \frac{(Frequency\ of\ infection\ in\ test\ sample)}{(Frequency\ of\ infection\ without\ serum)}$$

Then, neutralization curves were fitted by 4 parameter logistic regression in R using the drm function of drc R package or Graphpad Prism (full cohort, Lisa Lehmann). 50, 80 and 90 % FluoRNT values were interpolated from the curves.

Antibody titer determination in an enzyme-linked immunosorbent assay*

An in-house three-layer ELISA was employed to quantify antigen-specific IgG and IgM in the sera of vaccine recipients. Half-area 96-well plates (Corning) were coated overnight at 4°C with either 1 µg/ml of sE or DIII protein (this study or JenaBioscience for TBEV-DIII) and 3.5 µg/ml of full virus YF-17D. For the quantification of vaccinee-specific IgM, only full virus YF17D was used as the antigen. The coating was performed in sodium hydrogen carbonate/carbonate buffer at pH 9.5. After the coating step, the plates underwent 5 washes with 0.05% PBS tween-20. Subsequently, the plates were blocked for 3 hours at room temperature with gentle agitation at 200 rpm using a blocking solution composed of 10% goat serum in PBS with 0.05% tween-20. Following the blocking step, heat-inactivated serum samples were added to the plates at various three-fold dilutions (typically 1:100, 1:300, 1:900, and 1:1800 for IgG detection, and 1:200 and 1:400 for IgM). The serum samples were prepared in a blocking buffer and incubated for 2 hours. To eliminate non-specific immunoglobulins, the plates were thoroughly washed 10 times before the addition of anti-human IgG-HRP (Jackson ImmunoResearch, diluted at 1:5000) or anti-human IgM-HRP (ThermoFischer, diluted at 1:5000). An hour later, the plates were washed again 10 times with 0.05% PBS tween-20, and a TMB substrate (BD, 555214) was added. The plates were allowed to develop for 10-25 minutes before the addition of a 1M H_2SO_4 stop solution. The optical density was measured at 450 nm with a 570 nm correction. A signal was considered positive if it was at least three times higher than the background signal detected in wells without pre-coated antigen and at the same serum dilution. The background signal was

---

*With modifications from Santos-Peral et al. 2023 (see Disclaimers on page 8)

subtracted. To ensure comparability and reproducibility across different days and plates, the ELISA titers were expressed as relative units (RU) in reference to a standard anti-YF17D serum, which was arbitrarily assigned a value of 10,000 units. This standardization method has been described previously (Hofmann et al., 1983; Malafa et al., 2020; Stiasny et al., 2012). The corresponding values for the test serum samples were determined by reading from the standard curve, which was fitted using a four-parameter logistic regression model.

Antibody competition ELISA*

To assess the quantity of IgG antibodies in human serum targeting the FLE, the reduction in antibody binding to the sE protein when it competed with murine isotypes of 4G2 and 2D12 mAb using an ELISA assay was evaluated. As previously mentioned, ELISA plates were initially coated with 1 µg/ml of sE protein and then blocked with a solution consisting of 10% goat serum in PBS with 0.05% tween-20. In corresponding blocking conditions, an equimolar concentration of 35 nmol of either 4G2 or 2D12 mAb was added and incubated for 3 hours. The serum samples were tested at dilutions of 1:100 and 1:1000 in the presence of 35 nmol of either 4G2 or 2D12. The ELISA titers, expressed in relative units (RU), were compared to the titer determined in the absence of any competing antibody. The amount of anti-FLE antibodies present in the sample was calculated using the following formula:

% antifusion loop antibodies = [1-Sample with 4G2/ Sample without 4G2]*100%

ELISA for end-point titer determination for IgG antibodies in human serum*

The quantification of IgG antibody titers directed against locked-dimer, Locked-dimer^{N71K}, locked-dimer^{N71K,A240R}, breathing-dimer, and breathing-dimer^{W101H} antigens was performed as endpoint titrations. In brief, after the initial coating and blocking of ELISA plates, seven serial dilutions of serum samples were added to the plates, commencing at a 1:50 dilution and proceeding with a 1:3 dilution factor. After a 2-hour incubation, the plates underwent 10 washes, which included two washes with a solution containing 650 mM NaCl in PBS. The addition of this chaotropic agent serves the purpose of eliminating antibodies that bind with low affinity while preserving the quantification of antigen-specific antibodies and the structural integrity of the protein. The antibody titer is expressed as the interpolated dilution of donor serum at which the optical density (OD) value reaches the cutoff of 0.1 after subtracting the background. The frequency of FL-specific antibodies was calculated as follows:

% antifusion loop antibodies = [1- breathing-dimerW101H / breathing-dimer]*100%

Bulk IgM antibody depletion*

Serum samples, diluted at a 1:3 ratio in PBS, were applied to anti-human IgM agarose beads (Sigma) and allowed to incubate for 1.5 hours at room temperature (RT) in constant rotation. For each depletion round, double the volume of beads than serum was used. These beads had been pre-washed with PBS, and after a 5-minute centrifugation at 400 g, the supernatants were carefully removed. To ensure complete

*With modifications from Santos-Peral et al. 2023 (see Disclaimers on page 8)

IgM removal, two consecutive depletion rounds were carried out. The efficacy of IgM removal was confirmed through YF17D IgM and IgG ELISA assays.

Antigen-Specific IgG depletions*

To deplete antigen-specific IgG antibodies, we made use of the high-affinity binding of the double strep-tag located at the C-terminal end of the recombinant proteins with MagStrep XT beads (IBA). To ensure thorough depletion, a total of three rounds were performed. In each round, 20 µl of beads were first prepared by equilibrating them in a binding buffer (100 mM Tris-HCl, 150 mM NaCl, and 1mM EDTA at pH 8.0) and then conjugated with 5 µg of the recombinant protein for a minimum of 45 minutes at 4°C. Subsequently, unbound protein was removed using a magnetic separator, and the beads were washed with PBS before introducing the serum samples. Typically, the serum samples, which had undergone IgM depletion, were diluted in PBS to achieve a final volume of 160 µl (resulting in a final dilution of 1:7.5), and they were allowed to incubate for 1.5 hours at room temperature on a tube rotator. Depletions were confirmed by IgG ELISA as described above.

ADE of DENV VRP*

DENV-2, strain 16681, Reporter Replicon Particles (VRP) expressing a Gaussia luciferase was kindly provided by Dr. Kümmerer (Lücke et al., 2022).

In a 96-well plate, five serial dilutions for each test serum sample (1:20, $1:10^2$, $1:10^3$, $1:10^4$, $1:10^5$ for cohort samples or 1:50, 1:500, 1:5.000, 1:50.000 for antigen-specific depleted sera), were combined with VRPs at an MOI of 0.5 in uncomplemented RPMI-1640. After a 1-hour incubation at 37°C, 10.000 K562 cells were introduced into each well containing the serum-virus mixture. The cells were then allowed to incubate for an additional two hours at 37°C. Following this incubation period, the cells were washed three times with PBS, resuspended in R10 medium, and left to rest for an additional 72 hours. Supernatants were collected and stored for subsequent measurement. To measure luciferase activity, 20 µl of the sample was used. In each well, 20 µM of Coelenterazine substrate (Carl Roth) was injected and the signal was captured for 10 seconds in a FLUOstar Omega reader (BMG Labtech), following the method previously described (Tannous, 2009).

To account for variations between days and plates, each plate included the same internal control, which was serum from a donor vaccinated against TBEV and YF17D at a dilution 1:100. The test samples were then normalized against this internal control using the following procedure:

$$((\text{Sample-Cells}_{only}) / (\text{VRP}_{only} - \text{Cells}_{only})) / ((\text{control- Cells}_{only}) / (\text{VRP}_{only} - \text{Cells}_{only}))$$

2.4   Recombinant protein production and cloning*

The YF17D Envelope protein ectodomains, which lacked the anchor domains (amino acids 1-397), subdomains, and covalently bound dimers utilized in this research, were generated through recombinant production in stably transfected Drosophila S2 cell lines (Thermo Fisher). To introduce specific mutations site-directed mutagenesis was

*With modifications from Santos-Peral et al. 2023 (see Disclaimers on page 8)

performed using the QuikChange II kit (Agilent, 200523). Specific primers for the mutagenesis reactions were:

W101H	Forward	GATAGAGGCCACGGCAATGGCTGTGGCCTATTTGGG
W101H	Reverse	ACAGCCATTGCCGTGGCCTCTATCAGAATAAGTGCG
S253C	Forward	GGAAACCAGGAAGGCTGCTTGAAAACAG
S253C	Reverse	GAGCTGTTTTCAAGCAGCCTTCCTGG
L107C	Forward	CTGTGGCTGCTTTGGGAAAGG
L107C	Reverse	CCTTTCCCAAAGCAGCCACAG
T311C	Forward	GAACCCATGCGACACTGGC
T311C	Reverse	GCCAGTGTCGCATGGGTTC
N71K	Forward	GTTCTCACTCATGTGAAGATTAAAGACAAGTGCCC
N71K	Reverse	GGGCACTTGTCTTTAATCTTCACATGAGTGAGAAC
A240R	Forward	GAACCTCCGCATGCCCGCACTATCAGAGTACTG
A240R	Reverse	CAGTACTCTGATAGTGCGGGCATGCGGAGGTTC

To produce the protein of interest, a pT350 plasmid containing the desired construct, including a BiP signal sequence at the N-terminus and a double strep-tag at the C-terminus, was co-transfected with a puromycin-resistant plasmid (pCoPuro) (Iwaki et al., 2003) This transfection process was carried out using the Effectene reagent (Qiagen) as per the manufacturer's instructions. Following transfection, cells were subjected to puromycin selection to generate a polyclonal stable cell line expressing the desired protein. Protein expression was induced by the addition of 5 µM $CdCl_2$ in Insect-XPRESS medium from Lonza and was allowed to proceed for 5-7 days. The resulting supernatants were then concentrated and subjected to purification using strep-tactin affinity chromatography columns within an AKTA FPLC system. To distinguish properly folded protein from aggregates, an additional step of size exclusion chromatography was performed, and the elution peaks were validated by SDS-PAGE. The entire process of protein production and purification was confirmed through SDS-PAGE and Western blot analysis, conducted under both reducing and non-reducing conditions. To ensure that the protein had the proper folding and displayed the desired epitopes, the binding of 5A (specific to the FL-proximal region) and 4G2 (specific to FLE) mAbs was assessed. Finally, the purified protein was stored in a solution containing 150 mM NaCl and 10 mM Tris-HCL at pH 8.

2.5   Spectral flow cytometry stainings

For T and B cell analysis, cryopreserved PBMCs were thawed and incubated with Live/dead stain. Next, PBMC were stained with optimized concentrations of surface marker antibodies in the dark for 30 minutes at 37 °C. Cells were then washed twice with FACS buffer. For the intranuclear staining, the cells were fixed/permeabilized with TrueNuclear Fixation Buffer (BioLegend) for 1h at room temperature and protected from light. The cells were then washed twice in TrueNuclear Perm Buffer (BioLegend) and incubated with optimized concentrations of antibodies for 20h at 4°C. Cells were then

---

*With modifications from Santos-Peral et al. 2023 (see Disclaimers on page 8)

washed two more times in the True Nuclear Perm Buffer and fixed with 4% PFA for 10 minutes at room temperature. Antibodies used for the staining are listed in Apendix A. Samples were measured using the Cytek Aurora. Cell populations were gated manually using FlowJo v10. Panels and the gating strategy are found in Apendix A, B and C.

2.5.1 Enzymatic site-directed biotinylation

The biotinylation of the recombinant sE protein was accomplished through an enzymatic BirA ligase reaction (Mclab). 20 µg of sE per reaction were dialysed into Tris-HCl 10mM pH 8. The recombinant sE protein encodes an AviTag peptide at its C-terminus (sequence: GLNDIFEAQKIEWHE), which can be specifically monobiotinylated by the activity of BirA ligase in the presence of 10 mM ATP (Thermo Fisher), 10 mM MgAcCOO (Sigma Aldrich), 10 mM Tris at pH 8, and 2 mM D-Biotin (Sigma Aldrich). The reaction was maintained for 4h at 30°C. Free biotin was removed during the buffer exchange to PBS by dialysis. The success of the biotinylation was confirmed by WB. Following biotinylation, protein was stored at -80 °C.

2.5.2 B cell tetramer staining

The staining of antigen-specific B cells was done as described by Franz et al (Franz et al., 2011). Briefly, the tetramers were prepared freshly on the day of the experiment. Biotinylated sE protein at 1 µg/ml was incubated with fluorochrome-conjugated streptavidin at a molar ratio 4:1 in PBS 4°C for 30 minutes. Tetramers were formed conjugated to PE and APC to allow double-positive identification. Before the addition of the surface antibody markers, the cells are incubated with the pre-formed tetramers for 30 minutes at 37℃. Then, the viability dye was added and the staining protocol continued as described above.

2.5.3 CD4 T cell tetramer staining

Antigen-specific CD4 T cell staining was performed with HLA-peptide tetramers. In this study, four distinct peptide-loaded tetramers were utilized, all of which had previously been confirmed to stain YFV17D specific CD4 T cells (Huber et al., 2020). Two tetramers were used in combination for individuals carrying the HLA-DRB1*0101 allele, specifically targeting NS3 49-65 (HTMWHVTRGAFLVRNGK) and Capsid protein 49-65 (FFFLFNILTGKKITAHL). Additionally, two tetramers were used in combination for individuals with the HLA-DRB1*03:01 allele, specific for E 43-59 (ISLETVAIDRPAEVRKV) and NS1 85-101 (DISVVVQDPKNVYQRGT). These tetramers were produced by the NIH Tetramer Facility located at Emory University in Atlanta. Individuals with HLA-DRB1*03:01 and/or HLA-DRB1*01:01 matching genotypes were selected. Specifically, 62 individuals matched the HLA-DRB1*03:01 genotype, and 45 individuals matched the HLA-DRB1*01:01 genotype, with 10 individuals matching both genotypes. The process of tetramer staining involved a 30-minute incubation at 37°C in RPMI at a concentration of 20 µg/ml, before staining with surface antibody markers. The tetramers were fluorescently labeled with BV421 and APC and double-positive cells were gated as antigen-specific. Subsequent steps of the staining procedure were carried out as described previously.

2.6   *Ex vivo* restimulation of antigen-specific T cells

T cell re-stimulation with YF-17D virus. To measure antigen-specific T cells, cryopreserved PBMC were thawed and rested overnight at high density (5.10^6 million cells per mL) in R10 medium at 37°C in a 5% CO2 humidified atmosphere. PBMC were stimulated at a concentration of 5 million cells/mL in 200 µL. Cells were then incubated with live YF17D virus ($1.5 \ 10^7$ PFU/mL) or with the equivalent volume of purified supernatant of uninfected cells (unstimulated control). PBMC was stimulated for 20 hours and brefeldin A (Biolegend) was added for the last 4 hours of stimulation.

Intracellular Staining of ex vivo re-stimulated samples. The staining of the PBMC starts with the addition of anti-CD107a (clone H4A3, BD Biosciences) for the last 4 h of stimulation. After the stimulation, PBMC were stained for viability (fixable viability dye eFluor™ 780, Thermo Fischer) for 20 minutes in ice. Next, PBMC were blocked for 10 minutes with 10 % human AB serum (Sigma) in FACS buffer (BSA 0.5%, 2 mM EDTA in PBS). Surface staining was done in a blocking buffer with a combination of fluorochrome-labeled anti-human CD4 (clone OKT4, BD BioLegend), CD3 (clone SK7, BD Biosciences), CD8 (clone SK1, BioLegend), CD27 (clone O323, BioLegend), CCR7 (clone G043H7, BioLegend) and CD45RA (clone HI100, Biolegend) markers. Intracellular cytokine staining (ICS) was performed following fixation and permeabilization with Foxp3/Transcription Factor Staining Buffer Set (Invitrogen) for 20 minutes at RT. Cells were stained for 45 minutes with IFN-γ (clone B27, BD Biosciences), TNF-α (clone MAb11, Biolegend) IL-2 (clone MQ1-17H12, BD Biosciences), CD40L (Clone 24-31, BioLegend), IL21 (Clone 3A3-N2, BioLegend) antibodies in permeabilization buffer. Cytokine expression level obtained in the unstimulated control was subtracted in the analysis of YF17D-specific cytokine responses. Flow cytometric analyses were performed using Fortessa (BD) and data was analyzed with Flow Jo (v.10) software.

2.6.1   COMPASS: Combinatorial Polyfunctionality Analysis of Antigen-Specific T-cell Subsets

The functional (FS) and polyfunctional (PFS) score of the antigen-specific T-cell response was estimated using COMPASS analysis (Lin et al., 2015). COMPASS returns the posterior probability of the antigen specificity of each subset and sample provided that the number of counts is superior to five in the stimulated control in at least two of the samples. FS is defined as the proportion of antigen-specific subsets detected among all possible ones whereas PFS weighs the different subsets by their degree of functionality. Six parameters were included for CD4 responses: IL-2, TNFα, IFNγ, IL-21, CD107a, CD40L and four for CD8 responses: IL-2, TNFα, IFNγ, CD107a. The data was analyzed with COMPASSimple package from Bioconductor with a minimum of 100.000 iterations and 8 repetitions.

2.7   BCR repertoire sequencing

Genomic DNA was isolated using the GenElute miniprep kit (Sigma-Aldrich) from approximately 3 million PBMC, following the manufacturer's instructions. The concentration and purity of the genomic DNA were determined using a Nanodrop, and

500 ng of the DNA was subsequently used for VDJ amplification. The genetic loci were amplified in a multiplex PCR using BIOMED2-FR1 primer pools (Brüggemann et al., 2019; van Dongen et al., 2003). For V(D)J amplification, six V gene subgroups and a reverse consensus J primers (Metabion) were employed at a concentration of 5 pmol/µL.

Seq_VH1-FR1_FW	ACACTCTTTCCCTACACGACGCTCTTCCGATCTGGCCTCAGTGAAGGTCTCCTGCAAG
Seq_VH2-FR1_FW	ACACTCTTTCCCTACACGACGCTCTTCCGATCTGTCTGGTCCTACGCTGGTGAAACCC
Seq_VH3-FR1_FW	ACACTCTTTCCCTACACGACGCTCTTCCGATCTCTGGGGGGTCCCTGAGACTCTCCTG
Seq_VH4-FR1_FW	ACACTCTTTCCCTACACGACGCTCTTCCGATCTCTTCGGAGACCCTGTCCCTCACCTG
Seq_VH5-FR1_FW	ACACTCTTTCCCTACACGACGCTCTTCCGATCTCGGGGAGTCTCTGAAGATCTCCTGT
Seq_VH6-FR1_FW	ACACTCTTTCCCTACACGACGCTCTTCCGATCTTCGCAGACCCTCTCACTCACCTGTG
Seq_JH_RV	TGACTGGAGTTCAGACGTGTGCTCTTCCGATCTCTTACCTGAGGAGACGGTGACC

The PCR reaction was carried out using high-fidelity Phusion Hot Start II DNA Polymerase (NEB) with the following cycling conditions: 2 minutes at 98°C, followed by 30 cycles of 98°C for 30 seconds, 65°C for 30 seconds, and 72°C for 40 seconds, and a final extension step at 72°C for 10 minutes. PCR products were purified through gel extraction using the NucleoSpin Gel and PCR Clean-Up Kit (Macherey-Nagel). For the subsequent step, 2 µL of each amplicon, containing 8 nt barcodes, were subjected to a second PCR reaction. This reaction included the incorporation of Illumina i501 and i701 adaptors and followed these cycling conditions: 98°C for 30 seconds, 5 cycles of 98°C for 10 seconds, 52.2°C for 30 seconds, and 72°C for 30 seconds, followed by 20 cycles of 98°C for 10 seconds, 63.5°C for 30 seconds, and 72°C for 30 seconds, and concluding with a final extension at 72°C for 10 minutes. These primers were defined by Schmid-Burgk et al. (Schmid-Burgk et al., 2014):

Illu fwd1	AATGATACGGCGACCACCGAGATCTACACTATAGCCTACACTCTTTCCCTACACGACGCT
Illu fwd2	AATGATACGGCGACCACCGAGATCTACACATAGAGGCACACTCTTTCCCTACACGACGCT
Illu fwd3	AATGATACGGCGACCACCGAGATCTACACCCTATCCTACACTCTTTCCCTACACGACGCT
Illu fwd4	AATGATACGGCGACCACCGAGATCTACACGGCTCTGAACACTCTTTCCCTACACGACGCT
Illu fwd5	AATGATACGGCGACCACCGAGATCTACACAGGCGAAGACACTCTTTCCCTACACGACGCT
Illu fwd6	AATGATACGGCGACCACCGAGATCTACACTAATCTTAACACTCTTTCCCTACACGACGCT
Illu fwd7	AATGATACGGCGACCACCGAGATCTACACCAGGACGTACACTCTTTCCCTACACGACGCT
Illu fwd8	AATGATACGGCGACCACCGAGATCTACACGTACTGACACACTCTTTCCCTACACGACGCT
Illurev1	CAAGCAGAAGACGGCATACGAGATCGAGTAATGTGACTGGAGTTCAGACGTGTGCT
Illurev2	CAAGCAGAAGACGGCATACGAGATTCTCCGGAGTGACTGGAGTTCAGACGTGTGCT
Illurev3	CAAGCAGAAGACGGCATACGAGATAATGAGCGGTGACTGGAGTTCAGACGTGTGCT
Illurev4	CAAGCAGAAGACGGCATACGAGATGGAATCTCGTGACTGGAGTTCAGACGTGTGCT
Illurev5	CAAGCAGAAGACGGCATACGAGATTTCTGAATGTGACTGGAGTTCAGACGTGTGCT
Illurev6	CAAGCAGAAGACGGCATACGAGATACGAATTCGTGACTGGAGTTCAGACGTGTGCT
Illurev7	CAAGCAGAAGACGGCATACGAGATAGCTTCAGGTGACTGGAGTTCAGACGTGTGCT
Illurev8	CAAGCAGAAGACGGCATACGAGATGCGCATTAGTGACTGGAGTTCAGACGTGTGCT
Illurev9	CAAGCAGAAGACGGCATACGAGATCATAGCCGGTGACTGGAGTTCAGACGTGTGCT
Illurev10	CAAGCAGAAGACGGCATACGAGATTTCGCGGAGTGACTGGAGTTCAGACGTGTGCT
Illurev11	CAAGCAGAAGACGGCATACGAGATGCGCGAGAGTGACTGGAGTTCAGACGTGTGCT
Illurev12	CAAGCAGAAGACGGCATACGAGATCTATCGCTGTGACTGGAGTTCAGACGTGTGCT

Following gel electrophoretic separation, DNA was quantified using the QuantiFluor® dsDNA System (Promega) and assessed for quality on the Bioanalyzer using the DNA D1000 ScreenTape (Agilent). Subsequently, the samples were pooled to achieve a final concentration of 4 nM before undergoing NGS on the MiSeq V3 platform with 300X2 Illumina sequencing. The alignment of the fastq data to the genome was performed using Mixcr version 3.0.13 with the library imgt.202141-1.sv7.json by Edith Willscher at Halle University. Non-productive reads and sequences with fewer than 2 read counts were excluded from further analysis. Each unique complementarity-determining region 3 (CDR3) nucleotide sequence, along with the use of the same V gene, was defined as one clonotype. Data analysis was conducted using R, employing Immunarch (Samokhina et al., 2022) in combination with self-written code.

2.8   Statistical analysis

Multivariate linear regression analysis. Before linear model implementation, data used as dependent variables was adequately transformed as follows: 1) Replacing 0 values with half the value of the smallest value for each parameter; 2) Normalizing the data using the Box-Cox transformation approximation, which was performed using the "fpp" package in R. The multivariate regression analysis was performed in R (V 4.3.1) using the lm function from "stats" package and, unless they were the variable in question, the model included as covariates CMV infection status, age, sex, year of study inclusion, and, if necessary, the analysis batch of the corresponding variable. Comparisons were checked for homoscedasticity. Confidence intervals were calculated with a likelihood profile method. Information retrieved from the model was re-transformed to the original units and fold-changes were estimated as: (intercept + estimate)/intercept. A Benjamini-Hochberg procedure was implemented to adjust p-values for multiple hypothesis testing per analysis group.

Batch correction Flow cytometry data was corrected for batch effects before clustering or plotting. Briefly, 0 values were replaced with half the value of the smallest value for each parameter. The data was then normalized using the BoxCox approximation (package "fpp" in R) before adjusting for batch effects using ComBat ("sva" package in R). Data was then retransformed back to the original units inverting the BoxCox transformation.

Hierarchical clustering Data were scaled and clustered using hierarchical clustering with Ward's minimum variance method based on a similarity measure of Euclidean distance applied to normalized data. The optimal number of clusters was determined by the NbClust function (index = all) in R. The visualization was performed by factoextra R packages. Heatmaps were created using the ComplexHeatmap R package.

Other statistics. Determination of statistical significance included the Chi-square test, Wilcoxon Rank Sum test, and Spearman correlations. For radar plots, data was scaled, and student's t-test or ANOVA was used to test the significance. Other tests are indicated in the figure captions.

3. Results

3.1 Grouping of study subjects based on prior TBEV vaccination status*

250 healthy young individuals (81 male and 169 female; age 19-47 years, median 24) previously unvaccinated for JEV and YFV, were recruited for the study. Blood samples were collected longitudinally at baseline and on days 3, 7, 14, and 28 post-vaccination (pv) with the live attenuated YF17D vaccine (Stamaril) (Figure 2).
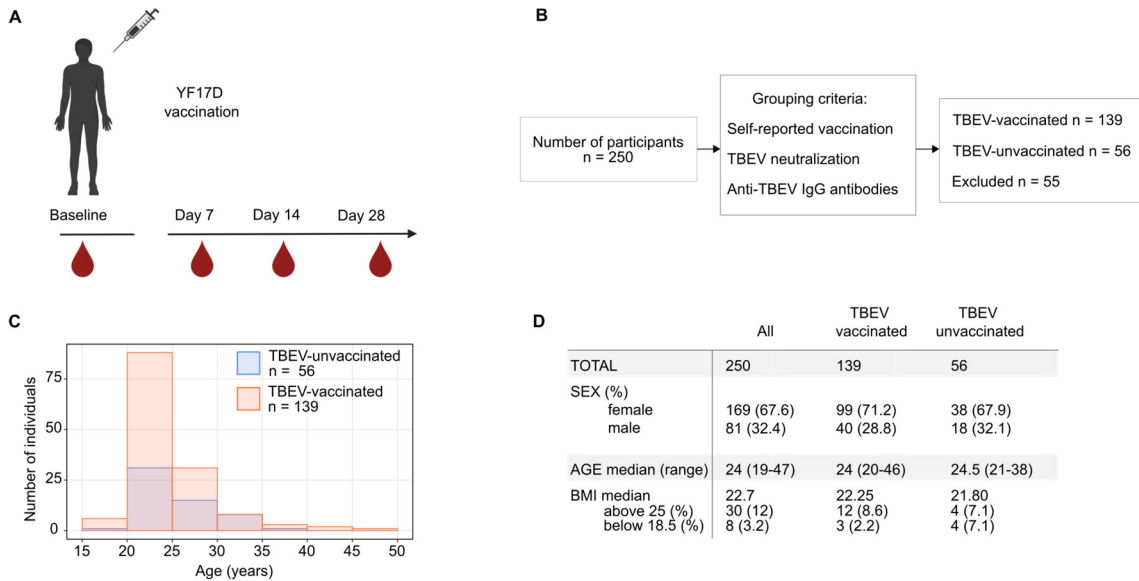
Figure 2. Study cohort characteristics.

A) PBMC, serum, and plasma samples were collected at baseline (before inoculation with the YF17D vaccine) and on days 7, 14, and 28 after vaccination.
B) 250 study participants were grouped based on prior vaccination status with the TBEV vaccine determined by self-reported vaccination history, their capacity to neutralize TBEV, and the presence of anti-TBEV IgG antibodies at baseline. The final grouping included 139 TBEV-vaccinated individuals and 56 TBEV-unvaccinated individuals.
C) Histogram depicting the age distribution of TBEV-pre-vaccinated and unvaccinated donors.
D) Table for sex, age, and BMI distribution for all participants and TBEV-vaccinated and unvaccinated subgroups.
Figure and figure legend modified from Santos-Peral et al. 2023 (see Disclaimers on page 8)

To investigate the effects of pre-existing immunity induced by TBEV vaccination on the response to the YF17D vaccine, the study participants were categorized retrospectively based on their previous vaccination status with the inactivated TBEV vaccine. In addition to the self-reported vaccination status, TBEV pre-immunity was confirmed by a positive result for an in-house TBEV neutralization assay (performed by Fabian Luppa and Dr. Michael Pritsch) and by the presence of anti-TBEV IgG antibodies in an enzyme-linked immunosorbent assay (ELISA) utilizing TBEV-DIII as the antigen. Individuals for which the self-reported pre-vaccination status contradicted the experimental validation were excluded as "unknown" from the analysis. Since the study was conducted in Bavaria, a German region where the TBEV vaccine is recommended, a significant number of the cohort had received at least one dose of a TBEV vaccine prior to study inclusion (139 TBEV positive, 56 TBEV negative and 55 unknown) (Figure 2B). This strict grouping is kept

---

*With modifications from Santos-Peral et al. 2023 (see Disclaimers on page 8)

throughout the rest of this dissertation. Even though it is possible to infer the pre-vaccination status of the 55 individuals classified as unknown, this grouping criteria ensures with high reliability the negativity for any previous flavivirus exposure in the TBEV-unvaccinated group, including a potential natural infection with DENV, WNV, or any other flavivirus that may have occurred before the initiation of this study. On the other hand, it also guarantees a correct determination for TBEV-pre-vaccinated individuals although, in this group, given the high antibody cross-reactivity among flaviviruses, we cannot be certain of the absence of prior flavivirus immunity resulting from a natural infection with DENV, ZIKV or other.

The specific vaccine (Encepur® or FSME-Immun), the number of doses, and the schedule for administering the TBEV vaccine were not recorded. As a result, TBEV-pre-vaccinated individuals showed considerable diversity in their IgG titer and levels of neutralizing antibodies against TBEV (data not shown). This situation, however, presents an added advantage in understanding the potential influence of pre-existing cross-reactive antibodies on the subsequent YF17D vaccination.

3.2 Effect of prior immunity to TBEV on the humoral response to the YF17D vaccine

3.2.1 TBEV pre-vaccination does not alter the neutralization response induced by YF17D, which is predominantly mediated by IgM antibodies, but it leads to higher IgG levels with limited neutralizing capacity*

The neutralizing antibody titer is the gold-standard correlate of vaccine-induced protection and is commonly used as an indicator of vaccine immunogenicity. The neutralizing antibody titer induced by YF17D was determined by FluoRNT (Scheck et al., 2022) by Lisa Lehmann (see disclaimer page 8). The YF17D vaccine induced a neutralizing response in all study participants as early as day 14 pv, which continued to increase by day 28 pv. The neutralizing antibody titer was equally strong in TBEV-unvaccinated and pre-vaccinated individuals indicating that TBEV-induced pre-immunity did not impair the neutralizing response to YF17D (Figure 3A).

To quantify the antigen-specific IgG serum levels induced upon YF17D vaccination, a recombinantly produced soluble E protein (sE), which contains the three ectodomains but lacks the stem and transmembrane domains, was used as antigen, and samples were measured longitudinally by ELISA. TBEV-pre-vaccinated study participants showed YF17D cross-reactive IgG antibodies at baseline and, upon vaccination, the IgG levels were further increased resulting in a 100-fold higher titer compared to the TBEV-unvaccinated group (Figure 3B). The expansion of anti-sE IgG antibodies started on day 14 pv for individuals with prior TBEV vaccination, while only a fraction of the TBEV-unvaccinated individuals showed detectable IgG levels at that timepoint, which indicates a more rapid response in individuals with pre-existing flavivirus immunity. The vaccine-induced IgG levels continued to increase by day 28 pv, at which point seroconversion was detectable for all the study participants (Figure 3B).

---

*With modifications from Santos-Peral et al. 2023 (see Disclaimers on page 8)

The remarkable difference in the sE-specific IgG levels on day 28 between individuals with and without TBEV-immune experience contrasts with the similar neutralization capacity observed in both groups. The IgG antibody titer on day 28 correlated weakly with the neutralization capacity (R = 0.29, p = 0.04 for TBEV-unvaccinated and R = 0.34, p < 0.0001 for TBEV-pre-vaccinated) (Figure 3C). Taken together, these results suggest that even though pre-immunization with the TBEV vaccine induced an IgG response that cross-reacts with YF17D, it did not hinder the generation of an effective neutralization response upon YF17D vaccination. In addition, TBEV-pre-immunized individuals elicited an earlier and stronger IgG response with limited neutralizing capacity.
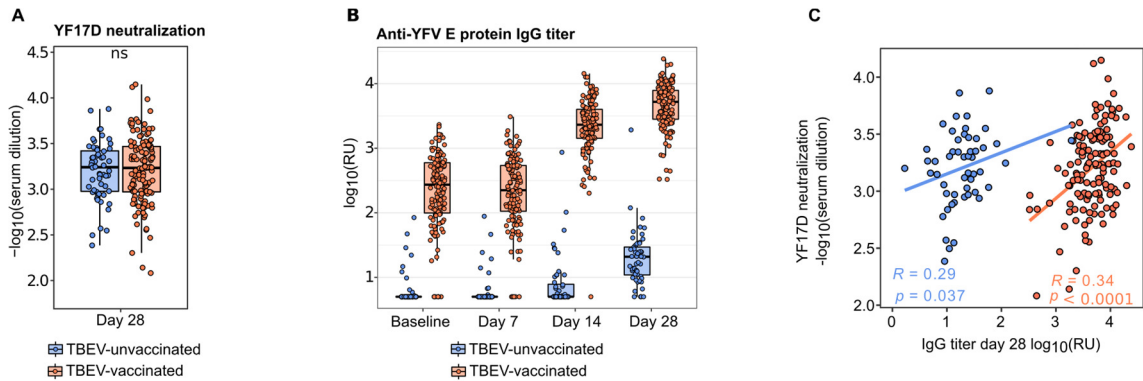
Figure 3. YF17D-induced neutralizing responses and anti sE-IgG antibodies in TBEV-vaccinated and unvaccinated individuals

A) YF17D 80% neutralization titer on day 28 (measured by Lisa Lehmann, disclaimer page 5)
B) Longitudinal anti-YF17D sE IgG titer in donor´s sera. Titer was estimated in Relative Units (RU) from a standard control given 10,000 arbitrary antibody units (AU)
C) Spearmann correlation of the IgG antibody titer against sE at day 28 with the neutralization titer at day 28.
TBEV-vaccinated individuals are depicted in orange and TBEV-unvaccinated donors in blue. Statistical significance in A was calculated with a Wilcoxon–Mann–Whitney test. Significance is depicted as follows: * p<0.05, ** p<0.01,*** p<0.001, **** p<0.0001. Figure and figure legend modified from Santos-Peral et al. 2023 (see Disclaimers on page 8)

The observed differences in the IgG titer did not correspond with a proportionally stronger neutralizing response in TBEV-pre-vaccinated individuals. To better define the capacity of the IgG fraction to neutralize, the neutralizing antibody titers were recalculated on donor sera depleted of IgM antibodies. IgM depletion resulted in a loss of approximately one order of magnitude on day 28 (Figure 4 A-B). The remaining neutralizing capacity was significantly higher in TBEV-pre-vaccinated individuals, indicating that the highly expanded IgG levels in this group could contribute, although weakly, to neutralization (Figure 4B). This slight benefit in neutralization was only apparent in the absence of IgM antibodies and was not proportional to the difference in the IgG levels in serum.

Altogether, on day 28 pv, the IgM antibody response had the most prominent neutralizing potential, accounting for 75% of the neutralizing capacity in both groups of vaccinees. The YF17D vaccine-induced IgG response can mediate neutralization, but the IgG fraction that is greatly expanded in TBEV-pre-vaccinated individuals has a poor neutralizing potential.

*With modifications from Santos-Peral et al. 2023 (see Disclaimers on page 8)
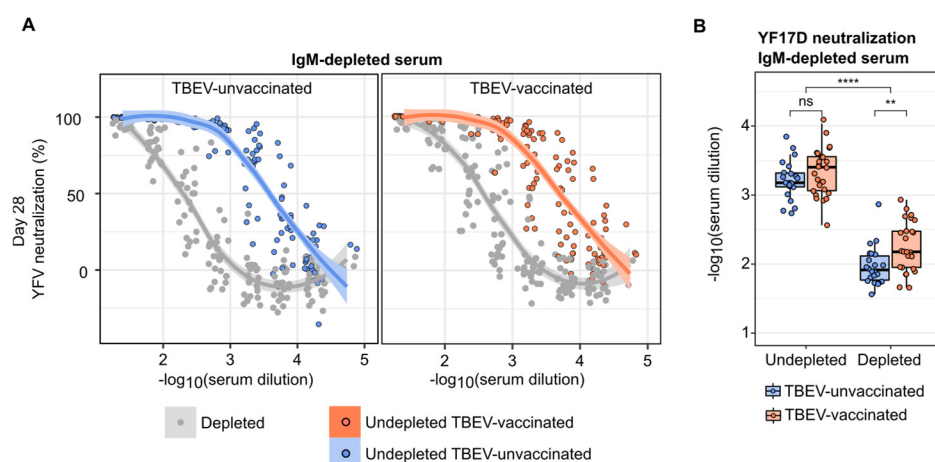
Figure 4. IgG-mediated YF17D neutralization

A) YF17D neutralization curves from TBEV-vaccinated and TBEV-unvaccinated individuals using serially diluted and IgM-depleted sera.

B) Comparison of the YF17D 80% neutralization titer for undepleted and IgM-depleted sera in the TBEV-vaccinated and unvaccinated participants shown in A

TBEV-vaccinated individuals (n = 26) are depicted in orange and TBEV-unvaccinated donors (n = 22) in blue. Curve fitting in A was calculated with local regression. Statistical differences between TBEV-vaccinated and unvaccinated individuals in B were calculated with a Wilcoxon–Mann–Whitney test and with a paired Wilcoxon signed-rank test for comparing undepleted with IgM-depleted conditions. Significance is depicted as follows: * p<0.05, ** p<0.01,*** p<0.001, **** p<0.0001. Figure and figure legend modified from Santos-Peral et al. 2023 (see Disclaimers on page 8)

3.2.2 Dissection of the YF17D epitope specificity of the IgG response*

Depending on the pre-vaccination status with TBEV, YF17D induced remarkable differences in the serum IgG titers. Nevertheless, both TBEV-unvaccinated and vaccinated individuals elicited an IgG response capable of effectively neutralizing YF17D. Investigating the same cohort, Fabian Luppa found that, following YF17D vaccination, TBEV-vaccinated individuals expanded a pan-flavivirus cross-reactive response whereas TBEV-unvaccinated elicited a non-cross-reactive response targeting uniquely YFV (Santos-Peral et al., 2023). These observations illustrate a shift in the vaccine epitope immunodominance resulting in different IgG antibody signatures targeting different epitopes. I hypothesized that the neutralizing antibodies preferentially target dimeric specificities or epitopes comprehending complex quaternary structures in the mature YF17D virion, akin to EDE, whereas the cross-reactive antibodies predominantly target the highly conserved FLE. Other neutralizing sites are likely to be found in the FL-proximal region and DIII. To test this hypothesis, a set of recombinant sE protein mutants displaying different epitopes was designed.

3.2.2.1 Toolbox: Recombinant proteins for the dissection and functional analysis of different antibody specificities*

In addition to the sE protein exposing the three ectodomains in a monomeric conformation, DI-II and DIII were produced separately (Figure 5 A-B). Additionally, constructs displaying quaternary dimeric epitopes, that more closely reproduce the epitope landscape of YF17D, were designed. The substitution S253C introduces a

---

*With modifications from Santos-Peral et al. 2023 (see Disclaimers on page 8)

cysteine in DII, within a region that comes into contact with the alternative protomer in the dimer. This modification enabled the formation of a disulfide bond, covalently binding both protomers and resulting in the formation of a stable dimer in solution (Crampon et al., 2023). This construct (hereinafter, breathing-dimer) displays quaternary dimeric epitopes. The breathing-dimer construct can oscillate dynamically (breathing) replicating the natural oscillating conformation that the E protein adopts in mature virions. This way, the breathing-dimer transiently exposes the FLE and all other monomeric epitopes as well as the FL-proximal epitope. In this setting, an additional mutation in W101H was introduced to disrupt the FLE (breathing-dimer[W101H]) (Figure 5C). Alternatively, the substitutions L107C and T311C allow the formation of a disulfide bond connecting DIII with DI-II of the opposing protomer. These modifications resulted in a stable dimer in pre-fusion conformation (locked-dimer). This strategy was used previously by Rouvinski et al. (Rouvinski et al., 2017) and Slon-Campos et al. (Slon-Campos et al., 2019) with DENV and ZIKV respectively, creating immunogens with the capacity to expose EDE while concealing FLE. In the locked dimer setting, two additional mutations were included, N71K (locked-dimer[N71K]) and A240R (locked-dimer[N71K,A240R]). The N71K substitution was mapped by Daffis et al (Daffis et al., 2005) in escape viral variants to a highly neutralizing monoclonal antibody which was found to bind a dimeric specificity. The recently published crystal structure of 5A also highlighted N71 as an important binding site (Lu et al., 2019). By introducing the A240R mutation, a large charged side chain is introduced in the ij loop, a location required for EDE-specific antibody binding (Figure 5A and D). Therefore, the mutations N71K and A240R were intended to disrupt an EDE-like epitope found in YF17D.

To validate the proper folding of the antigens as well as their binding capacity to mAb, an ELISA was used to test FLE and 5A-epitope display. W101H successfully prevented the binding of the pan-flavivirus FL-specific 4G2 antibody and reduced the binding of 5A in the breathing-dimer[W101H]. 5A bound to breathing-dimer and sE monomer but it did not bind the locked-dimer. Contrary to our expectations, the locked-dimer construct already failed to display the 5A-binding epitope as well as FLE. Given that both of these epitopes overlap with EDE, the locked-dimer construct might not be suitable for displaying complex quaternary epitopes (Figure 5 E-F).

3.2.2.2 YF17D epitope immunodominance is skewed in TBEV-pre-vaccinated donors towards the FLE*

The comparison between the IgG binding to the breathing—dimer and the breathing-dimer[W101H] served to quantify the IgG fraction directed against FLE and other specificities using the FL as a binding site. Notably, when compared to the breathing-dimer, the titer of IgG antibodies binding the breathing-dimer[W101H] was significantly reduced in baseline samples and in TBEV-pre-vaccinated individuals on day 28. In contrast, there were no significant differences in the levels of IgG antibodies binding to the breathing-dimer with or without a disrupted FLE in TBEV-unvaccinated individuals (Figure 6A). Correspondingly, the sE-specific IgG titer present in serum was quantified in binding competition with the pan-flavivirus FL-specific 4G2 monoclonal antibody. As expected, TBEV-pre-vaccinated serum samples exhibited over 80% binding competition with 4G2, both

*With modifications from Santos-Peral et al. 2023 (see Disclaimers on page 8)
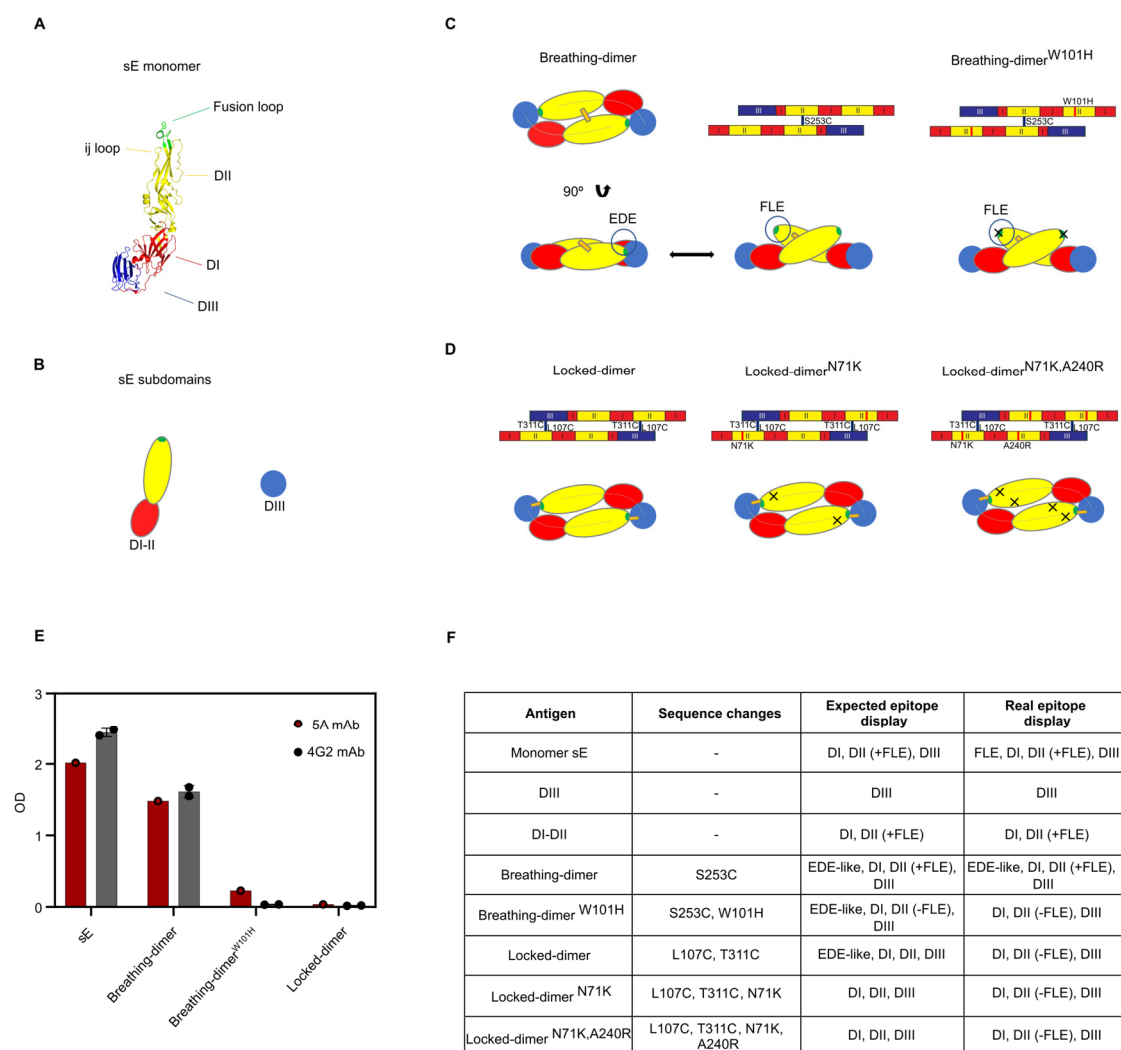
Figure 5. Toolbox for dissecting the specificities of the IgG response.

A) Illustration of the structure of sE. PDB: 6IW4 edited using Pymol.

B) Representation of DI-II, and DIII, produced separately.

C) Illustration of the folded breathing-dimer structure and its expected dynamic breathing together with the linear sequence depiction with the added mutations to form the dimer (S253C) and to disrupt the FLE (W101H)

D) Representation of the locked-dimer structure and the added mutations to form the dimer (L107C and T311C) in addition to mutations to potentially disrupt the EDE-like epitope (N71K and A240R)

E) Binding of the recombinantly produced proteins to 4G2 and 5A mAb by ELISA.

Table summarizing the recombinant proteins of the toolbox, the mutations introduced, the expected epitopes displayed, and the experimentally determined epitopes displayed (real epitope specificities) Figure and figure legend modified from Santos-Peral et al. 2023 (see Disclaimers on page 8).

Antigen	Sequence changes	Expected epitope display	Real epitope display
Monomer sE	-	DI, DII (+FLE), DIII	FLE, DI, DII (+FLE), DIII
DIII	-	DIII	DIII
DI-DII	-	DI, DII (+FLE)	DI, DII (+FLE)
Breathing-dimer	S253C	EDE-like, DI, DII (+FLE), DIII	EDE-like, DI, DII (+FLE), DIII
Breathing-dimer [W101H]	S253C, W101H	EDE-like, DI, DII (-FLE), DIII	DI, DII (-FLE), DIII
Locked-dimer	L107C, T311C	EDE-like, DI, DII, DIII	DI, DII (-FLE), DIII
Locked-dimer [N71K]	L107C, T311C, N71K	DI, DII, DIII	DI, DII (-FLE), DIII
Locked-dimer [N71K,A240R]	L107C, T311C, N71K, A240R	DI, DII, DIII	DI, DII (-FLE), DIII

at baseline and on day 28 post-vaccination. In contrast, flavivirus-unexperienced individuals showed a reduction of binding that ranged between 0-60% in competition with 4G2 (Figure 6B). Consistently, the binding loss caused by the W101H mutation correlated with the competition against 4G2 at both baseline and day 28 pv (R = 0.69, p = 0.0004 and R = 0.65, p = 0.0012, respectively) (Figure 6C). Collectively these results demonstrate that the FLE is a dominant binding site for the antibody response in TBEV-experienced individuals, but not in TBEV-unvaccinated individuals.

*With modifications from Santos-Peral et al. 2023 (see Disclaimers on page 8)
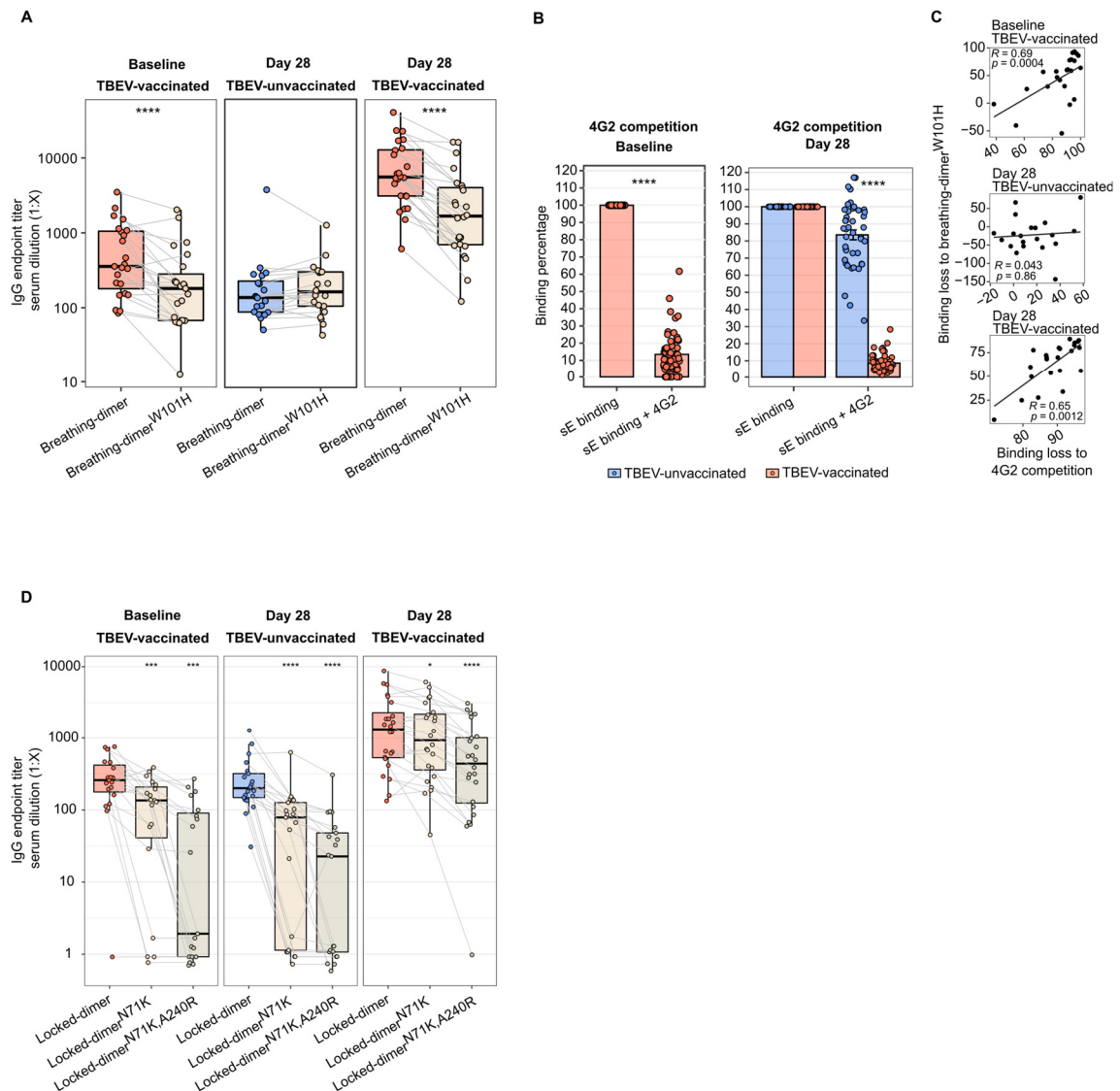
Figure 6. Dissection of the IgG epitope specificity

A) IgG endpoint titer for breathing-dimer and breathing-dimer[W101H] at baseline and on day 28 for TBEV-pre-vaccinated and TBEV-unvaccinated donors.

B) Percentage of IgG antibody binding to sE in competition with 4G2 mAb for baseline samples (left) and on day 28 pv (right)

C) Spearman correlation between the antibody binding loss observed in A with the loss quantified in B for TBEV-pre-vaccinated baseline samples and TBEV-pre-vaccinated and unvaccinated samples on day 28.

D) IgG endpoint titer directed against the locked-dimer, locked-dimer[N71K], and locked-dimer[N71KA240R] at baseline and on day 28 pv for TBEV pre-vaccinated and unvaccinated donors

For A and D, a subgroup of the study cohort was used (TBEV-vaccinated = 24, TBEV unvaccinated = 24). For B, all the study cohort was assessed. TBEV-vaccinated individuals are depicted in orange and TBEV-unvaccinated donors in blue. Statistical significance was calculated with a Wilcoxon–Mann–Whitney test for B and a paired Wilcoxon signed-rank test for A and D. Significance is depicted as follows: * $p<0.05$, ** $p<0.01$, *** $p<0.001$, **** $p<0.0001$. Figure and figure legend modified from Santos-Peral et al. 2023 (see Disclaimers on page 8)

Additionally, even though the antigens based on the locked-dimer setting failed to replicate the intended epitope display, a fraction of the IgG response was found to be specific for these constructs which still displayed monomeric epitopes other than FLE and FL-proximal and conventional EDE. Interestingly, the IgG titer targeting the locked-

dimer was 10-fold lower than for the breathing-dimer in TBEV-experienced individuals, likely given the high abundance of FLE-specific antibodies. A reduction in antibody levels targeting locked-dimer[N71K] and locked-dimer[N71KA240R] compared to the unmutated locked-dimer was apparent for TBEV-pre-vaccinated baseline samples and in both groups of vaccinees on day 28, particularly in the TBEV-unvaccinated group (Figure 6D). This observation suggests a differential direction of the antibody response other than FLE in which TBEV-unvaccinated individuals depend more on N71 to mount responses.

3.2.2.3 TBEV-pre-vaccination does not alter the generation of neutralizing antibodies that predominantly target dimeric quaternary epitopes*

The hyperexpanded IgG response towards the immunodominant FLE in TBEV-pre-vaccinated individuals did not explain the similar IgG-mediated neutralizing capacity in both groups. To identify the main neutralizing sites targeted by the IgG response, that presumably mediates the long-term protection, antigen-specific IgG depletions were performed in IgM-depleted sera. The different recombinant antigens were bound to strep-tactin-coated magnetic beads allowing antigen-specific IgG depletions, after which the remaining IgG antibody fraction was assessed for neutralization (Figure 7A).

As previously observed, IgM depletion from sera resulted in a great reduction of the neutralizing capacity. Further depletion with the breathing-dimer, which displays all the intra-dimeric and monomeric epitopes, significantly reduced the neutralizing capacity to a similar extent in TBEV-pre-vaccinated and unvaccinated individuals. The neutralizing capacity was recovered almost completely when the antigen used for depletions contained the disrupted FL W101H substitution. These results indicate that W101 in the FL serves as a binding site for the neutralizing IgG fraction targeting the dimer (Figure 7 left panel). To evaluate the existence and the neutralizing potential of dimer-antibodies, akin to EDE, antigen-specific IgG depletions were performed with DI-II and DIII subsequently. To this end, the use of full-length sE might have resulted in the unwanted depletion of EDE-like antibodies since IgG may assemble monomeric sE into dimers in solution (Slon-Campos et al., 2019). Sera depleted with DI-II had a significant loss of neutralizing capacity which could be potentially attributed to the depletion of both FL and FL-proximal antibodies. Nevertheless, DI-II and DIII failed to abrogate the neutralizing capacity of the remaining IgG fraction to the same extent as the breathing-dimer construct, indicating the central role of dimeric epitopes for effective neutralization (Figure 7 middle panel). The depletion with the locked dimer, which does not expose the FL and FL-proximal epitopes, resulted only in a slight decrease in neutralizing capacity. Further depletions with locked-dimer[N71K] or locked-dimer[N71KA240R] did not decrease the neutralizing capacity to a greater magnitude than the unmutated locked-dimer, demonstrating that these constructs are not exposing EDE-like epitopes, which remained in the undepleted fraction (Figure 7 right panel)

Taken together, these results highlight that the effective removal of neutralizing antibodies requires the FL and dimer oligomeric structures. Besides, neutralizing antibodies were produced against both monomeric or dimeric sites independently of prior TBEV vaccination.

---

*With modifications from Santos-Peral et al. 2023 (see Disclaimers on page 8)
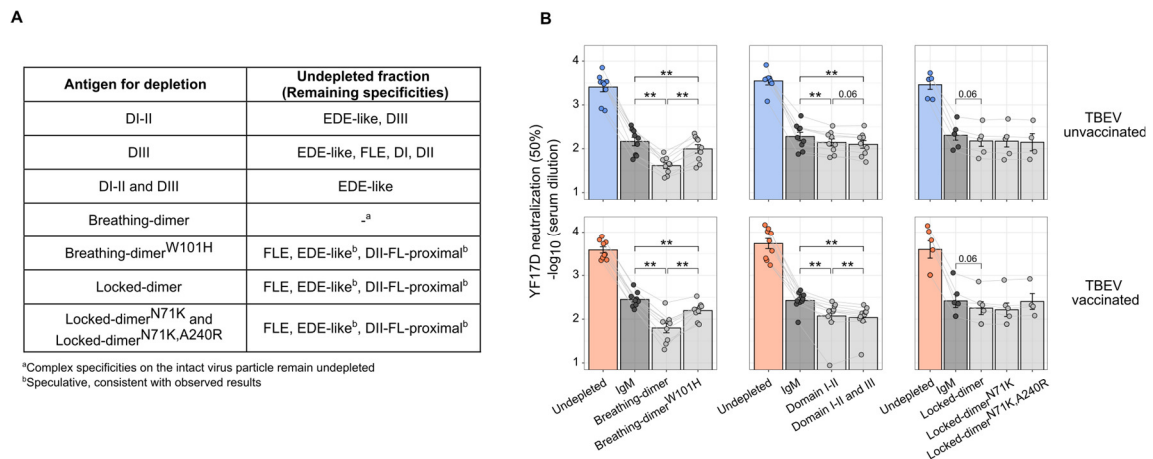
Figure 7. Neutralizing potential of different IgG specificities.

A) Summary table for the recombinant antigens used for antigen-specific IgG depletions and the expected specificities of the remaining undepleted fraction assessed for neutralization.

B) YF17D 50 % neutralization titer in undepleted, IgM-depleted, and antigen-specific IgG-depleted sera for TBEV-vaccinated (n =10) and unvaccinated (n = 10) donors. For locked-dimer-specific depletions, only 5 individuals were tested per group

Statistical significance was calculated with a paired Wilcoxon signed-rank test. Significance is depicted as follows: * $p<0.05$, ** $p<0.01$, *** $p<0.001$, **** $p<0.0001$. Figure and figure legend modified from Santos-Peral et al. 2023 (see Disclaimers on page 8)

3.2.2.4 YF17D vaccination expands cross-reactive IgG antibodies directed against the FLE with potential to mediate ADE of DENV infection in TBEV-pre-vaccinated individuals*

Individuals previously vaccinated against TBEV exhibited an IgG response directed towards the pan-flavivirus FLE following YF17D vaccination. These FLE antibodies are well-documented mediators of ADE during DENV infection (Beltramello et al., 2010). The potential of the polyclonal sera to mediate enhanced infection of DENV was addressed on K562 cells with viral reporter replicon particles (VRP) in vitro.

In contrast to TBEV-unvaccinated individuals, serum samples from TBEV-pre-vaccinated individuals enhanced the infection of DENV via ADE. After implementing the previously mentioned depletion strategy, the specific removal of antigens using DI-II and breathing-dimer effectively eliminated the enhancing capability observed in the non-depleted IgG fraction. Conversely, sera depleted using any of the locked-dimer constructs or the breathing-dimer[W101H] variant retained ADE capacity (Figure 8).

These results identify FLE-specific IgG antibodies as mediators of ADE of DENV infection in TBEV-pre-vaccinated individuals. Serum from flavivirus-naïve individuals did not facilitate DENV infection following YF17D vaccination, consistent with the lack of cross-reactive antibodies in these individuals. In TBEV-unvaccinated donors, YF17D seemed to conveniently conceal cross-reactive epitopes while priming for an effective neutralizing response.

*With modifications from Santos-Peral et al. 2023 (see Disclaimers on page 8)
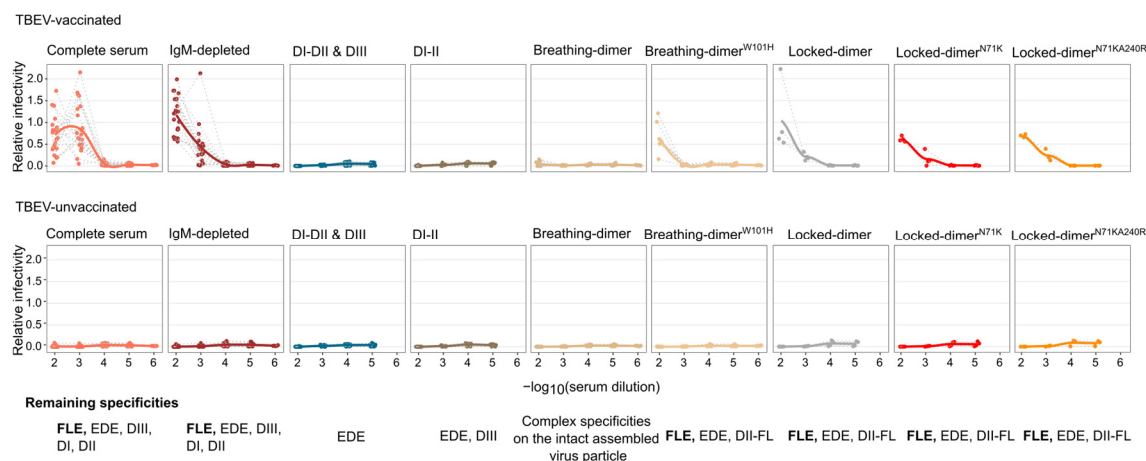
Figure 8. IgG specificities mediating ADE of DENV infection after YF17D vaccination

Antibody-dependent-enhancement of DENV2 VRP infection of TBEV pre-vaccinated and TBEV-unvaccinated samples. Serum was tested directly, after IgM depletion and antigen-specific IgG depletion with the following antigens: subsequent DI-II and DIII (monomer), DI-II only, breathing-dimer, breathing-dimer[W101H], Locked-dimer, locked-dimer[N71K], locked-dimer[N71KA240R]. The remaining IgG specificities in the undepleted fraction are indicated below the corresponding graph. Figure and figure legend modified from Santos-Peral et al. 2023 (see Disclaimers on page 8)

3.3 TBEV-pre-vaccination effect on vaccine immunogenicity and adaptive cellular immunity

In individuals with pre-existing immunity, various mechanisms may potentially act in concert. In addition to the expansion of pre-existing MBC clones induced by the TBEV vaccine, equivalent to an anamnestic response, cross-reactive antibodies may also play a role in modulating the GC reaction. This modulation can occur through the masking or exposure of cognate epitopes and the regulation of the activation thresholds for B cell selection (Muecksch et al., 2022; Schaefer-Babajew et al., 2023). In addition, Chan et al (2016) showed that individuals vaccinated against JEV generated cross-reactive antibodies that enhanced the immunogenicity of YF17D via ADE (Chan et al., 2016). We had shown that TBEV-pre-vaccinated individuals could facilitate YF17D infection of Fcγ-R expressing cell lines (experiments performed by Sebastian Goresch)(Santos-Peral et al., 2023). Therefore, I hypothesized that individuals pre-vaccinated with TBEV might simultaneously undergo different processes caused by pre-existing immunity. Firstly, an anamnestic response could have led to a quicker and stronger immune reaction, particularly against previously encountered epitopes. Secondly, there may be an enhanced immune response against YF17D, mediated by ADE. Both phenomena may be affecting not only the antibody response but also the cellular memory T-cell response.

3.3.1.1 Broader diversity of antibody targets and enhanced immunogenicity of the YF17D vaccine in TBEV-pre-vaccinated individuals*

Individuals pre-vaccinated against TBEV consistently exhibited higher IgG levels against all the different constructs of our toolbox. This observation extends to DIII, which lacks the immunodominant and cross-reactive FLE. In line with our previous observation, antigens displaying the FLE, like sE, YF17D virion, and the breathing-dimer captured an IgG response two orders of magnitude higher in TBEV-pre-vaccinated individuals on day

*With modifications from Santos-Peral et al. 2023 (see Disclaimers on page 8)

28. In addition, TBEV-pre-vaccinated individuals also exhibited higher antibody titers against constructs that either concealed or lacked the FLE, such as the breathing-dimer[W101H], all the locked dimer constructs and DIII. These results suggest that the IgG levels in serum of TBEV-pre-vaccinated donors were elevated across a broader range of specificities than just the dominant FLE (Figure 9A-B).
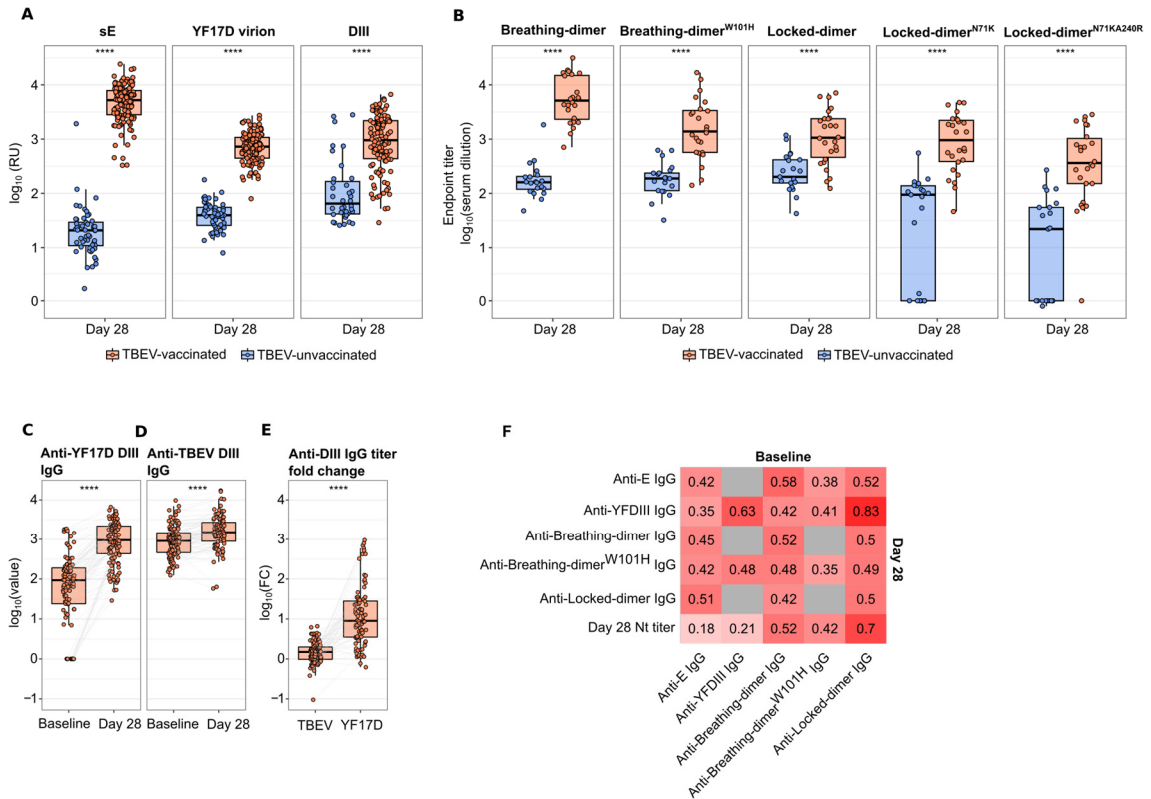
Figure 9. Diversity of antibody targets and enhanced immunogenicity of the YF17D vaccine in TBEV pre-vaccinated individuals.

A) Anti-YF17D sE, YF17D-virion and YF17D-DIII IgG titer in donor´s sera on day 28 pv. Titer was estimated in Relative Units (RU) from a standard control given 10,000 Arbitrary Units (AU)

B) IgG endpoint titer against breathing-dimer, breathing-dimer[W101H], locked-dimer, locked-dimer[N71K] and locked-dimer[N71K,A240R] on day 28 pv. A subset of the study cohort was used (TBEV-vaccinated n = 24 and TBE unvaccinated n = 24)

C) longitudinal anti-YF17D-DIII specific IgG titer (n = 117 TBEV-vaccinated individuals)

D) Longitudinal quantification of anti-TBE-DIII IgG titer (n = 114 pairs)

E) Paired comparison of the DIII-specific IgG fold-change between day 28 and day 0 for TBEV and YF17D specificities.

F) Spearmann correlation between baseline antibody titers and day 28 antibody and neutralization titer. Color scale and labeling indicates the correlation index for statistically significant comparisons (p < 0.05). Gray indicates p > 0.05.

Statistical significance was calculated with a Wilcoxon–Mann–Whitney test for A and B and a paired Wilcoxon signed-rank test for C, D and E. Significance is depicted as follows: * p<0.05, ** p<0.01,*** p<0.001, **** p<0.0001. Figure and figure legend modified from Santos-Peral et al. 2023 (see Disclaimers on page 8)

DIII can discriminate arthropod and mosquito-borne flavivirus serocomplexes (Holbrook et al., 2004). Nevertheless, sera from TBEV-pre-vaccinated individuals contained cross-reactive IgG antibodies to YF17D-DIII which confirmed the existence of cross-reactive epitopes conserved between TBEV and YF17D DIII (Figure 9C).

*With modifications from Santos-Peral et al. 2023 (see Disclaimers on page 8)

Interestingly, the IgG titer specific to YF17D-DIII increased by 10-100 fold following YF17D vaccination, whereas the increase in TBE-DIII specific IgG was more moderate, less than 10 fold (Figure 9 C-E). This result suggests that antibodies elicited by TBE-experienced individuals were also diversified towards non-cross-reactive epitopes in high levels. Altogether, TBEV pre-immunity not only amplified the response to cross-reactive epitopes due to the recall of TBEV vaccine-induced immune imprinting but also enhanced the IgG response to previously unencountered epitopes, for which no pre-existing memory existed.

Next, the linear association of pre-existing immunity with enhanced YF17D humoral immune responses was examined. Baseline IgG titers to sE, breathing dimer, and locked dimer mutants correlated not only with the final antibody titer but also with the neutralization capacity on day 28 pv (Figure 9F). Given the lack of known cross-neutralizing determinants between TBEV and YF17D and based on the higher titers of antibodies targeting non-cross-reactive epitopes observed in TBEV-experienced donors, these results support a more robust immune response compared to TBEV-unvaccinated individuals.

3.3.1.2 The cellular response to YF17D vaccination is moderately enhanced in TBEV-pre-vaccinated donors

T cell immunity is another indicator of vaccine immunogenicity and a central actor of an effective and protective anti-viral immunity elicited after infection or vaccination (Akondy et al., 2009; McKinstry et al., 2012; Miller et al., 2008; Wilkinson et al., 2012). The YF17D vaccine elicits a robust CD4 and CD8 immune response that transitions from an effector phase during the acute response to a long-lasting memory phenotype. YF17D vaccine effectiveness relies on the generation of wide-ranging and polyfunctional T-cell responses against both structural and non-structural viral proteins (Blom et al., 2013; Fuertes Marraco et al., 2015; James et al., 2013). This response is essential for directly mediating viral clearance and providing help to B cells for the generation of potent antibody responses and maturation within the GC reaction (Huber et al., 2020; Sandberg et al., 2021).

To investigate whether TBEV-induced immunity overall enhanced the immunogenicity of YF17D, we evaluated the antigen-specific memory T cell response following YF17D vaccination. The quantification of the number and functionality of the antigen-specific T cell response was achieved with an *ex vivo* re-stimulation assay, followed by intracellular cytokine staining (ICS), using live virus as the stimulating antigen. This approach, similar to the one used by Miller et al (2008) with vaccinia virus (Miller et al., 2008), allows the simultaneous detection of antigen-specific CD4 and CD8 T cell subsets (Figure 10A-D). The frequency of antigen-specific T cells was measured by detection of IFN-γ, TNFα, IL-2 and IL21 together with degranulation markers like CD107a and the activation-induced marker CD40L (CD154). CD40L is upregulated upon TCR engagement of the antigen allowing the accurate detection of antigen-specific T cells rather than bystander activated CD4 T cells.

Following the implementation of the *ex vivo* re-stimulation assay, a great expansion of antigen-specific CD4 and CD8 T cells was observed on day 28 pv (Figure 10A-D). T cell re-stimulation did not identify more pre-existing YF17D-specific T cells at baseline in TBEV-pre-vaccinated individuals than in the TBEV-unvaccinated donors. Consistent with the overall high immunogenicity of the YF17D vaccine, an elevated frequency of antigen-specific CD4 and CD8 T cells was observed (Figure 10C-D). Interestingly, the CD4 and CD8 T cell response on day 28 was comparable in magnitude between TBEV-pre-vaccinated and unvaccinated donors (Figure 10E-F).

Previously, we observed high heterogeneity in the strength of the humoral response against TBEV in baseline samples within the TBEV-pre-vaccinated group. A moderate effect of TBEV-prevaccination on the cellular immune response to YF17D may be overshadowed by other sources of natural variability in the human immune response to vaccinations. To gain insights into the effects of TBEV-pre-vaccination on cellular immune responses we grouped TBEV-pre-vaccinated individuals based on their baseline levels of sE-specific IgG antibodies. These cross-reactive antibodies, induced by TBEV, serve as a proxy for both the strength of the response to TBEV at the time of YF17D vaccination and the potential to enhance YF17D vaccine virus infection via ADE (results not shown). This way, we grouped individuals with intermediate and low TBEV-vaccine-induced IgG levels separately from the top quantile (high baseline anti-sE IgG titer). Interestingly, participants in the highest quantile showed significantly higher numbers of antigen-specific EM CD4 T cells (Figure 10E) and a trend to higher frequencies of antigen-specific CD8 T cells (Figure 10F). Thus, within the TBEV-pre-vaccinated group, a trend to enhanced CD4 T cell responses was observed.

The functionality and polyfunctionality scores (FS and PFS) of the YF17D-specific T cell response were calculated using a Combinatorial Polyfunctionality Analysis of Single Cells (COMPASS) analysis (Lin et al., 2015). COMPASS evaluates all the boolean combinations of activation markers in stimulated and unstimulated samples and returns the posterior probability of antigen-specificity for every combination (Figure 11 A-B). COMPASS analysis does not consider the number of antigen-specific cells with the assumption that all the identified functional combinations are equally important irrespective of their predominance. FS is defined as the proportion of antigen-specific subsets detected among all possible ones whereas PFS weighs the different subsets by their degree of functionality. TBEV-pre-vaccinated individuals had higher CD4 PFS than TBEV-unvaccinated individuals and TBEV-pre-vaccinated individuals with high anti-sE IgG titer at baseline had a better quality of final CD4 T cell response for both FS and PFS parameters whereas the CD8 T cell response was equally strong in both subgroups (Figure 11 C-D).

Collectively, YF17D vaccination induced a robust CD4 and CD8 response in all study participants regardless of their pre-vaccination status. However, TBEV pre-vaccination had a moderate enhancing effect on the magnitude and functionality of CD4 T cell responses, particularly notable in individuals with stronger anti-TBEV immunity at the time of YF17D vaccination.
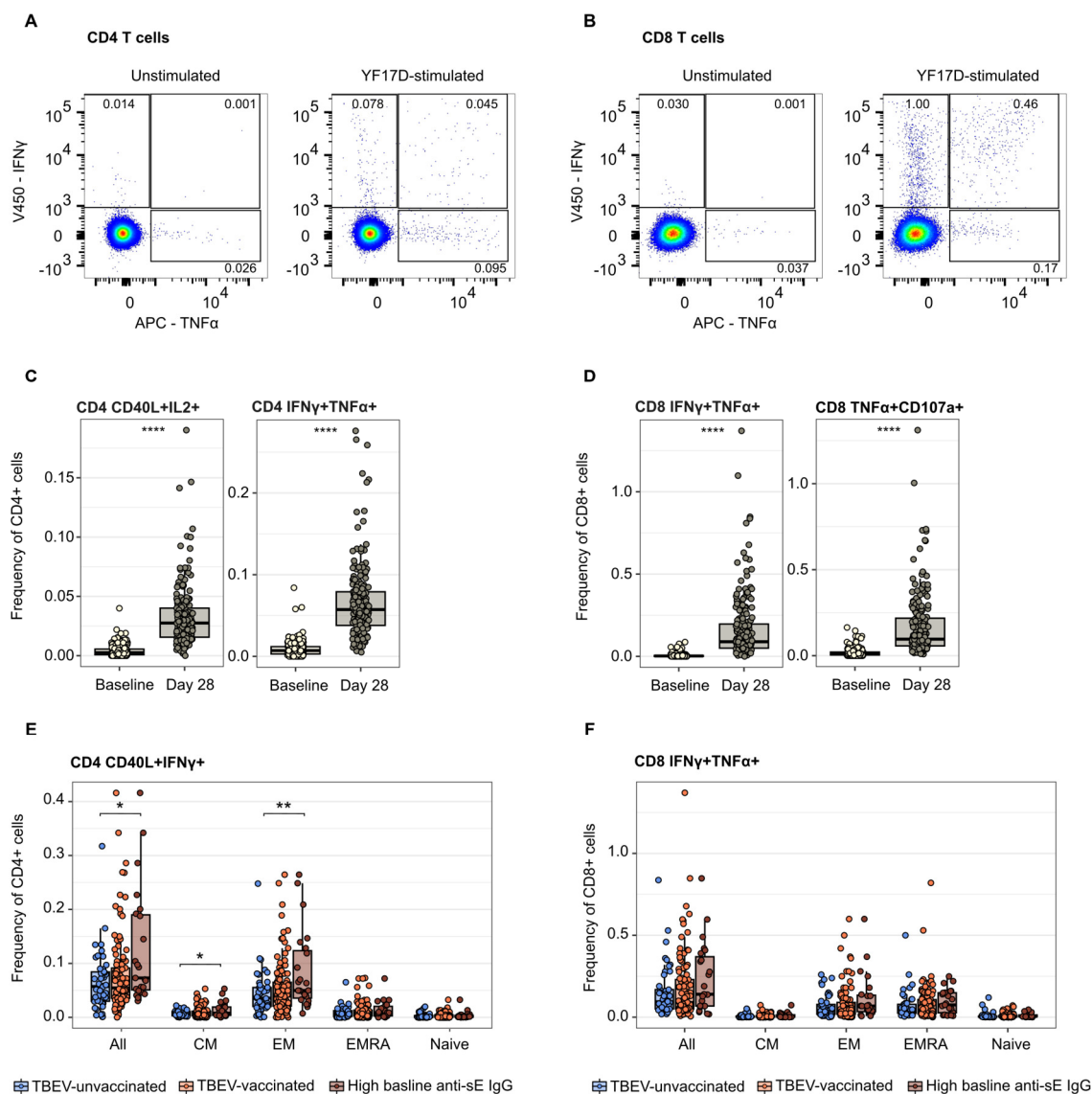
Figure 10. *Ex vivo* antigen-specific T-cell restimulation with live YF17D virus and ICS.

A) Representative flow cytometry plot of the expression of IFN-γ and TNFα by CD4 T cells in unstimulated and YF17D virus-restimulated samples 28 days after vaccination.
B) Representative flow cytometry plot of the expression of IFN-γ and TNFα by CD8 T cells in unstimulated and YF17D virus-restimulated samples 28 days after vaccination.
C) Frequency of CD4 T cells co-expressing CD40L and IL2 (left panel) and IFN-γ and TNFα (right panel) before and after YF17D vaccination
D) Frequency of CD8 T cells co-expressing IFN-γ and TNFα (left panel) and TNFα and CD107a (right panel) before and after YF17D vaccination
E) Frequency of CD4 T cells co-expressing CD40L and IFN-γ for all and different memory subpopulations after YF17D-restimulation on day 28 pv.
F) Frequency of CD8 T cells co-expressing IFN-γ and TNFα for all and different memory subpopulations after YF17D-restimulation on day 28 pv.

TBEV-vaccinated is depicted in orange and TBEV-unvaccinated in blue. The top quantile of individuals with high baseline anti-sE IgG titers are depicted in brown. Statistical significance was calculated with a Wilcoxon–Mann–Whitney test for C-F. Significance is depicted as follows: * p<0.05, ** p<0.01,*** p<0.001, **** p<0.0001.
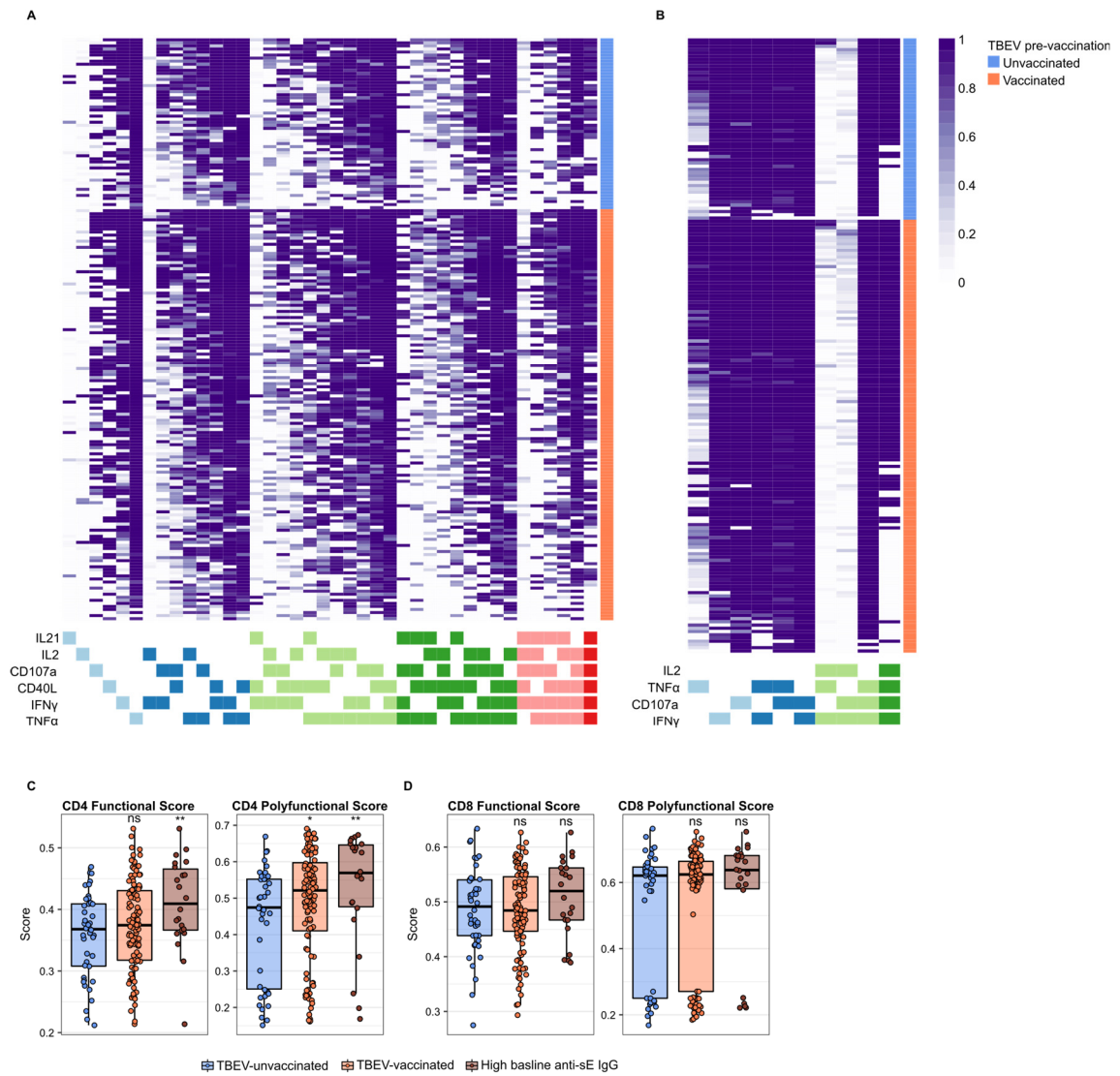
Figure 11. Combinatorial Polyfunctionality Analysis of Single Cells (COMPASS) of the antigen-specific CD4 and CD8 T cell response on day 28 pv.

A) Heatmap of the posterior probability of antigen-specificity for 64 functional CD4 subpopulations
B) Heatmap of the posterior probability of antigen-specificity for 16 functional CD8 subpopulations
C) Functional and polyfunctional score of the CD4 T cell response
D) Functional and polyfunctional score of the CD8 T cell response

Functional subpopulations that lacked antigen-specificity were excluded from visualization in A and B. TBEV-vaccinated donors are depicted in orange and TBEV-unvaccinated ones in blue. The top quantile of individuals with high baseline anti-sE IgG titers are depicted in brown. Statistical significance was calculated with a Wilcoxon–Mann–Whitney test for C-F. Significance is depicted as follows: * p<0.05, ** p<0.01,*** p<0.001, **** p<0.0001.

3.3.1.3 Influence of TBEV-pre-vaccination on the overall YFV17D vaccine response: classification into good and weak vaccine responders based on clustering of vaccination endpoints

Categorizing individuals based on their response as "good" or "weak" vaccine responders enhances the precise identification of factors influencing vaccine responses by reducing interference from average responders. This grouping also helps minimize

the impact of other sources of inter-individual variability in the response, such as genetic or intrinsic factors. Therefore, to evaluate whether TBEV-pre-vaccination improved the overall response to YF17D vaccination, study participants were grouped as good and weak vaccine responders based on different vaccination endpoints. To address this in a non-arbitrary manner, unsupervised hierarchical clustering of the three main vaccination endpoints: the number and function of antigen-specific CD4 and CD8 T cells and the neutralizing antibody titer, was performed (Figure 12A). For CD4 T cells, 4 clusters discretely separated the cohort into elite, good, average, and poor responders. Similarly, for CD8 and neutralizing antibody titers, 3 clusters divided the cohort into good, average, and poor responders. Finally, individuals present in the good or poor responder groups for every endpoint were classified as vaccine elite responders (n = 19) and vaccine poor responders (n = 23), respectively. Similarly, individuals classified as good responders in two of the indicators and average or good in the third were grouped as vaccine good responders (n = 46), while those classified as poor responders in two categories and average or poor in the third were named vaccine weak responders (n = 43) (Figure 12 A-B).

TBEV-pre-vaccinated individuals were categorized into two groups: those with high and those with average/low baseline anti-sE IgG titers. TBEV-pre-vaccinated groups and unvaccinated individuals were equally distributed across the elite/poor and good/weak responder groups (χ^2 p-value = 0.10, 0.24, respectively). Nevertheless, the elite and good responder groups were enriched with TBEV-pre-vaccinated individuals who had high baseline IgG antibodies (Figure 12C). Interestingly, this subgroup was significantly more represented in the elite CD4 T cell response cluster (χ^2 p value = 0.0027). In contrast, there was an equal distribution of individuals according to TBEV pre-vaccination status across the neutralizing antibody and CD8 response groups (Figure 12C).

To have a global perspective of the different vaccination endpoints, I compared the TBEV-pre-vaccinated and unvaccinated groups with the following vaccination endpoints: the polyclonal neutralizing antibody titer, the YF17D-specific IgM and IgG antibody titers, the functionality and the frequency of antigen-specific CD4 and CD8 T cell responses. As expected, the greatest impact was observed for the IgG and IgM antibody response. Interestingly, TBEV-pre-vaccinated individuals with high cross-reactive IgG levels at baseline showed a clear tendency to increased vaccine responses to all the endpoints reaching statistical significance for neutralization and CD4 T cell responses (Figure 12D).

Collectively, these results indicate that TBEV-pre-vaccination favors an enhanced response to the YF17D vaccine, with a pronounced effect on the humoral response and a moderate effect on the antigen-specific CD4 T cell response.
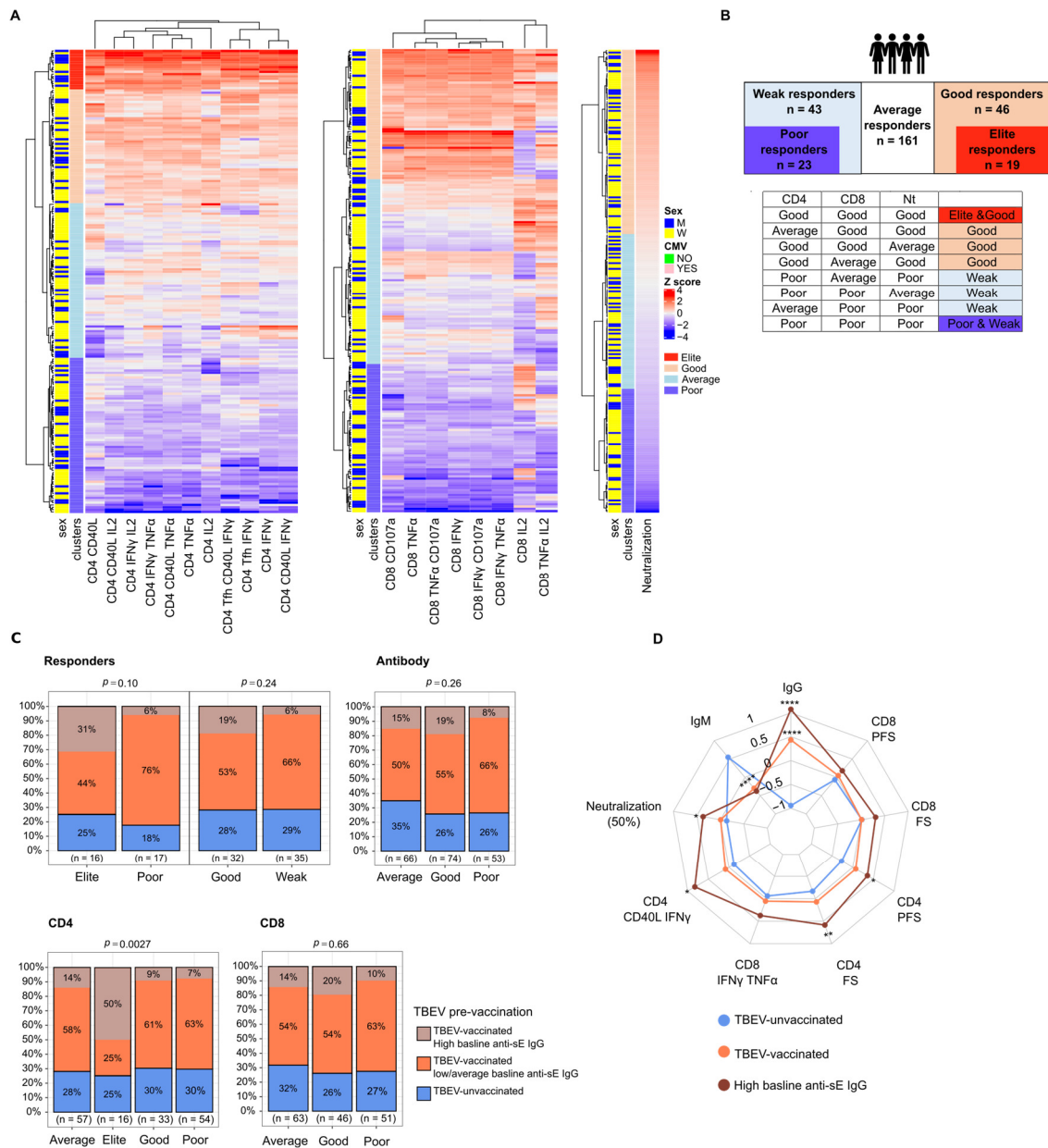
Figure 12. Overall effects of TBEV pre-vaccination. Vaccine response categories defined by hierarchical clustering of vaccination endpoints.

A) Hierarchical clustering of main vaccination endpoints: antigen-specific CD4 T cells, CD8 T cells and Neutralizing antibody titers. 3 to 4 clusters identify good, average and poor responders in each category.

B) Cohort grouping into 5 categories based on the clusters identified by hierarchical clustering in A. Individuals found in the good or poor responder groups for every endpoint were classified as vaccine elite responders (n = 19) and vaccine poor responders (n = 23). Individuals classified as good responders in two of the indicators and average or good in the third were grouped as vaccine good responders (n = 46), while those classified as poor responders in two categories and average or poor in the third were named vaccine weak responders (n = 43)

C) Response group allocation for TBEV-unvaccinated, TBEV-vaccinated with a low/average baseline anti-sE IgG titer and TBEV-vaccinated with a high baseline anti-sE IgG titer. Statistical significance was evaluated with a Chi-square test.

D) Radar plot for individual vaccination endpoints including YF17D-specific IgG, IgM and Neutralization antibody titers as well as CD4 and CD8 T cell responses. Data was scaled and statistical significance was estimated with a student T test. Significance is depicted as: * p<0.05, ** p<0.01,*** p<0.001, **** p<0.0001.

3.4 Effect of TBEV pre-vaccination on the T dynamics following YF17D vaccination

In the previous chapters, the outcome of YF17D vaccination in the context of prior flavivirus immunity has been examined. TBEV-pre-vaccination status was examined against different vaccination endpoints that acted as indicators of vaccine immunogenicity. Next, I examined how YF17D vaccination affected the longitudinal kinetics and activation of circulating immune subsets in individuals with and without prior TBEV-pre-existing immunity using multidimensional spectral flow cytometric analysis.

3.4.1.1 The longitudinal dynamics of the CD4 T cell response is independent of TBEV pre-vaccination

The blood lymphocyte concentration showed an initial decline by day 7 post-vaccination (pv), which was later reversed by day 14, resulting in a significant increase compared to baseline. By day 28 pv, the lymphocyte count in the blood had returned to baseline levels (Figure 13A). This early drop following vaccination has been described before and is associated with the strength of the final vaccine response (Bovay et al., 2020). The same pattern is followed by CD3 T cells, which represent the largest fraction of lymphocytes found in circulation and by both CD4 and CD8 T cell subsets (Figure 13A-C). The frequencies of CD4 and CD8 T cells within the circulating lymphocytes remained stable by day 7, indicating that YF17D triggered a similar mobilization of both subsets out of the peripheral blood circulation (Figure 13 A-C). Importantly, the magnitude of this immune perturbation was not affected by prior flavivirus immunity since the observed kinetics were equal for both TBEV-pre-vaccinated and unvaccinated individuals (Figure 13 A-C).

Using previously published YF17D-specific MHC-II tetramers (Huber et al., 2020), we could quantify and characterize antigen-specific CD4 T cells in a representative subset of the study cohort. Individuals matching for HLA-DRB1*03:01 and or DRB1*01:01, were selected (n = 62 and n = 45, respectively with 10 individuals matching for both). The reactive peptides were used in combination and included specificities against C, E, NS1 and NS3 viral proteins. Antigen-specific CD4 T cells could first be detected by day 14 pv, coinciding with the peak of the effector T cell response and by day 28, identifying memory CD4 T cells. At both timepoints, the frequency of tetramer-positive T cells showed no significant difference between TBEV-pre-vaccinated and unvaccinated individuals for either HLADR03:01 or 01:01 (Figure 13D). Tetramer-positive CD4 T cells encompassed a wide variety of CD4 T cell subpopulations, including regulatory T cells, cTfh, Th1, Th2, etc. (not shown). Interestingly, the frequency of tetramer-specific ctfh was significantly higher for TBEV-unvaccinated individuals by day 28 for the HLADR 01:01 type and the trend was present also for HLADR 0301 (Figure 13E). This result could indicate a prolonged or augmented expansion of cTfh cells in individuals undergoing a primary immune response in contrast to individuals with pre-existing flavivirus immunity.
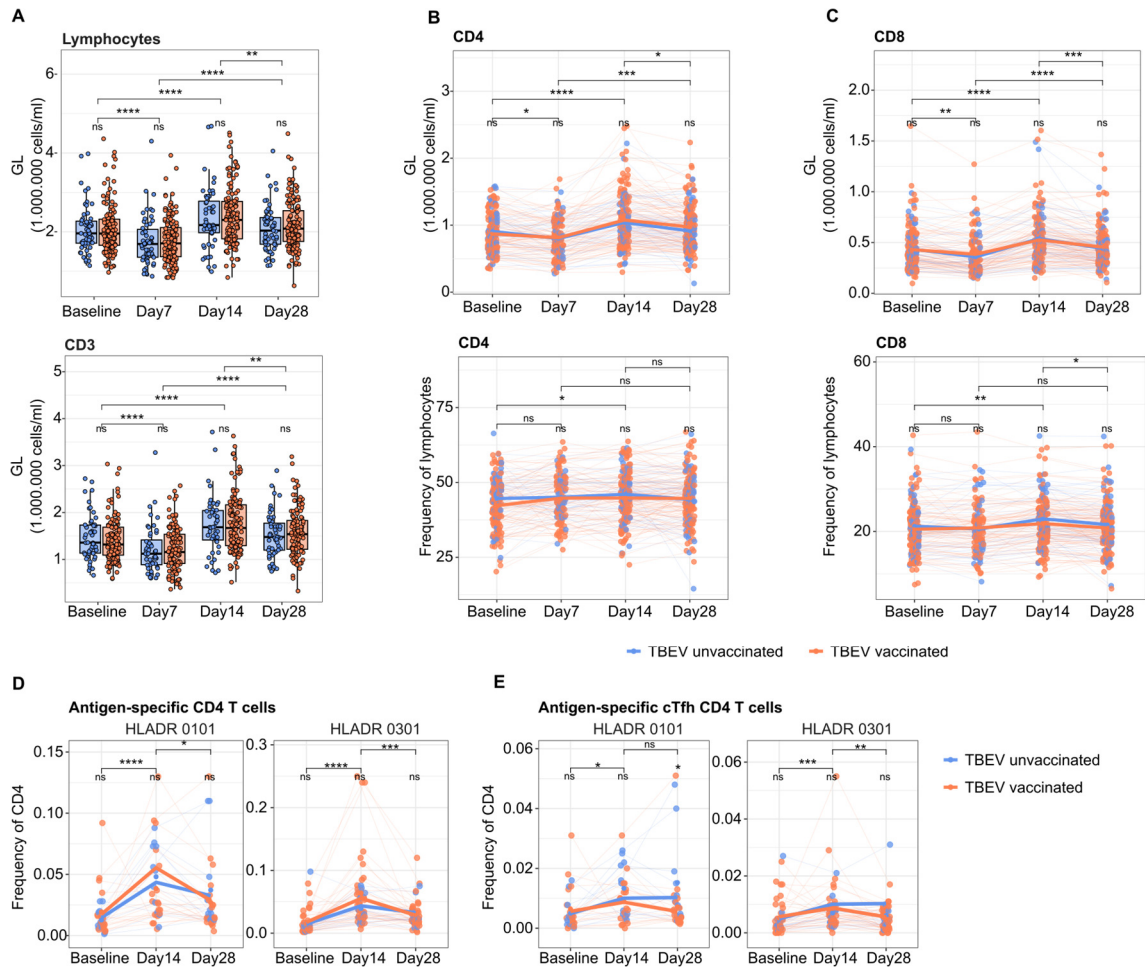
Figure 13. Longitudinal lymphocyte kinetics and tetramer-specific CD4 T cells.

A) Longitudinal concentration of lymphocytes (top panel) and CD3 T cells (bottom panel)

B) Longitudinal CD4 T cell kinetics quantified as blood cell concentration (top panel) and frequency of lymphocytes (bottom)

C) Longitudinal CD8 T cell kinetics quantified as blood cell concentration (top panel) and frequency of lymphocytes (bottom)

D) Antigen-specific CD4 T cells for HLADR0101 and HLADR0301 tetramers at baseline and at day 14 and 28 pv.

E) Antigen-specific cTfh cells for HLADR0101 and HLADR0301 tetramers at baseline and at day 14 and 28 pv.

Statistical differences between TBEV-vaccinated and unvaccinated individuals were calculated with a Wilcoxon–Mann–Whitney test and with a paired Wilcoxon signed-rank test for comparing longitudinal timepoints. Significance is depicted as follows: * $p<0.05$, ** $p<0.01$, *** $p<0.001$, **** $p<0.0001$.

The longitudinal characterization of the bulk CD4 T cell populations comprised 116 subpopulations in frequency of CD4 and blood cell concentration units. These included memory and helper subpopulations, cTfh, Tregs, and other subpopulations characterized by transcription factor expression and functional markers like PD1, ICOS, IL7Ra, CD57, and chemokine receptors like CCR7, CXCR3, CCR4, and CCR6. The analysis included known subpopulations to have relevance in primary, secondary or chronic immune reactions such us the populations defined by PD1/TCF1 that identify exhausted, and activated populations, or Tbet/Eomes which identified cells with effector, transient, or late differentiation status. As activation markers, the panel included CD25, CD38,

HLADR, and the proliferation marker Ki67 (panel in Appendix A, Table 2; gating strategy in Appendix B; full population list in Appendix E).

Consistent with prior studies, the activation kinetics of the CD4 T cell response peaked on day 14 pv. In fact, the proliferation of most of the populations tested peaked on day 14. This effect starts to be visible by day 7, especially for certain populations like CM, EM, Th1, Th1/17, PD1-TCF1+, and Tbet+Eomes+. The proliferation of these immune subsets seemed to be preceded by their activation, as indicated by the earlier expression of CD38 already by day 7pv (Figure 14A-B). The frequency of the bulk immune populations did not show profound variations following vaccination. The cell concentration in blood followed the same dynamics of the total CD4 compartment with no particular trend identified for CD4 subsets (not shown). Even though Th2 and Th17 were expanded upon vaccination, their relative frequencies were reduced by days 7 and 14 due to a more pronounced expansion of Th1 cells. In addition, Tbet+ CD4 T cells were also expanded following vaccination as well as Tregs and TCF1+ cells (Figure 14A). Collectively, the observed CD4 response reproduced the expected pattern of response to an acute viral infection for both TBEV-pre-vaccinated and unvaccinated individuals and was consistent with previous reports (Blom et al., 2013; Bovay et al., 2020; Hou et al., 2017; Huber et al., 2020; Kohler et al., 2012).

Notably, after correcting for multiple testing, none of these populations exhibited significant differences in the abundance or frequency between individuals pre-vaccinated for TBEV and unvaccinated (Figure 14A). Next, I investigated whether the longitudinal changes of the different populations varied between TBEV-pre-vaccinated groups implementing a multivariate regression model. This analysis included not only differences in the abundance or expansion of immune populations at a given timepoint but also the magnitude of change between timepoints: $\Delta(7,0)$, $\Delta(14,0)$, $\Delta(28,0)$, $\Delta(14,7)$, $\Delta(28,14)$ and $\Delta(28,7)$. The multivariate regression model included the T cell populations and deltas as the dependent variable and TBEV groups as independent variables while adjusting for sex, age, and experimental batch as fixed effects. This analysis allowed the quantification of the differences between groups at a given timepoint as a fold change as well as the differences between two timepoints. The implementation of this approach did not return any association with an p value < 0.05 adjusted for multiple testing. Nevertheless, it helped to identify trends for which pre-vaccination with TBEV had an influence. Of note, the dynamic change in cTfh exhibited a more significant reduction between day 7 and day 0 among TBEV-pre-vaccinated individuals (p = 0.05), with a longitudinal difference of -0.9%. Similarly, the frequency of PD1+CD38+ cTfh displayed distinct kinetics in TBEV-pre-vaccinated individuals, with a modest increase by day 7 (-0.08%), followed by a sharper rise by day 14. At this time point, it had already begun to decline in TBEV-unvaccinated individuals (0.05% difference for the change between day 14 and day 7; p = 0.03). In addition, Tbet^{low}Eomes^{+} CD4 T cells showed opposing trends between day 7 and day 0 with a tendency to increase for TBEV-unvaccinated and to decrease for TBEV-pre-vaccinated donors (-0.39%, p = 0.04). Lastly, consistent with previous reports, Tregs were expanded following vaccination and, interestingly, their

frequency remained high for TBEV-pre-vaccinated individuals by day 28 pv (0.24%, p = 0.024) (Figure 14C).

Altogether, the activation and kinetics of various CD4 T cell populations recapitulate the expected dynamic for an anti-viral immune response and were comparable in magnitude and characteristics for both TBEV-pre-vaccinated and unvaccinated study participants.

Figure 14. Longitudinal CD4 T cell dynamics following YF17D vaccination

A) Longitudinal changes in the frequency of selected CD4 T cell populations compared to their abundances on day 0. The frequency of batch-corrected CD4 T cell populations were scaled, and bubble size indicates the variation in the Z score with day 0. Colored filled bubbles represent statistically significant variations, determined using a Student's t-test with Welch correction. Red indicates increasing abundance and blue a decrease with respect day 0.

B) Longitudinal frequencies of CD38+ CD4 T cells (left) and proliferating Ki67+ CD4 T cells (right).

C) Longitudinal variation of the frequency of cTfh, Ctfh expressing PD1 and CD38, Tbet^{low}Eomes^{+} CD4 T cells, and Tregs negative for CXCR3 and CCR6 expression. Differences in the longitudinal variation influenced by TBEV-pre-vaccination as estimated by the multivariate linear model are indicated below each plot. The thick line connects the mean value of TBEV-pre-vaccinated individuals in orange and

TBEV-unvaccinated individuals in blue. Statistical significance in B and C plots was calculated with a Wilcoxon–Mann–Whitney test for comparing TBEV-pre-vaccination groups and with a paired Wilcoxon signed-rank test for comparing longitudinal timepoints. Significance is depicted as follows: * p<0.05, ** p<0.01,*** p<0.001, **** p<0.0001.

3.4.1.2 The longitudinal dynamics of the CD8 T cell response is independent of TBEV pre-vaccination

Similarly to the analysis performed with the CD4 T cell subsets, the longitudinal characterization of the CD8 T cell dynamics comprised 80 subpopulations both in frequency of CD8 and blood cell concentration units. These included memory subpopulations as well as different transcriptional factor profiles defined based on TCF1, Tbet, and Eomes. Included were phenotypic markers of stemness or exhaustion like CD127, CD57, and PD1. The expression of CD38, HLADR, and Ki67 was used as activation and proliferation markers (panel in Appendix A, Table 2; gating strategy in Appendix B; full population list in Appendix E).

As observed in the CD4 T cell response, the longitudinal kinetic of the bulk CD8 T cell response following YF17D vaccination was identical for both TBEV-pre-vaccinated and unvaccinated individuals. Post-vaccination, there were no significant changes in the bulk frequencies of the analyzed populations, except for the expansion of Naïve and TCF1+ CD8 T cells. Activation and proliferation of various CD8 immune subsets peaked at day 14 and were observed as early as day 7 (Figure 15). These results are consistent with previous reports (Akondy et al., 2009; Blom et al., 2013; Hou et al., 2017; Miller et al., 2008).

To account for differences in the dynamics of various CD8 T cell populations, I implemented the same linear model described above. However, TBEV pre-vaccination did not exert any effect.

Collectively, in response to the YFV17D vaccination CD8 T cells displayed robust activation and proliferation by day 14 in a comparable magnitude for both TBEV-pre-vaccinated and unvaccinated individuals.

3.5 Effect of TBEV pre-vaccination on the longitudinal analysis of B cell populations and B cell repertoire dynamics following YF17D vaccination

3.5.1 Prior TBEV vaccination does not impact the longitudinal kinetics of the bulk B cell response but enhances the expansion of differentiated IgG+ antigen-specific B cells following YF17D vaccination

The most profound differences caused by TBEV-pre-vaccination on the response to the YF17D vaccine were observed for the humoral response. Thus, the longitudinal phenotyping of the B cell response can help our understanding of the global effects of TBEV-pre-vaccination and the extent to which prior TBEV immunity may enhance vaccine immunogenicity, reshape epitope immunodominance, and to what extent the TBEV-induced signature primarily induces an anamnestic response, biased toward previously encountered epitopes and dominated by pre-existing MBC.
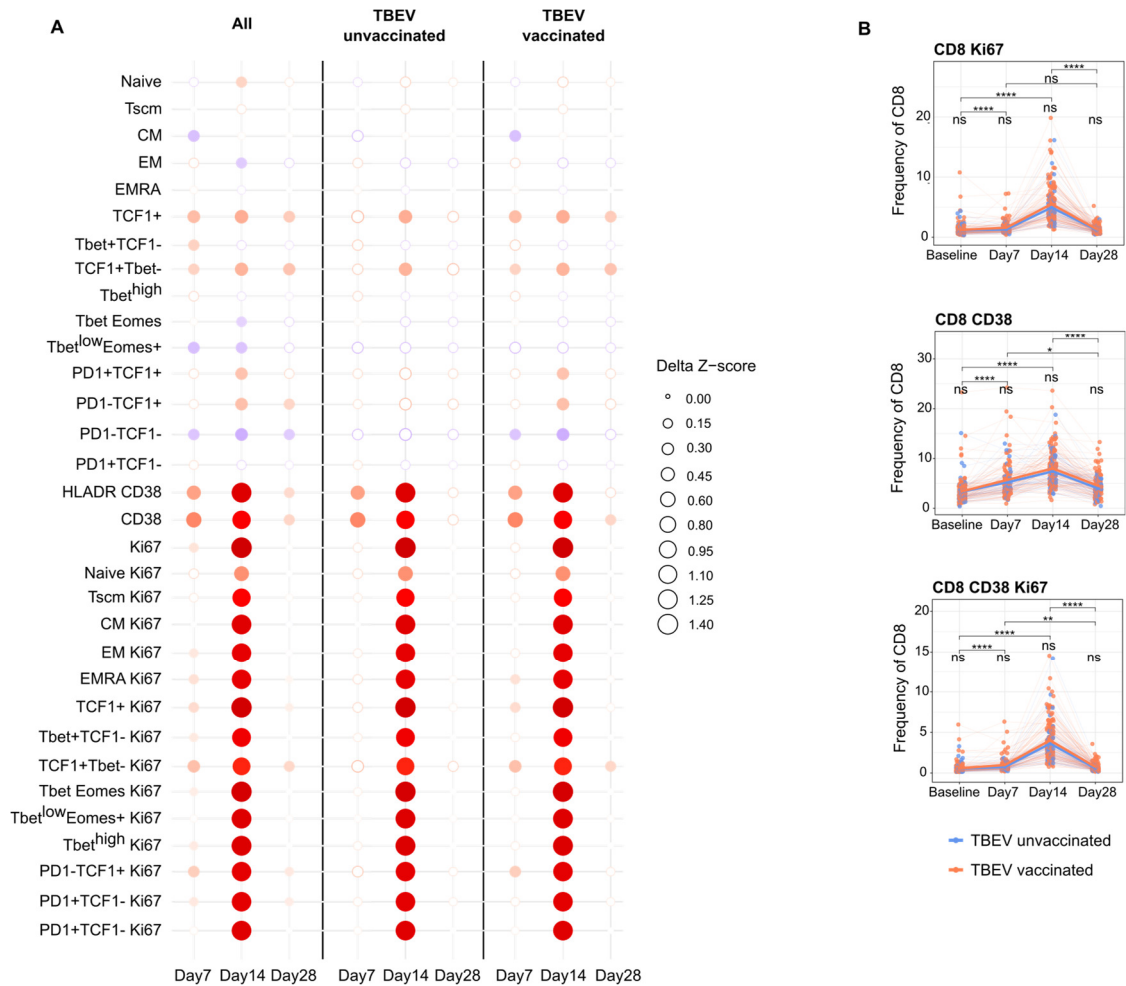
Figure 15. Longitudinal CD8 T cell dynamics following YF17D vaccination

A) Longitudinal changes in the size of selected CD8 T cell populations compared to their abundances on day 0. The frequency of batch-corrected CD8 T cell populations was scaled, and the differences from day 0 are visualized as bubbles, with their size indicating the variation in the Z score. Statistically significant variations, determined using a Student's t-test with Welch correction, are represented as colored filled bubbles, with increased abundances shown in red and decreased abundances in blue.

B) Longitudinal depiction of the frequencies of Ki67+, CD38+, and CD38+Ki67+ CD8 T cells. The thick line connects the mean value of TBEV-pre-vaccinated individuals in orange and TBEV-unvaccinated individuals in blue. Statistical significance in B plots was calculated with a Wilcoxon–Mann–Whitney test for comparing TBEV-pre-vaccination groups and with a paired Wilcoxon signed-rank test for comparing longitudinal timepoints. Significance is depicted as follows: * p<0.05, ** p<0.01,*** p<0.001, **** p<0.0001

Longitudinally, as observed with the lymphocyte concentration in peripheral blood, the concentration of CD19 cells experienced an early drop by day 7 pv which returned to baseline levels by day 14 (Figure 16A). The same trend was observed for the relative frequency of CD19 among all the lymphocytes, which suggests that among lymphocytes, the early drop is particularly affecting B cells (Figure 16B). Remarkably, this early drop was significantly more pronounced for TBEV-unvaccinated individuals, who consistently had lower B cell levels by day 28 pv (Figure 16 A-B). To identify which B cell population was relocating from circulation and causing the difference between both pre-vaccination groups, further characterization was done for the kinetics of activated memory (AM, CD21-CD27+), resting memory (RM, CD21+CD27+), tissue-like memory

(TLM, CD21-CD27-), and intermediate memory (IM, CD21+CD27-) B cell populations. Of note, with this gating strategy, the IM group included naive B cells. Longitudinally, both groups experienced a drop in the relative frequency of RM cells by day 7 (Figure 16C) and the circulating concentration declined for both RM and more strongly for IM (Figure 16D). Nevertheless, the IM population was significantly less represented in circulation for TBEV-unvaccinated individuals by day 7 (Figure 16E). This result could indicate that TBEV-unvaccinated individuals, who are undergoing a primary immune response against YF17D, required a greater mobilization of the circulating B cell subsets out of circulation that particularly affected the IM subpopulation.

For the characterization and quantification of the antigen-specific B cell response, an in-house monobiotinylated YF17D antigen was used to capture antigen-specific B cells as previously described (Franz et al., 2011). To this end, sE antigen (TBEV-unvaccinated n = 40; TBEV-vaccinated n = 92), and DI-II (TBEV-unvaccinated n = 11; TBEV-vaccinated n = 27) were used. Consistently with the serological results, the number of sE and DI-II-specific B cells was increased in TBEV-pre-vaccinated individuals (Figure 16F). At baseline, YF-cross-reactive B cells could not be detected in TBEV-pre-vaccinated donors. This was likely due to the very low abundance in circulation of MBC that fell below the sensitivity of the assay. Antigen-specific B cells could already be detected by day 14 for both subgroups although in higher amounts for TBEV-pre-vaccinated individuals and had further increased by day 28. This dynamic is consistent with the continuous increase in affinity maturation that antigen-specific B cells experience for months after infection or vaccination (Wec et al., 2020). As expected, the number of antigen-specific B cells targeting sE was higher than the number targeting DI-II. Phenotypically, antigen-specific B cells for both sE and DI-II were predominantly RM cells. However, TBEV-unvaccinated individuals had a significantly higher proportion of IM antigen-specific B cells (50%) and a smaller fraction of AM and RM cells than TBEV-pre-vaccinated individuals, who showed a phenotype dominated by AM (25%) and RM (60%) (Figure 16G). As expected, most of the sE-specific B cells were IgG positive in TBEV-pre-vaccinated individuals, while this was not the case for TBEV-negative individuals, who had mostly IM IgD+ cells (data not shown).

Altogether, these results highlight fundamental differences in the B cell response for TBEV-pre-vaccinated individuals, which expand higher amounts of antigen-specific B cells with a more differentiated phenotype in response to YF17D vaccination.

The longitudinal characterization of the bulk B cell response included 123 populations (panel in Appendix A, Table 3; gating strategy in Appendix C; full population list in Appendix E). Surprisingly, it did not show strong differences between TBEV-pre-vaccinated and unvaccinated individuals. The magnitude of activation and proliferation as well as the dynamic changes observed for various B cell populations, followed the same pattern for both subgroups (Figure 17A). Specifically, compared to baseline, the frequency of RM, CD27+ memory, CXCR5+, and CXCR4+ B cells were significantly reduced on day 7 pv. In contrast, the B cell frequency of TLM and double negative (DN, IgD-CD27-) populations increased.
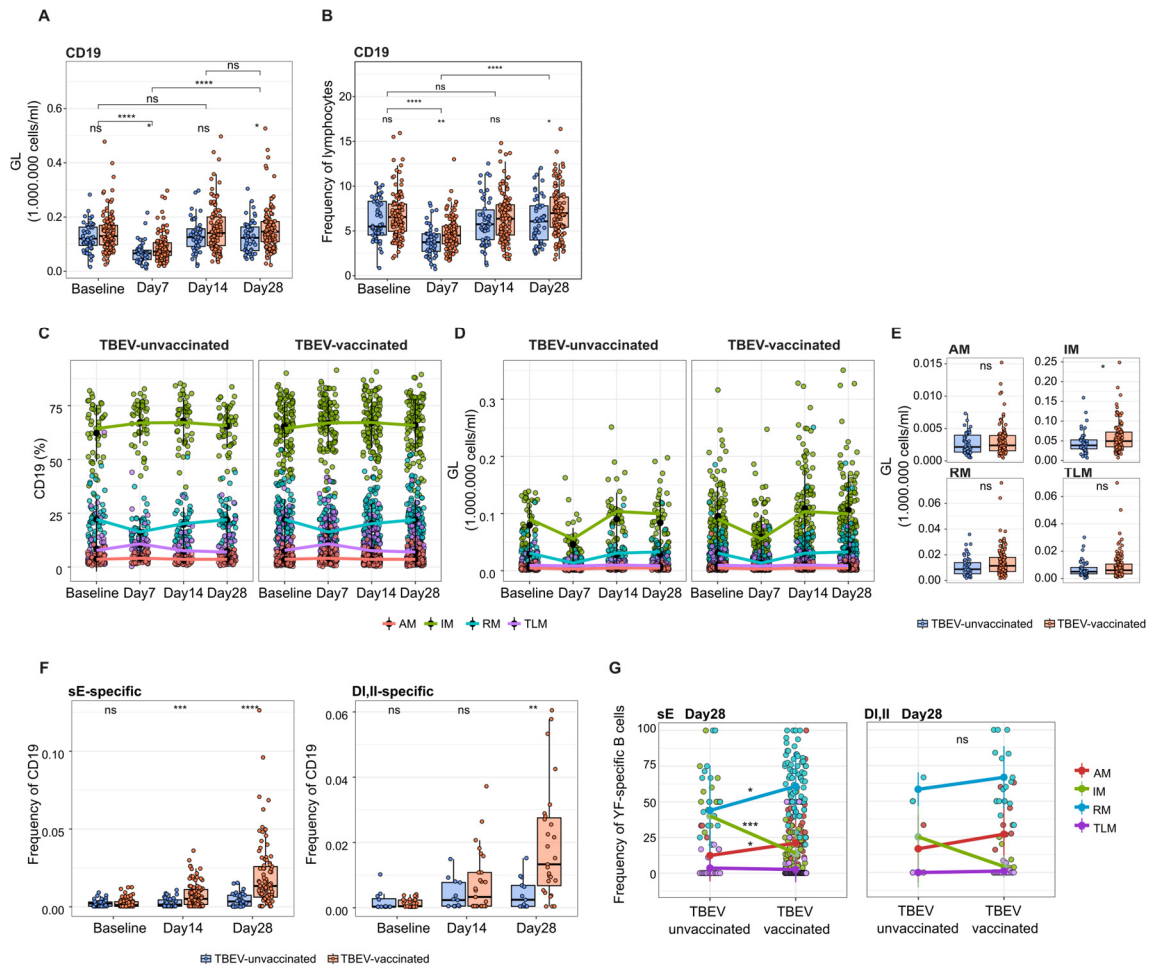
Figure 16. Longitudinal B cell kinetics and antigen-specific B cell phenotype.

A) Longitudinal blood concentration of CD19 B cells
B) Longitudinal CD19 B cell kinetics quantified as the frequency of lymphocytes
C) Longitudinal variation of the frequency of CD19 B cells for memory subpopulations for TBEV-unvaccinated (left) and TBEV-vaccinated (right).
D) Longitudinal variation in the circulating cell concentration for memory subpopulations for TBEV-unvaccinated (left) and TBEV-vaccinated (right).
E) Differences in the blood concentration of B cell memory subpopulations on day 7 pv.
F) Antigen-specific B cell quantification with sE (left) and DI-II (right).
G) Relative frequency of the antigen-specific B cells identified in F. Individuals with less than 2 high-affinity specific cells were excluded from representation.

Memory populations were identified as activated memory (AM, CD21-CD27+), resting memory (RM, CD21+CD27+), tissue-like memory (TLM, CD21-CD27-), and intermediate memory (IM, CD21+CD27+). Statistical significance was calculated with a Wilcoxon–Mann–Whitney test for comparing TBEV-pre-vaccination groups and with a paired Wilcoxon signed-rank test for comparing longitudinal timepoints. Significance is depicted as follows: * $p < 0.05$, ** $p < 0.01$, *** $p < 0.001$, **** $p < 0.0001$

As expected, plasmablast expansion following vaccination occurred by day 7 and peaked by day 14. This expansion was very pronounced for IgM+ plasmablasts as well as CXCR4-CD20-, and CD138+ B cells, which represent antibody-secreting cells with a commitment to develop into long-lasting plasma cells (Sanderson et al., 1989; Tellier & Nutt, 2017). Likewise, the proliferation of various B cell subsets by day 7 and 14 pv was stronger for RM, memory, class-switched, and CXCR3+ B cells (Figure 17A).
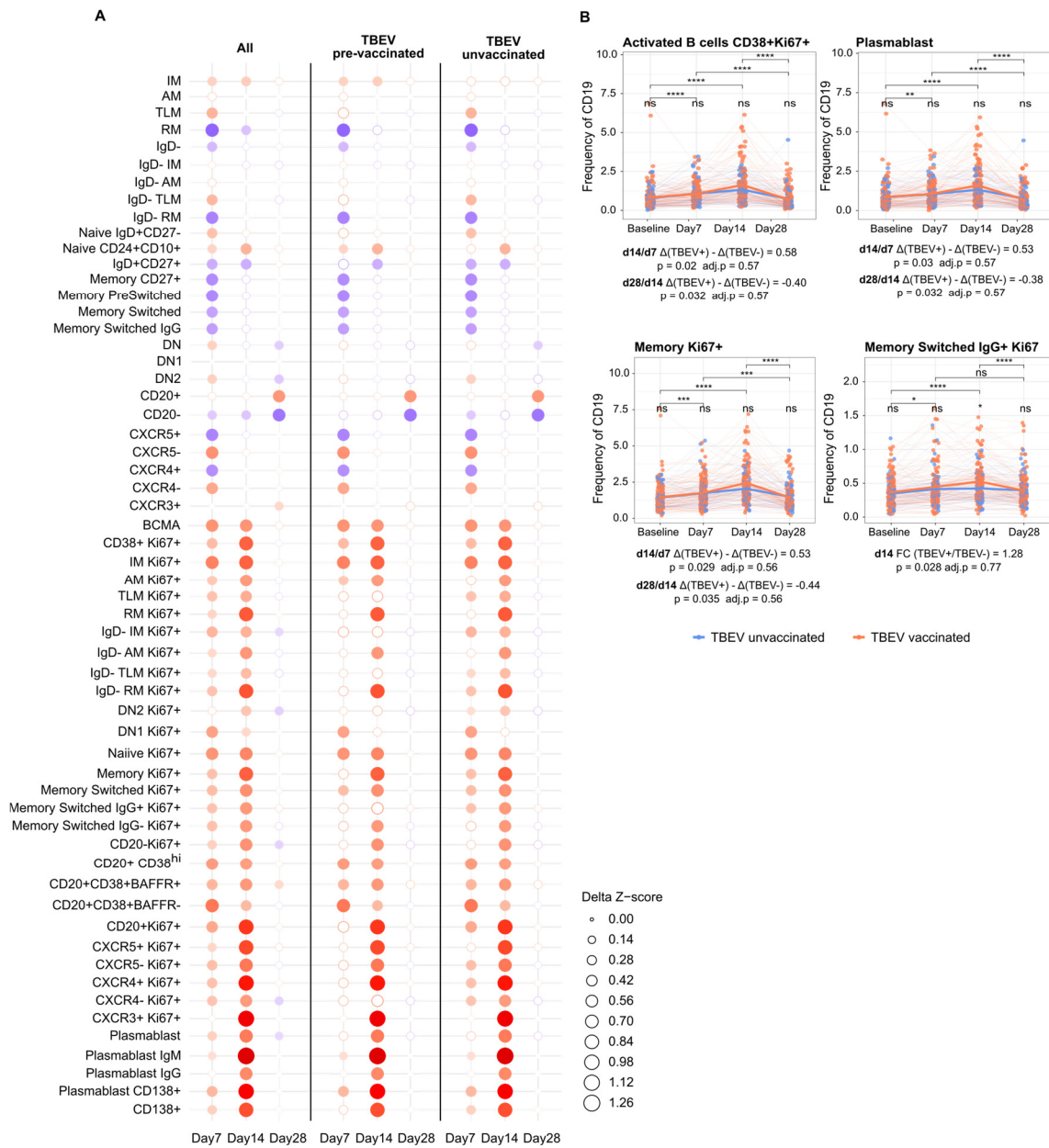
Figure 17. Longitudinal B cell dynamics following YF17D vaccination.

A) Longitudinal changes in the size of selected B cell subsets compared to their abundances on day 0. The frequency of batch-corrected CD19 B cell populations was scaled, and the differences from day 0 were visualized as bubbles, with their size indicating the variation in the Z score. Statistically significant variations, determined using a Student's t-test with Welch correction, were represented as colored filled bubbles, with increased abundances shown in red and decreased abundances in blue.

B) Longitudinal depiction of the frequencies of CD38+Ki67+ Activated B cells, CD20-CD38+ plasmablasts, CD27+Ki67+ proliferating memory B cells, and CD27+IgM-IgD-IgG+Ki67+ proliferating IgG class-switched B cells. Differences in the longitudinal variation influenced by TBEV-pre-vaccination as estimated by the multivariate linear model are indicated below each plot.

The thick line connects the mean value of TBEV-pre-vaccinated individuals in orange and TBEV-unvaccinated individuals in blue. Statistical significance was calculated with a Wilcoxon–Mann–Whitney test for comparing TBEV-pre-vaccination groups and with a paired Wilcoxon signed-rank test for comparing longitudinal timepoints. Significance is depicted as follows: * p<0.05, ** p<0.01,*** p<0.001, **** p<0.0001.

Even though the activation magnitude and kinetics of the overall B cell response detected by flow cytometry did not replicate the serology data nor the quantification of antigen-specific B cells in TBEV-pre-vaccinated individuals, TBEV-pre-vaccinated individuals had slightly higher levels of activated cells on day 14 as well as higher frequencies of plasmablasts, CD27+Ki67+, and class-switched IgG+Ki67+ B cells (Figure 17B). Additionally, the increase of these populations from day 7 to day 14 was found to be sharper for TBEV-pre-vaccinated individuals. For instance, the frequency of activated B cells (CD38+Ki67+) was increased an extra 0.58% more for TBEV-pre-vaccinated (p-value = 0.02) and an extra 0.53% for plasmablasts (p = 0.03) (Figure 17B). Nevertheless, these differences were not found to be statistically significant after correction for multiple testing.

Altogether, the bulk dynamic of the B cell response following YF17D vaccination was comparable for individuals with and without prior flavivirus immunity. This goes in line with the observations in the T cell kinetics and suggests that the immune perturbation induced by YF17D is largely unaffected by pre-existing immunity. Nevertheless, this result contrasts with the remarkable differences observed for the antibody titers in serum.

3.5.2 Bulk B cell receptor repertoire sequencing

The impact of TBEV pre-vaccination on the humoral response is driven by the selection and expansion of specific B cell clones. The selective expansion, dominant clones and diversity of the B cell response ultimately lead to the production of the polyclonal antigen-specific antibodies characterized in donors' sera. To better understand the changes in the B cell repertoire over time in both TBEV pre-vaccinated and unvaccinated individuals, I conducted next-generation sequencing of the IgH gene locus using longitudinal PBMC samples from 24 study donors, including 11 TBEV-unvaccinated and 13 TBEV-pre-vaccinated individuals. Following genomic DNA isolation, the genetic loci were amplified together in a multiplex PCR using BIOMED2-FR1 primers as previously described (Brüggemann et al., 2019; Schultheiß et al., 2020; van Dongen et al., 2003). The multiplexed primers allowed the simultaneous amplification of all V gene segments from 6 subgroups. Barcodes identifying donor samples were used for final amplification before sequencing on a MiSeq Illumina sequencer (V2X300 bp) (Figure 18A).

For clarity, as there is no consistent definition for what constitutes a clonotype, in this dissertation I adhere to the most widely accepted definition of a clonotype as a unique V(D)J nucleotide sequence, which naturally includes an identical CDR3 nucleotide sequence (Sofou et al., 2023).

3.5.2.1 Global diversity metrics of the BCR repertoire show a temporary reduction of diversity for both TBEV pre-vaccinated and unvaccinated individuals following YF17D vaccination

Analyzing global metrics in bulk BCR sequencing samples provided insights into the overall perturbations in the B cell repertoire induced by YF17D vaccination. Consistent with the flow cytometry data, the count of unique clonotypes exhibited a significant

decrease by day 7. This decrease was sustained through day 14 and eventually returned to baseline levels by day 28 pv (Figure 18B). This could be due either to the withdrawal of B cells from peripheral blood or to the emergence and expansion of clonotypes dominating the response to the YF17D vaccine. Interestingly, flow cytometry data showed a reduction in B cell concentration by day 7 that was not sustained by day 14.

Clonotype count depends on sequencing depth, and the number of sequenced clones varied significantly across samples. Therefore, other metric indexes were employed to examine longitudinal changes in repertoire diversity, evenness, and richness. The clonality index quantifies repertoire evenness on a scale from 0 to 1. A clonality index of 1 indicates that the analyzed sample contains only one clonotype, while 0 indicates complete clonal diversity. Interestingly, TBEV-pre-vaccinated individuals showed a significant increase in evenness at day 14 pv but overall the repertoire evenness remained relatively stable over time (Figure 18 C). This may suggest the emergence of dominant B cell clones within this subgroup. Global metrics indexes of repertoire diversity, like Shannon H index, the probability of interspecies encounter (PIE, also known as Simpson's evenness index and Gini-Simpson index) and the true diversity index reflected a decrease of diversity by day 7 that was maintained by day 14 pv (Figure 18 D-F). Unexpectedly, both TBEV-pre-vaccinated and unvaccinated individuals experienced the same degree of repertoire diversity variation.

Even though it failed to reach statistical significance, the PIE index, which indicates the probability that two clones selected at random from a sample will belong to different clonotypes, dropped more pronouncedly for a fraction of the TBEV-pre-vaccinated individuals analyzed. This result is consistent with the clonality index increase by day 14 for this group of individuals. Nevertheless, changes in the repertoire metrics did not vary across TBEV-pre-vaccinated individuals based on the level of baseline anti-sE IgG titers, a proxy of the strength of crossreactive anti-TBEV response at the moment of YF17D vaccination (Figure 18 B-F). Taken together, the BCR repertoire diversity metrics underwent longitudinal changes following YF17D vaccination, indicating a decrease in diversity from days 7 to 14 pv. These results potentially signify the emergence of dominant clonally expanded B cell families. Notably, within the TBEV-pre-vaccinated group, there was a more pronounced tendency towards a B cell repertoire with increased evenness on day 14 pv.

The variation in sequence identity from the germline-encoded V gene segment was used to quantify somatic hypermutation (SHM), a proxy for the GC reaction. Longitudinally, the frequency of SHM clones remained constant (Figure 18G, bottom panel). Only a slight increase in the mean frequency of germline V gene sequence identity was observed on day 14 (p = 0.07) (Figure 18G, upper panel). This result indicates an increase in "germline-likeness" or a higher abundance of clones that have not undergone SHM or GC reaction. Likewise, the global distribution of clones based on V-gene sequence identity included fewer mutated sequences by day 7 and 14 pv (Figure 18 H, upper panel). Even within SHM sequences, there was an increase of sequences with a low mutation distance from the germline by day 14 pv. (Figure 18H, lower panel). This suggests the appearance of clones in the repertoire that were newly generated upon

YF17D vaccination and that had a low degree of SHM given the short time since the vaccination. These results are consistent with previous observations in the response to acute viral infections like EBOV, RSV, Flu, and Sars-Cov-2 which also described a trend to increase germline-likeness in the bulk BCR repertoire (Kotagiri et al., 2022; Stewart et al., 2022).
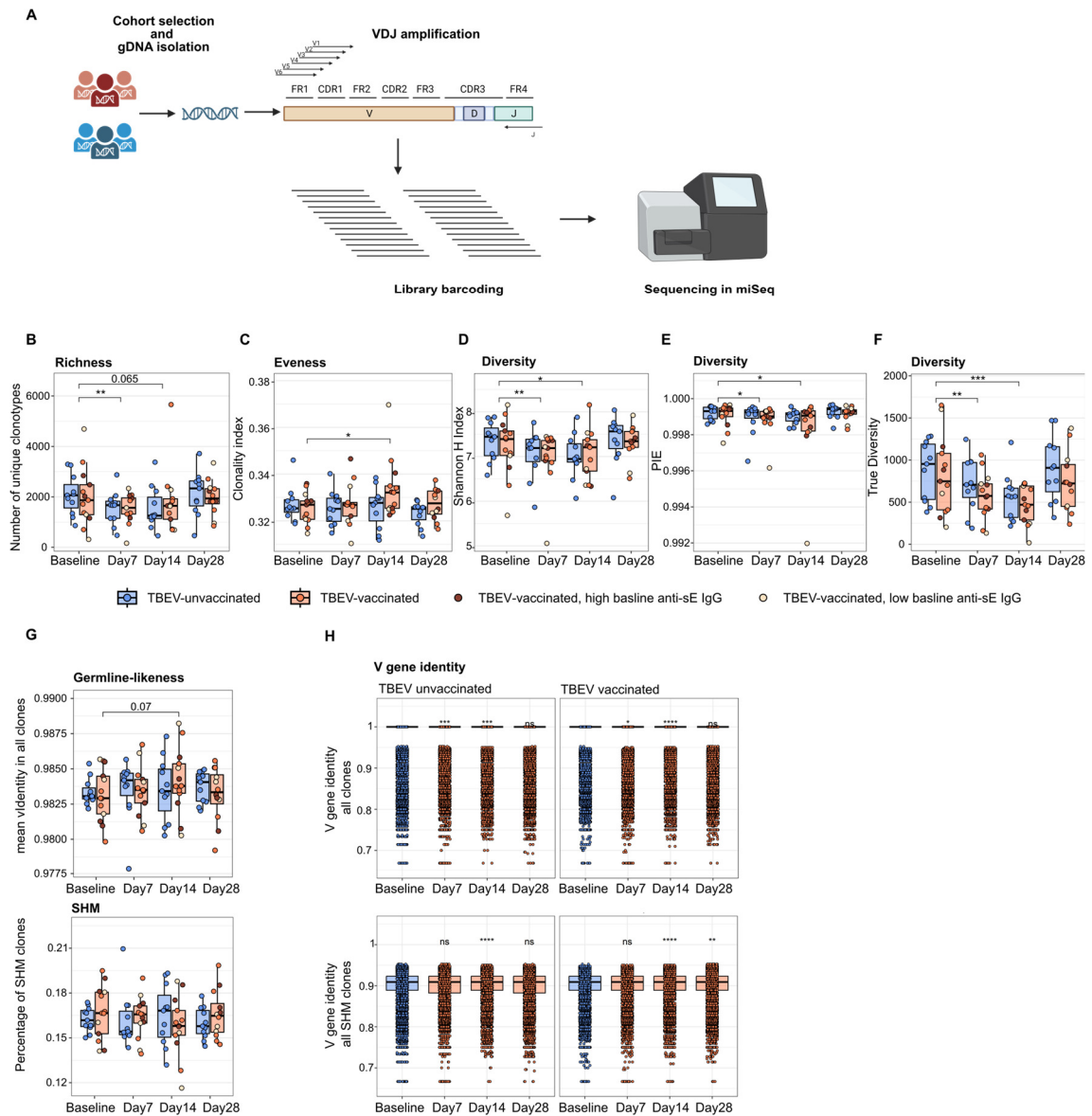
Figure 18. Longitudinal changes on the global metrics of the bulk B cell receptor repertoire.

A) Explanatory diagram illustrating the process for acquiring BCR repertoire data from genomic DNA material

B-F) Longitudinal changes in richness, measured as the number of unique clonotypes (B); eveness, measured as clonality index (C); diversity, estimated as Shannon H index (D), probability of interspecies encounter (E) and the true diversity index (F) for TBEV-vaccinated and unvaccinated individuals

G) Longitudinal changes in germline-likeness (top panel), measured as the mean distance from the germline-encoded V gene sequence (1 indicates identical sequence similarity). And longitudinal variation in the percentage of SHM sequences (bottom)

H) Distribution of all sequenced clones based on distance from the germline-encoded V gene sequence (top) and in the subset of all SHM clones (bottom)

TBEV-unvaccinated individuals are depicted in blue and TBEV-pre-vaccinated individuals in orange. Dark-brown dots indicate individuals with high-baseline anti-sE IgG titers, orange dots individuals with an intermediate level of baseline anti-sE IgG titers, and beige represents those with a low baseline anti-sE IgG titer. Statistical significance was calculated with a Wilcoxon–Mann–Whitney test for comparing TBEV-pre-vaccination groups and results displayed in H. A paired Wilcoxon signed-rank test was used for comparing longitudinal timepoints and significance in G. Significance is depicted as follows: * p<0.05, ** p<0.01,*** p<0.001, **** p<0.0001.

3.5.2.2 The YF-induced clonotype families: clonal expansion, tracking and meta- and sub-clonotypes

The bulk BCR repertoire measurement has limitations in revealing vaccine-induced changes in the repertoire as most sequences are likely not YF17D-specific. Flow cytometry results indicated that only around 2% of B cells were activated after vaccination, 1-4% were plasmablasts on day 14 pv, and 0.1% could be stained with sE on day 28. Nevertheless, BCR sequencing allowed the description of longitudinal changes in diversity metrics. To infer the emergence and dominance of YF17D-specific clones, I attempted to identify signs of clonally expanded sequences. Consistently with the longitudinal diversity changes, the number of clonotypes needed to fill 10% of the sequenced repertoire per individual and timepoint significantly decreased by about one-third on days 7 and 14 pv (Figure 19A). This suggests the expansion and increased abundance of certain clonotypes following YF17D vaccination.

The identification of YF-specific clones is challenging. An open question revolves around whether individuals previously vaccinated against TBEV were expanding pre-existing B cell clones or initiating a primary immune response directed towards cross-reactive and non-cross-reactive epitopes. To address this question, clonal tracking across various timepoints and individuals was conducted. Through this analysis, I sought to identify pre-existing clones that underwent expansion following vaccination, evaluate their relative abundance, and assess the extent of somatic hypermutation (SHM). Additionally, to infer antigen-specificity, the identification of public repertoires (shared clones across individuals) serves as a proxy for antigen-specific clones induced after vaccination. However, the number of shared clonotypes between individuals was very low, and only a small fraction was found in more than one timepoint (Figure 19B).

YF17D-specific B cell clones after vaccination can be identified based on their clonal expansion, clonotype diversification (sub-clonotypes) within an individual, and clonal convergence (meta-clonotypes) both between and within individuals. Related sequences and clonal families were identified by clustering based on the same V gene usage and a nucleotide sequence similarity of 95% in the CDR3 (Levenshtein distance of 0.05). Clustering all pooled sequences per timepoint and TBEV-pre-vaccination status identified a peak of interconnected sequences (clonal families defining either sub-clonotypes or meta-clonotypes) on day 14 pv. This peak was more pronounced for TBEV-pre-vaccinated individuals (0.24% of interconnected sequences), although this may be due to the inclusion of one more individual in this subgroup (Figure 18C and F). Similarly, clustering of all timepoints in a donor-independent manner served to identify and track B cell families across and within timepoints. Even though clonal families within baseline and post-vaccination samples were found, those were not more abundant in TBEV-pre-

vaccinated individuals, which would have indicated a potential recall of pre-existing clones following YF17D vaccination (Figure 19G).
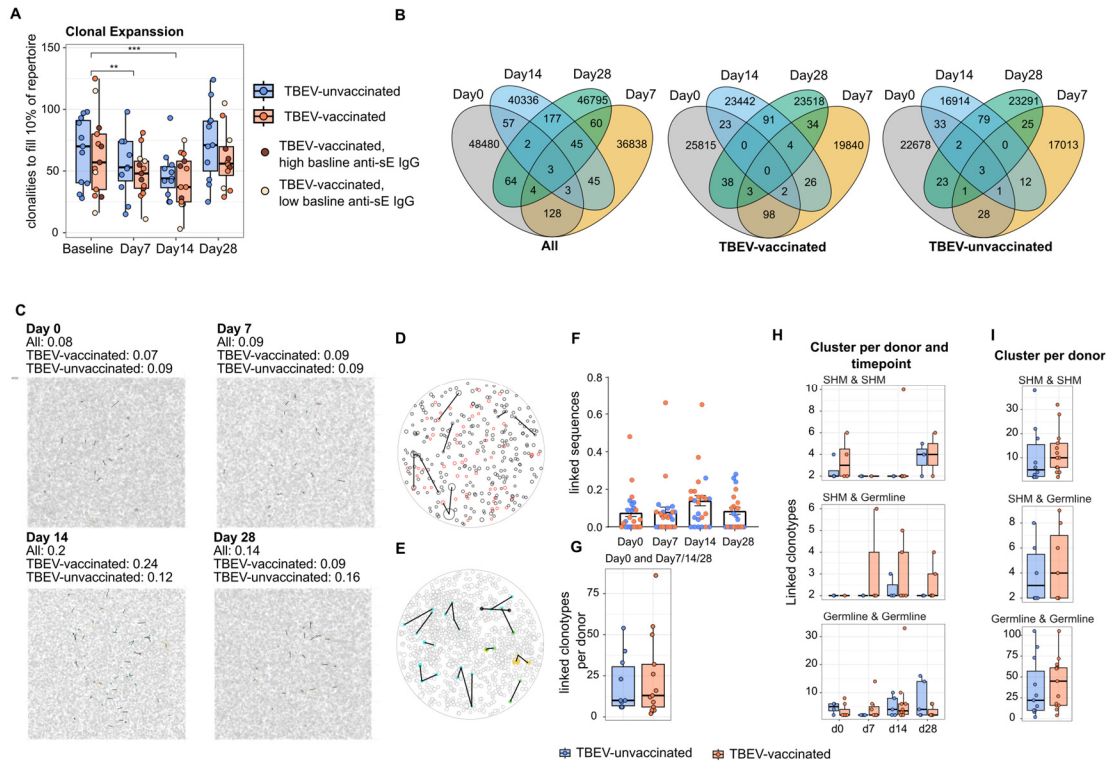
Figure 19. BCR clonal families

A) Longitudinal clonal expansion determination is based on the number of clonotypes that represent 10% of the sequenced repertoire per individual and timepoint.
B) Venn diagrams depicting the number of shared clonotypes between timepoints for all and TBEV pre-vaccinated and unvaccinated individuals. Matching clonotypes shared the same V gene and conserved CDR3 nucleotide sequence of 95% (0.05 Lavensthein distance).
C) Identification of interconnected clonal families, representing sub- and meta-clonotypes for all the individuals pooled in the corresponding timepoint and TBEV-pre-vaccinated group. Related sequences were linked based on shared V gene use and 95% similarity in the CDR3 nucleotide sequence. Each bubble represents a single clonotype, and its size corresponds to the abundance in the repertoire.
D) Representative visualization of connected clonotypes for one individual. Each bubble represents a clonotype, its size the abundance in the repertoire. Germline-encoded V gene sequences are depicted with a black border and SHM sequences in red.
E) Representative visualization of connected clonotypes between individuals and timepoints. Each bubble represents a clonotype, its size the abundance in the repertoire and the color the individual. Only connected clonotypes are colored.
F) Percentage of interconnected sequences (clustered in clonal families) per donor and timepoint for TBEV-pre-vaccinated individuals in orange and TBEV-unvaccinated in blue.
G) Number of connected clonotypes found in day 0 and following YF17D vaccination.
H) Number of connected clonotypes based on germline-encoded or SHM sequences per individual and timepoint.
I) Number of connected clonotypes based on germline-encoded or SHM sequences per individual at any timepoint.

TBEV-unvaccinated individuals are depicted in blue and TBEV-pre-vaccinated individuals in orange. Statistical significance was calculated with a Wilcoxon–Mann–Whitney test for comparing TBEV-pre-vaccination groups and a paired Wilcoxon signed-rank test for comparing longitudinal timepoints. Significance is depicted as follows: * $p<0.05$, ** $p<0.01$, *** $p<0.001$, **** $p<0.0001$.

From clonal lineages, the identification of sub-clonotypes (sequences using the same V gene and CDR3 yet with SHM in the V domain) could be achieved by connecting SHM sequences to unmutated sequences. These sub-clonotypes likely represent new B cells responding to YF17D vaccination that have begun maturing in a GC reaction. This approach successfully identified clonal families of that kind especially on days 7, 14, and 28 but not in greater abundance in any of both TBEV-pre-vaccinated subgroups (Figure 19H). Similarly, families including only SHM sequences could be identified, but they were rare since most of the families encompassed germline-encoded V genes, indicating a small level of convergence (Figure 19H-I)

Altogether, the analysis of the bulk BCR sequences showed low levels of clonal expansion peaking on day 14 pv. Additionally, the low number of responding cells and the rarity of shared clones, together with limitations attributed to sequencing depth and sampling stochasticity, did not allow the identification of pre-existing clones, antigen-specific clones nor to establish whether the B cell response to the YF17D vaccine followed the principles of a recall response for TBEV-pre-vaccinated individuals.

3.5.2.3 BCR repertoire comparison to public datasets enables the identification of YF17D-specific clones

Lastly, to identify antigen-specific B cells, I compared the dataset of YF17D-specific B cells generated by Wec et al. (Wec et al., 2020) with the data generated here. Wec et al isolated YF17D sE-specific B cells from two donors, naïve of prior flavivirus infection or vaccination, longitudinally following YF17D vaccination. There were 14 exact matches and 15 additional related sequences that shared the V gene and a maximum distance of 1 mismatch in the CDR3 aminoacidic sequence (Figure 20 A). Both TBEV-pre-vaccinated and unvaccinated groups contained matches with Wec's dataset on days 14 and 28. Since these clones were isolated from vaccinees undergoing a primary response to YF17D, they do not represent the signature expected in TBEV-pre-vaccinated individuals but rather the clones generated during the first encounter with the YF17D vaccine. Interestingly, TBEV-pre-vaccinated donors had 4 matches already at day 0. The sequences identified to coincide with Wec's dataset showed a longitudinal increase in SHM (Figure 20 A). Wec et al. studied the epitope specificity of the mAb they isolated. Some matching clones in our dataset coincided with mAb targeting the 5A binding site. One particular clone was found to be prevalent across different individuals and in Wec's dataset: IGHV3-72, CDR3 CTRGPPDYW. This clone was somatically hypermutated and was equally found in TBEV-pre-vaccinated and unvaccinated individuals after day 14 pv. Furthermore, this clone was also present in the dataset of Davydov et al. (Davydov et al., 2018) always with an IgM isotype. Based on this, I speculate that this clone represents a dominant high-affinity, selected YF-specific clone that binds accessible epitopes and lacks competition with 4G2 and 5A epitope (binding tested by Wec et al., 2020) (Figure 20 A-B).

Likewise, I compared our dataset with the one from Davydov et al (Davydov et al., 2018) which consists of plasmablast BCR sequences after YF17D vaccination. While Davidov's clones may not exclusively represent antigen-specific clones, as confirmed by the

identification of shared clones with baseline samples from TBEV-unvaccinated individuals, they are likely enriched for YF-specificity. Interestingly, TBEV-pre-vaccinated individuals had more shared clones with Davydov's dataset, also at day 0. SHM increased longitudinally suggesting that these clones were indeed representing clones elicited by YF17D vaccination. Strikingly, the number of SHM clones in the TBEV-pre-vaccinated group was high at all timepoints, possibly indicating the pre-existence of YF-specific clones (Figure 19C). This approach does not guarantee the identification of antigen-specific clones or clones sharing the same specificity. Although it is impossible to confirm the specificity of these clones without experimental validation, I addressed the reliability of this approach by comparing our dataset with the curated dataset generated by Stewart et al. (Stewart et al., 2022) consisting of 2044 clones with known antigen-specificity against RSV, Sars-Cov2, and EBOV. Only a very small number of matches were found between our dataset and Stewart's, which contrasts with the numerous matches identified in Wec's dataset, even though it contained significantly fewer clones (n=696). These results confirm the validity of this analysis to infer antigen-specific matches (Figure 20D). Lastly, to investigate whether TBEV-pre-vaccinated individuals expanded cross-reactive B cell clones, I compared our dataset with a pool of published sequences that had been experimentally proven to have antigen-specificity to either DENV, ZIKV or WNV (Cox et al., 2016; Dejnirattisai et al., 2015; Durham et al., 2019; Dussupt et al., 2020; Parameswaran et al., 2013; Robbiani et al., 2017; Rogers et al., 2017; Smith et al., 2013; Throsby et al., 2006; Tsioris et al., 2015; Waickman et al., 2020; Xu et al., 2012; Zanini et al., 2018) This dataset contains 570 clones. Exact CDR3 matches were not found except for one clone at day 0 for a TBEV-unvaccinated individual. Even though TBEV-pre-vaccinated individuals had a higher number of matching sequences this approach failed to identify pre-existing or expanded cross-reactive B cell clones in the TBEV-pre-vaccinated individuals (Figure 20E).

Taken together, gDNA bulk BCR sequencing showed global changes in diversity metrics and clonal expansion, which paralleled the observations in B cell population kinetics obtained through flow cytometry, contrasting with the serology results. Both TBEV-vaccinated and unvaccinated individuals underwent a reduction in circulating B cell diversity after vaccination, likely reflecting the mobilization of B cells to lymph nodes and the emergence of dominant B cell clones responding to YF17D. Additionally, there were indications of moderate clonal expansion in the first weeks post-vaccination. However, the limitations of this approach hindered the possibility of performing clonal tracking and identifying convergence signatures arising from pre-existing immunity. Nonetheless, when compared to published datasets, antigen-specific sequences were identified in both subgroups. To answer whether individuals previously vaccinated against TBEV were expanding pre-existing B cell clones or initiating a primary immune response directed towards cross-reactive and non-cross-reactive epitopes, more sensitive approaches such as antigen-specific BCR sequencing at the RNA level, which can include the constant antibody sequence, would be required. This would allow us to further infer the nature of B cell diversification, dependency on pre-existing immune clones and the shift in epitope immunodominance observed in TBEV-pre-vaccinated individuals.

A

YF17D-specific BCR (n = 696)
Wec et al 2020, PNAS)

TBEV unvaccinated

TBEV vaccinated

B

ID	TBEV vaccination	Timepoint	CDR3	V gene	Specificity (Competition)	Exact match
39	no	Day28	CAKHYDSSGYYYVDYW	IGHV3-23	ADI_45107	no
13	no	Day28	CAKSYDSSGYYYFDYW	IGHV3-30	nd	no
13	**no**	**Day14**	**CAKFYDSSGYYYFDYW**	**IGHV3-23**	**other**	**yes**
171	**yes**	**Day14**	**CAKYYDSSGYYYFDYW**	**IGHV3-23**	**5A_ADI_4510**	**yes**
171	**yes**	**Day14**	**CAKYYDSSGYYYFDYW**	**IGHV3-23**	**5A_ADI_4510**	**yes**
227	**yes**	**Day14**	**CAKYYDSSGYYYFDYW**	**IGHV3-23**	**5A_ADI_4510**	**yes**
241	**no**	**Day7**	**CAKYYDSSGYYYFDYW**	**IGHV3-23**	**5A_ADI_4510**	**yes**
241	no	Day28	CARDHYGMDVW	IGHV3-72	4G2_5A	no
229	yes	Day0	CARDRGGMDVW	IGHV3-7	nd	no
217	yes	Day14	CARDYYGMDVW	IGHV3-72	4G2_5A	no
211	yes	Day28	CARGHYGMDVW	IGHV3-72	4G2_5A	no
211	yes	Day14	CARQFGNWFDPW	IGHV4-39	4G2	no
237	yes	Day0	CARQRGNWFDPW	IGHV4-39	4G2	no
81	yes	Day14	CARQTGNWFDRW	IGHV4-39	4G2	no
171	yes	Day7	CARGPDYW	IGHV3-30	4G2_5A	no
43	**no**	**Day14**	**CSRGPPDYW**	**IGHV3-72**	**nd**	**yes**
13	no	Day14	CTRGPPDYW	IGHV3-72	nd	yes
171	**yes**	**Day28**	**CTRGPPDYW**	**IGHV3-72**	**nd**	**yes**
184	**no**	**Day14**	**CTRGPPDYW**	**IGHV3-72**	**nd**	**yes**
227	**yes**	**Day14**	**CTRGPPDYW**	**IGHV3-72**	**nd**	**yes**
236	**no**	**Day28**	**CTRGPPDYW**	**IGHV3-72**	**nd**	**yes**
81	**yes**	**Day14**	**CTRGPPDYW**	**IGHV3-72**	**nd**	**yes**
81	yes	Day28	CAKGDPDYW	IGHV3-30	4G2_5A	no
43	no	Day28	CARDSWPADYW	IGHV3-7	4G2	no
178	**yes**	**Day14**	**CARETANNWFDPW**	**IGHV4-59**	**nd**	**yes**
227	yes	Day0	CARGPPDYW	IGHV3-72	nd	no
229	yes	Day14	CARGPPDYW	IGHV3-72	nd	no
227	**yes**	**Day28**	**CARGNIAAAVVYW**	**IGHV4-34**	**nd**	**yes**
217	yes	Day14	CARVYDGAFDIW	IGHV3-72	4G2	no

Exact match ● no ▲ yes

C

YF17D plasmablasts (n=15.269)
Davydov et al (2018, Front. Immunol.)

TBEV unvaccinated

TBEV vaccinated

D

SARS-CoV2/RSV/EBOV-specific BCR (n = 2.044)
Curated database by Stewart et al (2022, Front. Immunol.)

TBEV unvaccinated

TBEV vaccinated

E

Flavivirus-specific BCR (n = 570)

TBEV unvaccinated

TBEV vaccinated

● DENV ● WNV ● ZIKV/DENV ● ZIKV DIII

Figure 20. B cell sequences shared with other datasets

A) Longitudinal SHM levels of the BCR sequences found to match with the Wec et al PNAS 2019 dataset of YF17D-specific B cell clones.

B) Table summarizing the matching clones with Wec's dataset and their epitope specificity.

C) Longitudinal SHM levels of the BCR sequences found to match with the Davydov et al Front. immunol. 2018 dataset of YF17D vaccine-induced plasmablasts.

D) Longitudinal SHM levels of the BCR sequences found to match with the Stewart et al Front. Immunol. 2022 dataset of EBOV, RSV and Sars-Cov2 -specific B cell clones.

E) Longitudinal SHM levels of the BCR sequences that were found to match with 570 clones specific for DENV, WNV, or ZIKV.

The color indicates the CDR3 sequence except for E, which indicates the matching flavivirus. Dots reflect a convergence of same V gene and 95% aminoacidic similarity with the CDR3, triangles indicate a perfect, 100% sequence match with the CDR3.

4. Discussion

4.1 Overview*

The live-attenuated YF17D vaccine exhibits an outstanding performance and offers a unique opportunity to study a potent and protective anti-flavivirus response. YF17D was empirically developed (Theiler & Smith, 1937) and achieved an optimal balance between immunogenicity and attenuation. However, the mechanisms underlying YF17D attenuation remain poorly understood. The virulent Asibi strain, from which YF17D is derived, differs in only 32 amino acid positions, with 12 of these changes located in the E protein, which regulates virus tropism, and cell entry, and is the primary target of the antibody response (Hahn et al., 1987). Although beyond the scope of this dissertation, subtle variations in virus tropism, cell entry, structure, and immunomodulation induced by these 32 substitutions likely underlie the optimal performance of the YF17D vaccine strain.

Flavivirus infections represent a significant public health concern. Vaccination remains the most effective approach for mitigating the spread of flaviviruses, such as DENV and ZIKV. Given the global prevalence of flaviviruses, it is urgent to understand the influence of pre-existing immunity on immune responses to current vaccines, such as YF17D, and to design new vaccination strategies. Nevertheless, vaccine efficacy in the context of pre-existing immunity to other flaviviruses remains poorly studied. In this dissertation, the influence of pre-existing cross-reactive immunity on the response to the live YF17D vaccine was investigated in a longitudinal cohort of 250 young, healthy YF17D vaccine recipients, stratified based on their prior immunization with the inactivated TBEV vaccine.

Pre-existing immunity induced by the TBEV vaccine profoundly influences the immunogenicity and epitope immunodominance of the YF17D vaccine. This study presents a comprehensive characterization of the humoral immune response elicited by YF17D in both groups, aiming to delineate the differences in antibody abundance, epitope specificity, and antibody-mediated functionality. Furthermore, the effect of TBEV pre-immunity on vaccine immunogenicity was assessed by considering not only the neutralizing antibody titer but also the magnitude and functionality of the antigen-specific CD4 and CD8 T cell response. Additionally, in-depth phenotyping of the longitudinal dynamics of CD4, CD8, and B cells following vaccination together with bulk BCR sequencing data is presented to further describe the impact of TBEV pre-vaccination on the kinetics, epitope-dominance, and magnitude of the YF17D response. Collectively, by assessing vaccine epitope immunodominance, vaccine immunogenicity, and response kinetics, this dissertation aimed to comprehensively explore the key aspects of the adaptive immune response induced by the YF17D vaccine within the context of pre-existing TBEV immunity.

While the mechanisms governing the outcome of immunization with the YF17D vaccine in the presence of pre-existing immunity remain unclear and require further

investigation with advanced methodologies, the results presented here underscore the potentially combined influence of three phenomena in TBEV pre-immunized individuals. These include the enhancement of vaccine immunogenicity via ADE, the elicitation of a recall response with a potential original antigenic sin effect, and the impact of pre-circulating antibodies on B cell development and vaccine responses via antibody feedback.

4.2   Pre-existing immunity and the humoral response to the YF17D vaccine*

IgG and IgM mediated neutralization and cross-reactivity in TBEV-pre-vaccinated and unvaccinated individuals

Given the high immunogenicity of the YF17D vaccine, all participants in the study exhibited seroconversion and developed protective neutralizing antibody titers by day 28 pv. By day 28, the polyclonal neutralizing response was predominantly reliant on the IgM fraction. The neutralizing mechanism of IgM thereby likely benefits from the multivalent binding to the virion (Singh et al., 2022). At this timepoint, a clear distinction emerged between TBEV-pre-vaccinated and unvaccinated vaccinees. In individuals without previous exposure to flaviviruses, the YF17D vaccine induced a non-cross-reactive neutralizing antibody response. In contrast, TBEV-experienced individuals produced significant quantities of cross-reactive IgG antibodies directed against the pan-flavivirus FLE. This cross-reactivity represents an undesirable effect that can lead to ADE of DENV infection.

The YF17D vaccine virus appears to possess a unique ability to mask cross-reactive epitopes while promoting the production of neutralizing antibodies in individuals with no previous exposure to flaviviruses. This characteristic is not observed in other flavivirus infections or vaccinations, which typically lead to the production of cross-reactive antibodies (Chih-Yun et al., 2008; Dejnirattisai et al., 2015; Malafa et al., 2020). For example, in the cases of DENV or ZIKV infection, the immunodominance of the FLE results in a preferential generation of cross-reactive antibodies that have limited cross-neutralizing capacity but can induce ADE (Beltramello et al., 2010). Moreover, our study demonstrates that TBEV vaccination alone induced a cross-reactive response that had the potential to enhance DENV infection (Santos-Peral et al., 2023). This optimal non-crossreactive YF17D priming could explain the lack of an association between YF17D vaccination and dengue severity (Luppe et al., 2019) in contrast to the JEV vaccine, which induces a cross-reactive response and is associated with severe dengue disease (Anderson et al., 2011; Saito et al., 2016). This unique epitope presentation may contribute to the exceptional performance of the YF17D vaccine. We hypothesize that this capability is inherently present in the YF17D vaccine strain and may have been achieved during the virus's attenuation process, resulting in a structurally more stable virion, with limited breathing that could result in FLE exposure. This stability would favor the priming of anti-EDE-like antibodies while minimizing anti-FLE antibody generation. Whether the Asibi strain and currently circulating strains retain the ability to conceal cross-reactive epitopes or this feature is exclusive to the vaccine strain requires further

investigation. Murine studies have revealed distinct serocomplexes induced by the YF17D vaccine and the Asibi strain (Cammack & Gould, 1986; Davis & Barrett, 2020) highlighting fundamental differences in epitope display. Nevertheless, these murine studies are restricted by the low number of mAbs tested, which likely do not comprehend the full epitope-landscape of YFV. A comprehensive understanding of this aspect, along with the identification of amino acids or structural determinants contributing to it, could serve as a stepping stone for the development of anti-flavivirus vaccines with minimal cross-reactivity. In the pursuit of concealing the FLE and priming for quaternary epitopes, vaccination approaches involving the use of covalently locked recombinant dimers have been considered for dengue and Zika (Rouvinski et al., 2017; Slon-Campos et al., 2019). However, further research on the YF17D vaccine may provide insights into alternative methods for achieving optimal antibody priming.

To date, only four studies have successfully produced human monoclonal antibodies against YFV. Daffis et al (Daffis et al., 2005) identified monoclonal antibodies with a strong neutralizing capacity that were elicited following wild-type YFV infection and vaccination. These antibodies were specific to YFV only. In the second study, Li et al. characterized 8 mAb isolated from infected patients using sE to sort B cells. These antibodies mapped to the Pr binding site (Y. Li et al., 2022). Doyle et al created hybridomas with MBC from a YF17D vaccinee (Doyle et al., 2022). Lastly, Wec et al. (Wec et al., 2020) used sE to sort antigen-specific MBC to generate a large panel of mAb. It's worth noting that these studies were inherently biased towards detecting antibodies with monomeric specificities. However, a representative subset of the isolated monoclonal antibodies competed with 4G2 for binding and approximately 6% demonstrated cross-reactivity with other flaviviruses such as ZIKV, DENV, and WNV. This finding suggests that the YF17D vaccine alone can also induce antibodies that target a broader range of flaviviruses. Nevertheless, based on the findings presented in this dissertation, the detection and expansion of cross-reactive antibodies in the polyclonal serum appear to be minimal (Santos-Peral et al., 2023) Furthermore, recently generated data indicated a similar outcome one year after vaccination, suggesting that the antibody response had not significantly diversified toward the FLE.

The expansion of FLE antibodies by TBEV-pre-vaccinated individuals depends on MBC recognition of the epitope. However, close concealment of the FLE by the YF17D virion would hamper this process. Nevertheless, there may still be a transient exposure of the FLE, during natural viral oscillations (Stiasny et al., 2022), enough to trigger a recall response from a MBC even though not enough to trigger a primary response in a naïve B cell (Vratskikh et al., 2013; Wec et al., 2020). Consistent with this study, minimal cross-reactivity following YF17D vaccination was observed by others (Pond et al., 1967; Souza et al., 2019). Collectively, the FLE-dominant response in TBEV pre-vaccinated individuals may result from a recall response by MBC to a reduced but sufficiently exposed FLE. Alternatively, the accessibility of the FLE may be modulated by the binding of cross-reactive antibodies to the YF17D virion, stabilizing a state with exposed FLE.

The B cell response to the YF17D vaccine continues to mature for 6 to 9 months after vaccination (Wec et al., 2020). As the immune response progresses, the antibody

response becomes more diversified in terms of epitope recognition and binding affinity (Hägglöf et al., 2023). To extend our understanding beyond day 28 post-vaccination, the long-term effects of pre-existing immunity on the antibody response to YF17D were assessed using one-year samples from a separate, independent cohort. Since these results have only recently been generated with an independent cohort, they are not presented in this dissertation. In summary, the findings described on day 28 samples were replicated in the one-year samples, with TBEV-pre-vaccinated individuals exhibiting high titers of cross-reactive, ADE-enhancing, but poorly neutralizing antibodies, and TBEV-unvaccinated individuals developed an expanded non-cross-reactive, effective-neutralizing antibody response. The IgM fraction retained significant neutralizing potential, which can persist for several years (Gibney et al., 2012).

Determination of epitope specificities and neutralization determinants

To gain a more comprehensive understanding of the humoral response and to unravel the function mediated by IgG antibodies against different epitopes, I utilized a series of recombinant envelope protein mutants. In addition to the E protein subdomains, the antigen design was focused on creating constructs containing quaternary dimeric epitopes, aiming to replicate the epitope diversity found on the YF17D virus particle. Through targeted removal of antibodies from sera, I could show that quaternary epitopes were the primary focus of neutralizing antibodies. Additionally, I identified the FLE as the target of the cross-reactive IgG response in individuals with prior TBEV exposure.

Previous studies have emphasized the importance of the FL-proximal site in DII for YFV neutralization (Doyle et al., 2022; Y. Li et al., 2022; Lu et al., 2019; Wec et al., 2020). Here, the impact of FL-proximal epitopes on neutralization became evident when a DI-II construct was employed for antibody depletions. The influence of DI-II-specific epitopes was more pronounced among TBEV-pre-vaccinated individuals. Nevertheless, using covalently bound dimers, I could show that quaternary epitope binders represent the most substantial fraction of neutralizing activity within the IgG-fraction of the polyclonal human sera post-YF17D vaccination. To date, a precise mapping of EDE-like antibodies for YFV has not been published and their characterization was impossible in studies using monomeric sE for B-cell sorting (Y. Li et al., 2022; Wec et al., 2020). The relevance of EDE-like antibodies in anti-YFV immunity has been previously suggested, as monomeric specificities alone did not fully account for the neutralizing activity in polyclonal human sera (Vratskikh et al., 2013), and viral escape variants to potent neutralizing antibodies mutated sites compatible with an EDE-like epitope in YFV (Daffis et al., 2005).

The dissection of antibody specificities in polyclonal serum is challenging given that FLE, dimeric, and FL-proximal epitopes can overlap at certain positions. Furthermore, the absence of a clearly defined EDE on YFV complicates our understanding of the exact amino acids that make up this epitope. The design of the locked-dimer construct forced the structural occlusion of the FL together with an added modification in position L107. This construct was designed to deplete EDE antibodies, thus significantly reducing serum

neutralization activity while preserving undepleted FLE-specific antibodies. A similar construct for DENV (Rouvinski et al., 2017), was able to bind most EDE antibodies but showed reduced binding for specific EDE variants. Unfortunately, the YF17D E locked-dimer construct failed to deplete the principal antibody fraction responsible for the virus neutralization. In this study, I created a locked-dimer antigen that incorporated the N71K mutation. This mutation was identified in neutralization escape variants to a highly effective neutralizing mAb 7A, the binding site of which is compatible with EDE (Daffis et al., 2005). The N71K substitution introduces a positive charge and a large lysine side chain in the contact region for mAb 5A. This area in DII is an important binding site for neutralizing antibodies. In fact, new infectious strains circulating in South America with increased evasion of neutralization induced by vaccination carry amino acid substitutions in this area, such as H67N and A83E (Haslwanter et al., 2022). Other variations in these strains include the introduction of a glycan at position D270N, as well as additional variations like N271S and N272K, which are located in a region proximal to DI and may interfere with an EDE-like epitope equivalent to the one found in DENV. To complement the toolbox of designed antigens, a second mutation, A240R, was introduced with the idea that a large, polar, positively charged arginine residue would disrupt EDE epitopes in the ij loop. Unfortunately, the locked-dimer construct failed to display the EDE in the first place, rendering the locked-dimer[N71K] and locked-dimer[N71KA240R] constructs ineffective for our purposes. Future research could potentially benefit from the breathing-dimer construct to optimize epitope display and to study N71K and 240R mutations in this setting to investigate whether these positions indeed serve as binding sites for an effective neutralizing response.

Collectively, despite the limitations of the constructs, this toolbox proved useful for the dissection of the antibody specificities and function in serum. Moreover, the breathing-dimer construct introduced in this context has the potential to be an excellent candidate for use as bait in B cell studies, facilitating the capture of B cells and the mapping of antibodies that target quaternary specificities.

Risk of ADE of DENV infection

The effectiveness of both TBEV and YF17D vaccines is excellent (Kling et al., 2022; Santonja et al., 2022). When individuals are vaccinated against TBEV followed by YF17D, they maintain and generate protective immunity to both of these vaccines with no compromise in the immunogenicity and the generation of a neutralizing response. Nevertheless, the antibody profile elicited by this sequential TBEV and YF17D vaccination consists of elevated cross-reactive antibodies that could enhance DENV infection in vitro. This raises concerns because the risk of severe dengue disease is elevated in heterotypic secondary DENV infections due to ADE (Dejnirattisai et al., 2010; Katzelnick et al., 2017). While tertiary and quaternary DENV infections are clinically silent (Olkowski et al., 2013), a DENV infection in individuals with one previous ZIKV infection or one previous ZIKV followed by a first DENV infection, have also been associated with elevated risk of severe dengue disease (Katzelnick et al., 2020). This suggests that subsequent infections with heterologous viruses do not have the same effect as sequential tertiary or quaternary infections with different DENV serotypes,

which are likely to broaden the diversity of the B cell receptor repertoire towards cross-neutralizing determinants rather than boosting cross-reactivity with ADE potential. Clinical associations have also linked JEV vaccination to increased dengue severity (Anderson et al., 2011). In contrast, there is minimal or negligible cross-reactivity between YF17D and DENV (This study and Souza et al., 2019) which probably underlays the lack of association between YF17D vaccination and a worsened course of dengue disease (Luppe et al., 2019). I hypothesize that subsequent TBEV and YF17D vaccination, and not YF17D vaccination alone, would result in a humoral response comparable to that after a primary DENV infection. These findings imply that consecutive TBEV and YF17D vaccinations, by increasing cross-reactive antibodies with ADE potential, may render individuals vulnerable to severe dengue disease. Furthermore, there are no known shared cross-neutralizing determinants between YF17D and DENV, or TBEV and DENV, which could lead to clinically silent DENV infections. Additionally, YF17D-induced T cells show limited cross-reactivity (Grifoni et al., 2020) and are unlikely to mitigate DENV ADE effects, as observed with the Dengvaxia vaccine which has a YF17D genetic backbone (Ferguson et al., 2016). The double vaccination for TBEV and YF17D is not uncommon among European and Asian travelers living in TBEV-endemic areas and dengue has become one of the most important emerging diseases among European travelers (Gossner et al., 2022). Nevertheless, these observations should be interpreted with caution before an epidemiological study evaluates the clinical impact of subsequent TBEV/YF17D vaccination on dengue disease.

4.3   The combined impact of antibody feedback, epitope rearrangement, ADE-mediated increased immunogenicity, and recall response on the YF17D-induced response in TBEV-pre-vaccinated individuals

The adaptive immune response is characterized by its ability to mount stronger and quicker T and B cell responses upon secondary exposures to a challenge. This relies on memory T and B cells elicited during the primary challenge, which persist in circulation or lymphoid organs for years. The TBEV vaccine, an adjuvanted inactivated vaccine, is capable of inducing durable T, B, and antibody responses (Costantini et al., 2020; Varnaitė et al., 2020). As a result, the immune memory conferred by the TBEV vaccine can be reactivated in response to the related YF17D vaccine. Cross-reactive clones within the MBC compartment may dominate over de novo activated naïve B cells undergoing germinal center reactions, consequently limiting the final diversity of the B cell response to a new challenge (Wong et al., 2020). This phenomenon, often referred to as Original Antigenic Sin (OAS) (Vatti et al., 2017) would ultimately lead to a robust expansion of pre-existing cross-reactive B and T cell clones targeting conserved epitopes between TBEV and YF17D. The more rapid seroconversion of individuals pre-vaccinated with TBEV and the higher final titer of antibodies directed against cross-reactive epitopes are compatible with a secondary recall response and OAS. Nevertheless, at the cellular level, TBEV-induced YF17D-cross-reactive B and T cells could not be distinguished from background at baseline in flow cytometry using tetramer staining or ex vivo re-stimulation. This could be due to the very low frequency of these cells in circulation, being at the sensitivity threshold of these assays. However, no significant

difference in the magnitude of the T cell response was observed between TBEV-vaccinated and unvaccinated individuals at later timepoints, despite clearly detectable antigen-specific T-cell responses. BCR-repertoire sequencing also failed to identify a distinct B cell signature in the bulk B cell repertoire between TBEV-naïve and TBEV-pre-vaccinated individuals. These results suggest a limited effect of TBEV-pre-vaccination on the diversity and re-activation of memory B and T cells following YF17D vaccination. In line with a secondary response signature, and consistent with serology data, antigen-specific B cells found in circulation occurred at higher frequencies in TBEV-pre-vaccinated individuals versus TBEV-unvaccinated. However, this detection is inherently biased towards epitopes displayed in the monomeric sE and tends to capture high-affinity B cell clones. Consequently, the detected antigen-specific B cells were predominantly memory, class-switched IgG+ B cells that had undergone a germinal center reaction and were expanded upon vaccination. Overall, YF17D vaccination might induce a recall or anamnestic response in TBEV pre-vaccinated individuals, this effect is particularly evident in the antibody response but does not significantly impact circulating T and B cell activation.

Nevertheless, the extended breadth of the antibody response to previously unseen epitopes in TBEV-experienced individuals cannot be explained exclusively by a recall response to conserved epitopes. Consequently, additional mechanisms might be at play alongside the recall response in TBEV-pre-vaccinated individuals.

Antibodies induced by TBEV, present at baseline, can bind to the YF17D virus without neutralizing it (This study and Bradt et al., 2019). These antibodies may exert influence by either masking or exposing epitopes presented by follicular dendritic cells in the GC (Schaefer-Babajew et al., 2023). In this context, pre-existing cross-reactive antibodies might have contributed to broadening antibody specificities, as observed with DIII specificities. The antibody feedback mechanism depends on a complex interplay between the antigen dose, antibody titers, and time intervals between immunological challenges. In a malaria vaccine study, repeated boosting resulted in antibody diversification towards subdominant epitopes due to dominant epitope masking, while shorter vaccination intervals limited the recruitment of new B cells, subsequently weakening the response (McNamara et al., 2020). Similarly, in SARS-CoV-2 vaccination, individuals treated with a therapeutic antibody cocktail before vaccination exhibited a difference in quality of the response. Therapeutic antibodies redirected the response towards IgM-memory B cells and away from the dominant epitopes covered by the therapeutic antibodies to subdominant, poor-neutralizing epitopes while lowering the activation threshold of new B cells in the GC and favoring the development of low-affinity antibody clones (Schaefer-Babajew et al., 2023). However, subsequent vaccination with the original Sars-Cov-2 vaccine formulation led to protection against emerging variants of concern due to the continuous diversification of the antibody response towards subdominant but conserved epitopes (Muecksch et al., 2022). Similar to these studies, antibody feedback mechanisms might be occurring during YFV17D vaccination in individuals previously vaccinated against TBEV. These mechanisms could

contribute to the observed phenomenon, wherein the antibody response is directed at higher levels not only to FLE but also to non-cross-reactive epitopes.

Another observation that is not solely accounted for by the stimulation of a memory response is the expansion of FLE antibodies exclusively in TBEV-pre-vaccinated individuals and not in flavivirus-naive individuals. As previously discussed, the FLE epitope on the YF17D surface is effectively concealed. Thus, I hypothesize that the accessibility of the FLE might be modulated by the binding of cross-reactive antibodies to the YF17D virion. This binding could stabilize a conformation that exposes the FLE, thereby favoring its prominence and triggering a robust de novo cross-reactive response. E glycoprotein rearrangement upon antibody binding has been observed in other viruses like DENV (Lok et al., 2008). Furthermore, filament-shaped conformations of DENV and ZIKV were shown to be stabilized upon the binding of the C10 mAb, altering the conventional arrangement of the envelope protein dimeric structure (Morrone et al., 2020). Similarly, the administration of mAb A3, which targets TBEV DII, led to an increase in DII-specific antibodies in mice immunized with sE dimers. A3 mediated the dissociation of dimers and promoted a specific antibody response to the FLE (Tsouchnikas et al., 2015). Altogether, epitope rearrangement within the YF17D structure might explain the observed difference in epitope immunodominance between TBEV-pre-vaccinated and unvaccinated individuals. Nevertheless, further experiments, such as electron microscopy visualization of the virus structure, are required to confirm this hypothesis.

Lastly, cross-reactive antibodies induced by the TBEV vaccine can enhance YF17D infection via ADE as shown by data from Sebastian Goresch (Santos-Peral et al., 2023) in our group-. We observed that higher titers of enhancing antibodies before YF17D vaccination were associated with a stronger neutralizing antibody response in TBEV-pre-vaccinated individuals, indicating increased vaccine immunogenicity. Moreover, higher baseline TBEV-induced YF17D-specific antibody titers, reflecting the strength of TBEV-induced cross-reactive immunity, correlated with stronger CD4 T cell responses in both function and magnitude, as well as with enhanced neutralizing capacity. The enhanced immunogenicity is compatible with a previous study by Chan et al (2019) which showed that JEV vaccine-induced cross-reactive antibodies enhance YF17D vaccine immunogenicity via ADE (Chan et al., 2016). However, further research is necessary to determine the extent to which YF17D-ADE affects virus replication, antigen dose, and virus sensing by pattern recognition receptors and FcyR-triggering.

Taken together, the humoral response in TBEV-pre-vaccinated individuals is directed preferentially towards the FLE and reaches a higher magnitude. This response appears stronger, more vigorous, and faster but is misdirected toward non-neutralizing epitopes, without a clear advantage in mediating virus neutralization for these individuals. This immune response is probably the result of combined mechanisms including YF17D vaccine epitope rearrangement, antibody feedback, anamnestic response, and enhanced immunogenicity through ADE.

4.4   Pre-existing immunity and cellular immune responses to YF17D vaccine.

To comprehend the influence of TBEV pre-vaccination on the YF17D-induced cellular responses and the longitudinal response to the vaccine, this study integrated the detection and characterization of antigen-specific B and T cells using a 24- and 27-marker panel in spectral flow cytometry. Furthermore, an *ex vivo* re-stimulation assay was employed to assess the function and enumeration of the antigen-specific T-cell response. This readout serves as an endpoint assay evaluating YF17D-induced immunity and functions as a correlate of vaccine immunogenicity. Lastly, longitudinal bulk gDNA BCR repertoire sequencing was implemented to better understand the differences observed in the humoral response. BCR repertoire data is useful to illustrate variations in clone dominance, diversity, and to explain the origin of responding B cells upon YF17D vaccination. These efforts aimed to shed more light on the discussed shift in epitope immunodominance and vaccine immunogenicity in the context of TBEV pre-existing immunity (as discussed in Chapter 4.3).

The flow cytometric analysis uncovered a consistent increase in the frequency of YF17D-specific B cells by day 28 in both vaccine groups. However, individuals pre-vaccinated against TBEV exhibited a notably higher frequency of YF17D-E protein specific B cells. Both TBEV pre-vaccinated and naïve individuals displayed an equally expanded plasmablasts response (including YF17D-specific and unspecific cells), detectable at day 7 and peaking at day 14 post-vaccination. This suggests that the frequency of antigen-specific memory B cells post-vaccination is dissociated from the intensity of the plasmablasts response. Moreover, the longitudinal kinetics of the B cell response revealed that activated and proliferating B cells, representing approximately 2% of the bulk B cells in circulation and peaking by day 14, displayed a similar dynamic in both groups. However, these dynamics did not align with the substantial changes observed in serology or with the quantification of antigen-specific B cells using flow cytometric tetramer staining or ELISpot (Santos-Peral et al., 2023). This discrepancy might be due to the low frequency of antigen-specific B cells in circulation and their weak affinity in binding to sE antigens when utilized as bait. This might bias the detection towards IgG-positive, class-switched B cells. Moreover, a significant proportion of YF-specific plasmablasts is presumably producing IgM antibodies (Quach et al., 2016), which are produced to a similar extent in both subgroups and that we were unable to capture by tetramer-staining or ELISpot. Furthermore, the chosen detection methods might have limitations in identifying antigen-specific MBC that are selected by higher avidity in the GC rather than for high affinity (Viant et al., 2020). Additionally, plasmablasts or activated B cells in circulation even though expanded after exposure to YF17D may not represent antigen-specific cells, as observed in other viruses like Ebola virus (Davis CW et al, 2019), DENV (Appanna et al., 2016) and influenza virus (Ellebedy et al., 2016). Importantly, TBEV-induced plasma cells residing in the bone marrow might be significant producers of the antibodies found in serum, and their kinetics might not reflect the behavior of the MBC compartment. In this study, MBC with a resting memory phenotype showed a decrease in their circulating frequency, indicating a possible recirculation to lymph nodes for further maturation in the GC reaction (Viant et al., 2020). MBC with a

higher affinity were identified in TBEV pre-vaccinated donors on day 28 post-vaccination, hinting at further optimization of the B cell response.

The analysis of the bulk BCR repertoire, conducted without specific enrichment for YF17D-specific B cells, revealed identifiable longitudinal changes induced by YF17D vaccination. However, these changes did not entirely mirror the differences observed in serology. The decrease in diversity observed and the increase in germline-like sequence by day 14 pv are in line with previous studies (Kotagiri et al., 2022; Stewart et al., 2022) and could signify the emergence of dominant clones induced by the vaccine. Yet, these vaccine-induced effects may be overshadowed by the presence of numerous unrelated B cells in circulation. Only about 2% of B cells were responsive to vaccination based on flow cytometric analysis. Moreover, the methodology used for BCR sequencing can only capture a fraction of YF17D-induced B cells in circulation, and approximately 30,000 clones per sample are sequenced. This limitation means that rare clones induced by the YF17D vaccine might go undetected.

Unfortunately, YF17D-specific clones at baseline could not be conclusively identified by the methods used, probably, due to the scarce number of TBEV-induced cross-reactive memory B cell clones in circulation, that falls below the assay's sensitivity. This limitation obstructed the efforts to determine the origin of the high levels of FLE antibodies and the immunodominance shift to cross-reactive epitopes. A more targeted approach, like isolating and sequencing antigen-specific B cell clones or generating monoclonal antibodies from the plasmablast or activated B cell compartment, would likely be necessary to establish a clear signature of their origin, maturation level, and clonal composition.

In this study, a surprising discovery was the similarity in activation dynamics observed in the circulating immune populations between TBEV pre-vaccinated individuals and those without prior vaccination. Typically, an anamnestic response in T or B cells would result in a stronger and earlier activation of T or B cell populations in circulation. The general activation of T and B cells induced by YF17D vaccination was evident for both groups, consistent with earlier reports showing a similar expansion of CD38+ T cells in both primary and secondary cases of DENV for both bulk and tetramer-specific T cells (Friberg et al., 2011). Likewise, this activated phenotype, characterized by CD38, Ki67, BCL2lo, HLA-DR, and perforin expression is consistently triggered after vaccination for all T cell memory subtypes, including CM, EM, Naïve, Tscm, and EMRA including tetramer-specific CD8 T cells (Fuertes Marraco et al., 2022). Good vaccine responders showed a more pronounced perturbation of these activation markers (not shown), which indicates an association of the magnitude of T cell activation with vaccine immunogenicity. Nevertheless, the T cell kinetics remained unaltered by the presence/absence of previous immunity to TBEV and was consistently induced after vaccination. It is well documented that infection or vaccination can lead to the expansion and activation of T cells that are not specific for the immunological challenge (Tough et al., 1996). This bystander T cell activation affects mostly memory T cells, whose threshold for activation is lower than for naïve CD4 T cells (Paprckova et al., 2023) and might underlay the high frequencies of activated T cells detected by flow cytometry.

The detailed characterization of the T cell response to YF17D vaccination was beyond the scope of this study, but a predominant activation of Th1 cells concurrent with Tfh cells was observed, known to be a good indicator of vaccine immunogenicity (Huber et al., 2020). However, none of the previously identified correlates of vaccine-induced responses like BCMA expression, frequency of CD4 Tfh CXCR3, and CD38+CD20+ B cells (Kotliarov et al., 2020; Querec et al., 2009; Tsang et al., 2014) showed differences between TBEV pre-vaccinated and unvaccinated individuals longitudinally after vaccination. The homogeneity in the T cell response observed for both groups could be explained by the absence of cross-reactive T cells or the dissociation between the activation profile and the magnitude or generation of long-lived populations. Though T cell cross-reactivity across flaviviruses exists, it is limited (Grifoni et al., 2020) and the inactivated nature of the TBEV vaccine restricts the T cell response to the structural proteins, limiting the impact of TBEV pre-vaccination on the T cell response induced by YF17D vaccination.

In summary, the longitudinal T cell kinetics did not indicate a signature attributable to a recall response. The findings suggest the absence of a dominant cross-reactive T cell response induced by TBEV immunization.

4.5   Summary and Future Research.

Flaviviruses pose a significant public health concern, and vaccination is the most effective measure to mitigate their impact and prevent their spread. The highly effective YF17D vaccine was empirically developed, and little is known about the factors that determine its immunogenicity. Typically, studies evaluate the effectiveness of live vaccines in individuals with no prior immunological exposure. However, the impact of pre-existing immunity to related vaccines or viruses is often unknown and understudied. Given the high prevalence of flaviviruses, YF17D is frequently administered to individuals with cross-reactive immunity. The way this impacts the vaccine response and the clinical course in secondary infections with DENV remains a highly relevant and open question. Furthermore, unlike other flaviviruses, the epitopes crucial for neutralizing YF17D have not been clearly defined yet. In this study, TBEV pre-vaccination was used to assess the impact of pre-existing cross-reactive immunity on the response to the YF17D vaccine in humans. Our findings can be summarized in six key points:

1. The response to YF17D is skewed towards the cross-reactive FLE in TBEV-vaccinated individuals. Consequently, the expanded cross-reactive IgG response can mediate ADE of DENV infection.

2. YF17D vaccine elicits a protective neutralizing response that is not cross-reactive in flavivirus-naïve individuals.

3. Neutralizing antibodies predominantly target the quaternary dimeric arrangement of the envelope protein of YF17D, whereas cross-reactive antibodies specifically bind to the conserved FLE.

4. TBEV-pre-vaccinated individuals manifest a humoral response consistent with a secondary anamnestic response dominated by cross-reactive specificities but in

addition exhibit a further diversification of the antibody response against non-crossreactive epitopes.

5. TBEV-induced immunity may enhance YF17D immunogenicity, leading to increased antibody and CD4 T cell responses.

6. TBEV pre-vaccination does not alter the longitudinal dynamics of cellular responses following vaccination.

An important finding of this study is that the YF17D vaccine induces non-cross-reactive protective immunity in individuals who have not received the TBEV vaccine. This distinctive characteristic is a cornerstone of effective anti-flavivirus protective immunity and represents an optimal epitope presentation by the YF17D virion. Further research is needed to uncover why the YF17D can effectively mask cross-reactive epitopes when administered to individuals with no prior flavivirus exposure, but not to those with pre-existing flavivirus immunity.

In this context, further research is required to gain a better understanding of the B cell response. It remains an open question whether the YF17D vaccine induces a de novo cross-reacting immune response or relies on pre-existing memory B cells. Additionally, how pre-existing antibodies may influence the arrangement of the E protein on the virion, potentially reshaping the epitope dominance in the vaccine response, is a highly relevant and still unanswered question. Analyzing the antigen-specific BCR repertoire is crucial for a deeper comprehension of cross-reactivity in TBE pre-vaccinated individuals and for distinguishing disparities in the B cell response between individuals with and without prior TBEV exposure. BCR sequencing will provide insights into whether the response in TBEV-experienced individuals is characterized by the emergence of new B cell clones or the expansion of existing ones. Furthermore, this study has not explored the impact of other functions mediated by pre-existing antibodies on the YF17D response. ADCC, ADCP, and antibody-mediated complement activation may all play a pivotal role in shaping the immune response against YF17D and could contribute to the reshaping of the epitope immunodominance described here.

It is important to note that the affinity or avidity of antibody binding have not been directly considered in this dissertation. Furthermore, the serology assays did not take into account potential cooperative and/or competitive interactions between antibody populations targeting the same antigen but with different specificities, avidities, and concentrations. These interactions can be crucial in understanding the overall immune response.

The usage of E monomer moieties in previous studies for studying the humoral response or as bait for antigen-specific B cell responses in BCR and monoclonal antibody production has limited the understanding of the complete antibody response (Haslwanter et al., 2022; Vratskikh et al., 2013; Wec et al., 2020) This limitation has constrained previous studies to identify only the FL-proximal region as an essential neutralizing site for YFV (Daffis et al., 2005; Doyle et al., 2022; Y. Li et al., 2022; Lu et al., 2019). In this work, I propose the use of the breathing-dimer as a valuable tool for

identifying quaternary antibodies. Future research can benefit from this construct to isolate and map monoclonal antibodies with high neutralizing potential.

I have presented mechanistic evidence suggesting that the response in TBEV-pre-vaccinated individuals may increase their susceptibility to severe dengue disease. Given that the YF17D vaccine is administered to travelers or in areas where DENV and YFV co-circulate, these results potentially impact real-life scenarios. It is worth noting that ADE of DENV was measured in vitro. To the best of my knowledge, there is no clinical data demonstrating a direct association between subsequent TBEV and YF17D vaccination and dengue disease. The Robert Koch Institute in Germany and the European Center for Disease Control report the annual number of dengue cases in Europe per country, but the severity of the disease is not noted, and patient data that could help infer previous vaccinations received is lacking. Therefore, there is an urgent need for an epidemiological study to evaluate whether TBEV/YFV vaccination has clinical implications for dengue severity. Considering the findings of other researchers such as Anderson et al. in 2011, which showed an association between JEV vaccination and Dengue disease, and Katzelnick et al. in 2020, showing that antibody levels elicited after a single ZIKV, DENV, or ZIKV/DENV infections are also associated with worsened clinical dengue disease, together with the data presented here, we believe there is substantial evidence to support this hypothesis (Anderson et al., 2011; Katzelnick et al., 2017, 2020).

In summary, the development of new vaccines requires new antigens and knowledge. Our understanding of protective epitopes, their dominance, and B cell responses remains limited, constraining our ability to design successful vaccines. Additionally, in real-life scenarios, individuals are exposed to or vaccinated against related pathogens, which can have a significant impact on vaccine effectiveness. This work provides new insights into the interplay between vaccine virus biology and human immunology in determining the antigenicity and immunogenicity of the YF17D vaccine in the context of cross-reactive pre-existing immunity. These insights have implications for vaccine design, aiming to direct responses to protective antigenic sites with minimal cross-reactivity.

.

References

Akondy, R. S., Fitch, M., Edupuganti, S., Yang, S., Kissick, H. T., Li, K. W., Youngblood, B. A., Abdelsamed, H. A., McGuire, D. J., Cohen, K. W., Alexe, G., Nagar, S., McCausland, M. M., Gupta, S., Tata, P., Haining, W. N., McElrath, M. J., Zhang, D., Hu, B., … Ahmed, R. (2017). Origin and differentiation of human memory CD8 T cells after vaccination. *Nature*, *552*(7685), 362–367. https://doi.org/10.1038/nature24633

Akondy, R. S., Monson, N. D., Miller, J. D., Edupuganti, S., Teuwen, D., Wu, H., Quyyumi, F., Garg, S., Altman, J. D., Del Rio, C., Keyserling, H. L., Ploss, A., Rice, C. M., Orenstein, W. A., Mulligan, M. J., & Ahmed, R. (2009). The Yellow Fever Virus Vaccine Induces a Broad and Polyfunctional Human Memory CD8 + T Cell Response . *The Journal of Immunology*, *183*(12), 7919–7930. https://doi.org/10.4049/jimmunol.0803903

Allwinn, R. (2011). Significant increase in travel-associated dengue fever in Germany. *Medical Microbiology and Immunology*, *200*(3), 155–159. https://doi.org/10.1007/s00430-011-0185-2

Anderson, K. B., Gibbons, R. V, Thomas, S. J., Rothman, A. L., Nisalak, A., Berkelman, R. L., Libraty, D. H., & Endy, T. P. (2011). Preexisting Japanese Encephalitis Virus Neutralizing Antibodies and Increased Symptomatic Dengue Illness in a School-Based Cohort in Thailand. *PLOS Neglected Tropical Diseases*, *5*(10), e1311. https://doi.org/10.1371/journal.pntd.0001311

Appanna, R., KG, S., Xu, M. H., Toh, Y.-X., Velumani, S., Carbajo, D., Lee, C. Y., Zuest, R., Balakrishnan, T., Xu, W., Lee, B., Poidinger, M., Zolezzi, F., Leo, Y. S., Thein, T. L., Wang, C.-I., & Fink, K. (2016). Plasmablasts During Acute Dengue Infection Represent a Small Subset of a Broader Virus-specific Memory B Cell Pool. *EBioMedicine*, *12*, 178–188. https://doi.org/10.1016/j.ebiom.2016.09.003

Austin, S. K., Dowd, K. A., Shrestha, B., Nelson, C. A., Edeling, M. A., Johnson, S., Pierson, T. C., Diamond, M. S., & Fremont, D. H. (2012). Structural Basis of Differential Neutralization of DENV-1 Genotypes by an Antibody that Recognizes a Cryptic Epitope. *PLoS Pathogens*, *8*(10). https://doi.org/10.1371/journal.ppat.1002930

Barba-Spaeth, G., Dejnirattisai, W., Rouvinski, A., Vaney, M.-C., Medits, I., Sharma, A., Simon-Lorière, E., Sakuntabhai, A., Cao-Lormeau, V.-M., Haouz, A., England, P., Stiasny, K., Mongkolsapaya, J., Heinz, F. X., Screaton, G. R., & Rey, F. A. (2016). Structural basis of potent Zika–dengue virus antibody cross-neutralization. *Nature*, *536*(7614), 48–53. https://doi.org/10.1038/nature18938

Barba-Spaeth, G., Longman, R. S., Albert, M. L., & Rice, C. M. (2005). Live attenuated yellow fever 17D infects human DCs and allows for presentation of endogenous and recombinant T cell epitopes. *The Journal of Experimental Medicine*, *202*(9), 1179–1184. https://doi.org/10.1084/jem.20051352

Beltramello, M., Williams, K. L., Simmons, C. P., Macagno, A., Simonelli, L., Quyen, N. T. H., Sukupolvi-Petty, S., Navarro-Sanchez, E., Young, P. R., de Silva, A. M., Rey, F. A.,

Varani, L., Whitehead, S. S., Diamond, M. S., Harris, E., Lanzavecchia, A., & Sallusto, F. (2010). The Human Immune Response to Dengue Virus Is Dominated by Highly Cross-Reactive Antibodies Endowed with Neutralizing and Enhancing Activity. *Cell Host & Microbe*, *8*(3), 271–283. https://doi.org/10.1016/j.chom.2010.08.007

Blitvich, B., & Firth, A. (2015). Insect-Specific Flaviviruses: A Systematic Review of Their Discovery, Host Range, Mode of Transmission, Superinfection Exclusion Potential and Genomic Organization. *Viruses*, *7*(4), 1927–1959. https://doi.org/10.3390/v7041927

Blom, K., Braun, M., Ivarsson, M. A., Gonzalez, V. D., Falconer, K., Moll, M., Ljunggren, H.-G., Michaëlsson, J., & Sandberg, J. K. (2013). Temporal Dynamics of the Primary Human T Cell Response to Yellow Fever Virus 17D As It Matures from an Effector- to a Memory-Type Response. *The Journal of Immunology*, *190*(5), 2150–2158. https://doi.org/10.4049/jimmunol.1202234

Bovay, A., Speiser, D. E., & Fuertes Marraco, S. A. (2020). Early drop of circulating T cells negatively correlates with the protective immune response to Yellow Fever vaccination. *Human Vaccines & Immunotherapeutics*, *16*(12), 3103–3110. https://doi.org/10.1080/21645515.2020.1750249

Bradt, V., Malafa, S., von Braun, A., Jarmer, J., Tsouchnikas, G., Medits, I., Wanke, K., Karrer, U., Stiasny, K., & Heinz, F. X. (2019). Pre-existing yellow fever immunity impairs and modulates the antibody response to tick-borne encephalitis vaccination. *NPJ Vaccines*, *4*, 38. https://doi.org/10.1038/s41541-019-0133-5

Brüggemann, M., Kotrová, M., Knecht, H., Bartram, J., Boudjogrha, M., Bystry, V., Fazio, G., Froňková, E., Giraud, M., Grioni, A., Hancock, J., Herrmann, D., Jiménez, C., Krejci, A., Moppett, J., Reigl, T., Salson, M., Scheijen, B., Schwarz, M., … group, on behalf of the E.-N. working. (2019). Standardized next-generation sequencing of immunoglobulin and T-cell receptor gene recombinations for MRD marker identification in acute lymphoblastic leukaemia; a EuroClonality-NGS validation study. *Leukemia*, *33*(9), 2241–2253. https://doi.org/10.1038/s41375-019-0496-7

Cammack, N., & Gould, E. A. (1986). Topographical analysis of epitope relationships on the envelope glycoprotein of yellow fever 17D vaccine and the wild type asibi parent virus. *Virology*, *150*(2), 333–341. https://doi.org/10.1016/0042-6822(86)90298-9

Chan, K. R., Wang, X., Saron, W. A. A., Gan, E. S., Tan, H. C., Mok, D. Z. L., Zhang, S. L. X., Lee, Y. H., Liang, C., Wijaya, L., Ghosh, S., Cheung, Y. B., Tannenbaum, S. R., Abraham, S. N., St John, A. L., Low, J. G. H., & Ooi, E. E. (2016). Cross-reactive antibodies enhance live attenuated virus infection for increased immunogenicity. *Nature Microbiology*. https://doi.org/10.1038/nmicrobiol.2016.164

Chan, K. R., Zhang, S. L.-X., Tan, H. C., Chan, Y. K., Chow, A., Lim, A. P. C., Vasudevan, S. G., Hanson, B. J., & Ooi, E. E. (2011). Ligation of Fc gamma receptor IIB inhibits antibody-dependent enhancement of dengue virus infection. *Proceedings of the National*

Academy of Sciences, *108*(30), 12479–12484.
https://doi.org/10.1073/pnas.1106568108

Chen, D., Duan, Z., Zhou, W., Zou, W., Jin, S., Li, D., Chen, X., Zhou, Y., Yang, L., Zhang, Y., Shresta, S., & Wen, J. (2020). Japanese encephalitis virus–primed CD8+ T cells prevent antibody-dependent enhancement of Zika virus pathogenesis. *Journal of Experimental Medicine*, *217*(9), e20192152. https://doi.org/10.1084/jem.20192152

Cherrier, M. V, Kaufmann, B., Nybakken, G. E., Lok, S.-M., Warren, J. T., Chen, B. R., Nelson, C. A., Kostyuchenko, V. A., Holdaway, H. A., Chipman, P. R., Kuhn, R. J., Diamond, M. S., Rossmann, M. G., & Fremont, D. H. (2009). Structural basis for the preferential recognition of immature flaviviruses by a fusion-loop antibody. *The EMBO Journal*, *28*(20), 3269–3276. https://doi.org/10.1038/emboj.2009.245

Chih-Yun, L., Wen-Yang, T., Su-Ru, L., Chuan-Liang, K., Hsien-Ping, H., Chwan-Chuen, K., Han-Chung, W., Gwong-Jen, C., & Wei-Kung, W. (2008). Antibodies to Envelope Glycoprotein of Dengue Virus during the Natural Course of Infection Are Predominantly Cross-Reactive and Recognize Epitopes Containing Highly Conserved Residues at the Fusion Loop of Domain II. *Journal of Virology*, *82*(13), 6631–6643. https://doi.org/10.1128/JVI.00316-08

Cochet, A., Calba, C., Jourdain, F., Grard, G., Durand, G. A., Guinard, A., team, I., Noël, H., Paty, M.-C., & Franke, F. (2022). Autochthonous dengue in mainland France, 2022: geographical extension and incidence increase. *Eurosurveillance*, *27*(44). https://doi.org/10.2807/1560-7917.ES.2022.27.44.2200818

Costantini, M., Callegaro, A., Beran, J., Berlaimont, V., & Galgani, I. (2020). Predicted long-term antibody persistence for a tick-borne encephalitis vaccine: results from a modeling study beyond 10 years after a booster dose following different primary vaccination schedules. *Human Vaccines & Immunotherapeutics*, *16*(9), 2274–2279. https://doi.org/10.1080/21645515.2019.1700712

Cox, K. S., Tang, A., Chen, Z., Horton, M. S., Yan, H., Wang, X.-M., Dubey, S. A., DiStefano, D. J., Ettenger, A., Fong, R. H., Doranz, B. J., Casimiro, D. R., & Vora, K. A. (2016). Rapid isolation of dengue-neutralizing antibodies from single cell-sorted human antigen-specific memory B-cell cultures. *MAbs*, *8*(1), 129–140. https://doi.org/10.1080/19420862.2015.1109757

Crampon, E., Covernton, E., Vaney, M. C., Dellarole, M., Sommer, S., Sharma, A., Haouz, A., England, P., Lepault, J., Duquerroy, S., Rey, F. A., & Barba-Spaeth, G. (2023). New insight into flavivirus maturation from structure/function studies of the yellow fever virus envelope protein complex. *MBio*, *0*(0), e00706-23. https://doi.org/10.1128/mbio.00706-23

Crill, W. D., & Chang, G.-J. J. (2004). Localization and characterization of flavivirus envelope glycoprotein cross-reactive epitopes. *Journal of Virology*, *78*(24), 13975–13986. https://doi.org/10.1128/JVI.78.24.13975-13986.2004

Daffis, S., Kontermann, R. E., Korimbocus, J., Zeller, H., Klenk, H. D., & Ter Meulen, J. (2005). Antibody responses against wild-type yellow fever virus and the 17D vaccine strain: Characterization with human monoclonal antibody fragments and neutralization escape variants. *Virology*, *337*(2), 262–272. https://doi.org/10.1016/j.virol.2005.04.031

Dai, L., Song, J., Lu, X., Deng, Y.-Q., Musyoki, A. M., Cheng, H., Zhang, Y., Yuan, Y., Song, H., Haywood, J., Xiao, H., Yan, J., Shi, Y., Qin, C.-F., Qi, J., & Gao, G. F. (2016). Structures of the Zika Virus Envelope Protein and Its Complex with a Flavivirus Broadly Protective Antibody. *Cell Host & Microbe*, *19*(5), 696–704. https://doi.org/10.1016/j.chom.2016.04.013

Davis CW, Jackson KJL, McElroy AK, Halfmann P, Huang J, Chennareddy C, Piper AE, Leung Y, Albariño CG, Crozier I, Ellebedy AH, Sidney J, Sette A, Yu T, Nielsen SCA, Goff AJ, Spiropoulou CF, Saphire EO, Cavet G, Kawaoka Y, Mehta AK, Glass PJ, Boyd SD, A. R. (2019). Longitudinal Analysis of the Human B Cell Response to Ebola Virus Infection. *Cell*, *177*(6), 1566-1582.e17. https://doi.org/10.1016/j.cell.2019.04.036

Davis, E. H., & Barrett, A. D. T. (2020). Structure–Function of the Yellow Fever Virus Envelope Protein: Analysis of Antibody Epitopes. *Viral Immunology*, *33*(1), 12–21. https://doi.org/10.1089/vim.2019.0107

Davis, E. H., Wang, B., White, M., Huang, Y.-J. S., Sarathy, V. V, Wang, T., Bourne, N., Higgs, S., & Barrett, A. D. T. (2022). Impact of yellow fever virus envelope protein on wild-type and vaccine epitopes and tissue tropism. *Npj Vaccines*, *7*(1), 39. https://doi.org/10.1038/s41541-022-00460-6

Davydov, A. N., Obraztsova, A. S., Lebedin, M. Y., Turchaninova, M. A., Staroverov, D. B., Merzlyak, E. M., Sharonov, G. V., Kladova, O., Shugay, M., Britanova, O. V., & Chudakov, D. M. (2018). Comparative Analysis of B-Cell Receptor Repertoires Induced by Live Yellow Fever Vaccine in Young and Middle-Age Donors. *Frontiers in Immunology*, *9*. https://doi.org/10.3389/fimmu.2018.02309

de Alwis, R., Williams, K. L., Schmid, M. A., Lai, C.-Y., Patel, B., Smith, S. A., Crowe, J. E., Wang, W.-K., Harris, E., & de Silva, A. M. (2014). Dengue Viruses Are Enhanced by Distinct Populations of Serotype Cross-Reactive Antibodies in Human Immune Sera. *PLOS Pathogens*, *10*(10), e1004386. https://doi.org/10.1371/journal.ppat.1004386

Dejnirattisai, W., Jumnainsong, A., Onsirisakul, N., Fitton, P., Vasanawathana, S., Limpitikul, W., Puttikhunt, C., Edwards, C., Duangchinda, T., Supasa, S., Chawansuntati, K., Malasit, P., Mongkolsapaya, J., & Screaton, G. (2010). Cross-Reacting Antibodies Enhance Dengue Virus Infection in Humans. *Science*, *328*(5979), 745–748. https://doi.org/10.1126/science.1185181

Dejnirattisai, W., Supasa, P., Wongwiwat, W., Rouvinski, A., Barba-Spaeth, G., Duangchinda, T., Sakuntabhai, A., Cao-Lormeau, V.-M., Malasit, P., Rey, F. A., Mongkolsapaya, J., & Screaton, G. R. (2016). Dengue virus sero-cross-reactivity drives

antibody-dependent enhancement of infection with zika virus. *Nature Immunology*, *17*(9), 1102–1108. https://doi.org/10.1038/ni.3515

Dejnirattisai, W., Wongwiwat, W., Supasa, S., Zhang, X., Dai, X., Rouvinski, A., Jumnainsong, A., Edwards, C., Quyen, N. T. H., Duangchinda, T., Grimes, J. M., Tsai, W.-Y., Lai, C.-Y., Wang, W.-K., Malasit, P., Farrar, J., Simmons, C. P., Zhou, Z. H., Rey, F. A., … Screaton, G. R. (2015). A new class of highly potent, broadly neutralizing antibodies isolated from viremic patients infected with dengue virus. *Nature Immunology*, *16*(2), 170–177. https://doi.org/10.1038/ni.3058

Dowd, K. A., Jost, C. A., Durbin, A. P., Whitehead, S. S., & Pierson, T. C. (2011). A dynamic landscape for antibody binding modulates antibody-mediated neutralization of West Nile virus. *PLoS Pathogens*, *7*(6). https://doi.org/10.1371/journal.ppat.1002111

Dowd, K. A., Mukherjee, S., Kuhn, R. J., & Pierson, T. C. (2014). Combined Effects of the Structural Heterogeneity and Dynamics of Flaviviruses on Antibody Recognition. *Journal of Virology*, *88*(20), 11726–11737. https://doi.org/10.1128/jvi.01140-14

Dowd, K. A., & Pierson, T. C. (2011). Antibody-mediated neutralization of flaviviruses: A reductionist view. *Virology*, *411*(2), 306–315. https://doi.org/10.1016/j.virol.2010.12.020

Doyle, M. P., Genualdi, J., Bailey, A., Nurgun, K., Christopher, G., Jessica, R., Reeder, K., Nelson, C., Jethva, P., Sutton, R., Bombardi, R., Gross, M., Julander, J., Fremont, D., Diamond, M., Crowe, J., & Projan, S. (2022). Isolation of a Potently Neutralizing and Protective Human Monoclonal Antibody Targeting Yellow Fever Virus. *MBio*, *13*(3), e00512-22. https://doi.org/10.1128/mbio.00512-22

Durham, N. D., Agrawal, A., Waltari, E., Croote, D., Zanini, F., Fouch, M., Davidson, E., Smith, O., Carabajal, E., Pak, J. E., Doranz, B. J., Robinson, M., Sanz, A. M., Albornoz, L. L., Rosso, F., Einav, S., Quake, S. R., McCutcheon, K. M., & Goo, L. (2019). Broadly neutralizing human antibodies against dengue virus identified by single B cell transcriptomics. *ELife*, *8*. https://doi.org/10.7554/eLife.52384

Dussupt, V., Sankhala, R. S., Gromowski, G. D., Donofrio, G., De La Barrera, R. A., Larocca, R. A., Zaky, W., Mendez-Rivera, L., Choe, M., Davidson, E., McCracken, M. K., Brien, J. D., Abbink, P., Bai, H., Bryan, A. L., Bias, C. H., Berry, I. M., Botero, N., Cook, T., … Krebs, S. J. (2020). Potent Zika and dengue cross-neutralizing antibodies induced by Zika vaccination in a dengue-experienced donor. *Nature Medicine*, *26*(2), 228–235. https://doi.org/10.1038/s41591-019-0746-2

ECDC. (2022). *Dengue. In: ECDC. Annual epidemiological report for 2020*.

Ellebedy, A. H., Jackson, K. J. L., Kissick, H. T., Nakaya, H. I., Davis, C. W., Roskin, K. M., McElroy, A. K., Oshansky, C. M., Elbein, R., Thomas, S., Lyon, G. M., Spiropoulou, C. F., Mehta, A. K., Thomas, P. G., Boyd, S. D., & Ahmed, R. (2016). Defining antigen-specific plasmablast and memory B cell subsets in human blood after viral infection or vaccination. *Nature Immunology*, *17*(10), 1226–1234. https://doi.org/10.1038/ni.3533

Ferguson, N. M., Rodríguez-Barraquer, I., Dorigatti, I., Mier-y-Teran-Romero, L., Laydon, D. J., & Cummings, D. A. T. (2016). Benefits and risks of the Sanofi-Pasteur dengue vaccine: Modeling optimal deployment. *Science*, *353*(6303), 1033–1036. https://doi.org/10.1126/science.aaf9590

Fernandez-Garcia, M. D., Meertens, L., Chazal, M., Hafirassou, M. L., Dejarnac, O., Zamborlini, A., Despres, P., Sauvonnet, N., Arenzana-Seisdedos, F., Jouvenet, N., & Amara, A. (2016). Vaccine and Wild-Type Strains of Yellow Fever Virus Engage Distinct Entry Mechanisms and Differentially Stimulate Antiviral Immune Responses. *MBio*, *7*(1), e01956-15. https://doi.org/10.1128/mBio.01956-15

Fibriansah, G., Lim, E. X. Y., Marzinek, J. K., Ng, T. S., Tan, J. L., Huber, R. G., Lim, X. N., Chew, V. S. Y., Kostyuchenko, V. A., Shi, J., Anand, G. S., Bond, P. J., Crowe, J. E., & Lok, S. M. (2021). Antibody affinity versus dengue morphology influences neutralization. *PLoS Pathogens*, *17*(2), 1–30. https://doi.org/10.1371/JOURNAL.PPAT.1009331

Fourati, S., Tomalin, L. E., Mulè, M. P., Chawla, D. G., Gerritsen, B., Rychkov, D., Henrich, E., Miller, H. E. R., Hagan, T., Diray-Arce, J., Dunn, P., Deckhut-Augustine, A., Haddad, E. K., Hafler, D. A., Harris, E., Farber, D., McElrath, J., Montgomery, R. R., Peters, B., … (HIPC), T. H. I. P. C. (2022). Pan-vaccine analysis reveals innate immune endotypes predictive of antibody responses to vaccination. *Nature Immunology*, *23*(12), 1777–1787. https://doi.org/10.1038/s41590-022-01329-5

Franz, B., May, K. F., Dranoff, G., & Wucherpfennig, K. (2011). Ex vivo characterization and isolation of rare memory B cells with antigen tetramers. *Blood*, *118*(2), 348–357. https://doi.org/10.1182/blood-2011-03-341917

Friberg, H., Bashyam, H., Toyosaki-Maeda, T., Potts, J. A., Greenough, T., Kalayanarooj, S., Gibbons, R. V., Nisalak, A., Srikiatkhachorn, A., Green, S., Stephens, H. A. F., Rothman, A. L., & Mathew, A. (2011). Cross-Reactivity and Expansion of Dengue-Specific T cells During Acute Primary and Secondary Infections in Humans. *Scientific Reports*, *1*(1), 51. https://doi.org/10.1038/srep00051

Fuertes Marraco, S. A., Alpern, D., Lofek, S., Lourenco, J., Bovay, A., Maby-El Hajjami, H., Delorenzi, M., Deplancke, B., & Speiser, D. E. (2022). Shared acute phase traits in effector and memory human CD8 T cells. *Current Research in Immunology*, *3*, 1–12. https://doi.org/10.1016/j.crimmu.2021.12.002

Fuertes Marraco, S. A., Soneson, C., Cagnon, L., Gannon, P. O., Allard, M., Abed Maillard, S., Montandon, N., Rufer, N., Waldvogel, S., Delorenzi, M., & Speiser, D. E. (2015). Long-lasting stem cell-like memory CD8+ T cells with a naive-like profile upon yellow fever vaccination. *Science Translational Medicine*, *7*(282), 282ra48. https://doi.org/10.1126/scitranslmed.aaa3700

García San Miguel Rodríguez-Alarcón, L., Fernández-Martínez, B., Sierra Moros, M. J., Vázquez, A., Julián Pachés, P., García Villacieros, E., Gómez Martín, M. B., Figuerola Borras, J., Lorusso, N., Ramos Aceitero, J. M., Moro, E., de Celis, A., Oyonarte, S.,

Mahillo, B., Romero González, L. J., Sánchez-Seco, M. P., Suárez Rodríguez, B., Ame-yugo Catalán, U., Ruiz Contreras, S., … Simón Soria, Fernando. (2021). Unprecedented increase of West Nile virus neuroinvasive disease, Spain, summer 2020. *Eurosurveillance*, *26*(19). https://doi.org/10.2807/1560-7917.ES.2021.26.19.2002010

Gaucher, D., Therrien, R., Kettaf, N., Angermann, B. R., Boucher, G., Filali-Mouhim, A., Moser, J. M., Mehta, R. S., Drake, D. R. 3rd, Castro, E., Akondy, R., Rinfret, A., Yassine-Diab, B., Said, E. A., Chouikh, Y., Cameron, M. J., Clum, R., Kelvin, D., Somogyi, R., … Sekaly, R.-P. (2008). Yellow fever vaccine induces integrated multilineage and poly-functional immune responses. *The Journal of Experimental Medicine*, *205*(13), 3119–3131. https://doi.org/10.1084/jem.20082292

Gibney, K. B., Edupuganti, S., Panella, A. J., Kosoy, O. I., Delorey, M. J., Lanciotti, R. S., Mulligan, M. J., Fischer, M., & Staples, J. E. (2012). Detection of Anti-Yellow Fever Vi-rus Immunoglobulin M Antibodies at 3–4 Years Following Yellow Fever Vaccination. *The American Society of Tropical Medicine and Hygiene*, *87*(6), 1112–1115. https://doi.org/10.4269/ajtmh.2012.12-0182

Goo, L., VanBlargan, L. A., Dowd, K. A., Diamond, M. S., & Pierson, T. C. (2017). A sin-gle mutation in the envelope protein modulates flavivirus antigenicity, stability, and pathogenesis. In *PLoS Pathogens* (Vol. 13, Issue 2). https://doi.org/10.1371/jour-nal.ppat.1006178

Gossner, C. M., Fournet, N., Frank, C., Fernández-Martínez, B., Del Manso, M., Gomes Dias, J., & de Valk, H. (2022). Dengue virus infections among European travellers, 2015 to 2019. *Euro Surveillance : Bulletin Europeen Sur Les Maladies Transmissibles = Euro-pean Communicable Disease Bulletin*, *27*(2). https://doi.org/10.2807/1560-7917.ES.2022.27.2.2001937

Gould, E. A., & Solomon, T. (2008). Pathogenic flaviviruses. *Lancet*, *371*(9611), 500–509. https://doi.org/10.1016/S0140-6736(08)60238-X

Grifoni, A., Voic, H., Dhanda, S. K., Kidd, C. K., Brien, J. D., Buus, S., Stryhn, A., Durbin, A. P., Whitehead, S., Diehl, S. A., De Silva, A. D., Balmaseda, A., Harris, E., Weiskopf, D., & Sette, A. (2020). T Cell Responses Induced by Attenuated Flavivirus Vaccination Are Specific and Show Limited Cross-Reactivity with Other Flavivirus Species. *Journal of Vi-rology*, *94*(10). https://doi.org/10.1128/JVI.00089-20

Guo, Z., Jing, W., Liu, J., & Liu, M. (2022). The global trends and regional differences in incidence of Zika virus infection and implications for Zika virus infection prevention. *PLOS Neglected Tropical Diseases*, *16*(10), e0010812. https://doi.org/10.1371/jour-nal.pntd.0010812

Hagan, T., Gerritsen, B., Tomalin, L. E., Fourati, S., Mulè, M. P., Chawla, D. G., Rychkov, D., Henrich, E., Miller, H. E. R., Diray-Arce, J., Dunn, P., Lee, A., Deckhut-Augustine, A., Gottardo, R., Haddad, E. K., Hafler, D. A., Harris, E., Farber, D., Kleinstein, S. H., …

Pulendran, B. (2022). Transcriptional atlas of the human immune response to 13 vaccines reveals a common predictor of vaccine-induced antibody responses. *Nature Immunology*, *23*(12), 1788–1798. https://doi.org/10.1038/s41590-022-01328-6

Hägglöf, T., Cipolla, M., Loewe, M., Chen, S. T., Mesin, L., Hartweger, H., ElTanbouly, M. A., Cho, A., Gazumyan, A., Ramos, V., Stamatatos, L., Oliveira, T. Y., Nussenzweig, M. C., & Viant, C. (2023). Continuous germinal center invasion contributes to the diversity of the immune response. *Cell*, *186*(1), 147-161.e15. https://doi.org/10.1016/j.cell.2022.11.032

Hahn, C. S., Dalrymple, J. M., Strauss, J. H., & Rice, C. M. (1987). Comparison of the virulent Asibi strain of yellow fever virus with the 17D vaccine strain derived from it. *Proceedings of the National Academy of Sciences*, *84*(7), 2019–2023. https://doi.org/10.1073/pnas.84.7.2019

Haslwanter, D., Lasso, G., Wec, A. Z., Furtado, N. D., Raphael, L. M. S., Tse, A. L., Sun, Y., Stransky, S., Pedreño-Lopez, N., Correia, C. A., Bornholdt, Z. A., Sakharkar, M., Avelino-Silva, V. I., Moyer, C. L., Watkins, D. I., Kallas, E. G., Sidoli, S., Walker, L. M., Bonaldo, M. C., & Chandran, K. (2022). Genotype-specific features reduce the susceptibility of South American yellow fever virus strains to vaccine-induced antibodies. *Cell Host & Microbe*, *30*(2), 248-259.e6. https://doi.org/10.1016/j.chom.2021.12.009

Heinz, F. X., & Stiasny, K. (2012). Flaviviruses and their antigenic structure. *Journal of Clinical Virology*, *55*(4), 289–295. https://doi.org/10.1016/j.jcv.2012.08.024

Hofmann, H., Heinz, F. X., & Dippe, H. (1983). ELISA for IgM and IgG antibodies against tick-borne encephalitis virus: Quantification and standardization of results. *Zentralblatt Für Bakteriologie, Mikrobiologie Und Hygiene. 1. Abt. Originale. A, Medizinische Mikrobiologie, Infektionskrankheiten Und Parasitologie*, *255*(4), 448–455. https://doi.org/10.1016/S0174-3031(83)80002-X

Holbrook, M., Shope, R., & Barrett, A. D. (2004). Use of Recombinant E Protein Domain III-Based Enzyme-Linked Immunosorbent Assays for Differentiation of Tick-Borne Encephalitis Serocomplex Flaviviruses from Mosquito-Borne Flaviviruses. *Journal of Clinical Microbiology*, *42*(9), 4101–4110. https://doi.org/10.1128/JCM.42.9.4101-4110.2004

Hou, J., Wang, S., Jia, M., Li, D., Liu, Y., Li, Z., Zhu, H., Xu, H., Sun, M., Lu, L., Zhou, Z., Peng, H., Zhang, Q., Fu, S., Liang, G., Yao, L., Yu, X., Carpp, L. N., Huang, Y., … Shao, Y. (2017). A Systems Vaccinology Approach Reveals Temporal Transcriptomic Changes of Immune Responses to the Yellow Fever 17D Vaccine. *The Journal of Immunology*, *199*(4), 1476–1489. https://doi.org/10.4049/jimmunol.1700083

Huber, J. E., Ahlfeld, J., Scheck, M. K., Zaucha, M., Witter, K., Lehmann, L., Karimzadeh, H., Pritsch, M., Hoelscher, M., von Sonnenburg, F., Dick, A., Barba-Spaeth, G., Krug, A. B., Rothenfußer, S., & Baumjohann, D. (2020). Dynamic changes in circulating T follicular helper cell composition predict neutralising antibody responses after yellow fever

vaccination. *Clinical & Translational Immunology*, *9*(5), e1129–e1129. https://doi.org/10.1002/cti2.1129

Iwaki, T., Figuera, M., Ploplis, V. A., & Castellino, F. J. (2003). Rapid selection of Drosophila S2 cells with the puromycin resistance gene. *BioTechniques*, *35*(3), 482–486. https://doi.org/10.2144/03353bm08

James, E. A., LaFond, R. E., Gates, T. J., Mai, D. T., Malhotra, U., & Kwok, W. W. (2013). Yellow Fever Vaccination Elicits Broad Functional CD4 T Cell Responses That Recognize Structural and Nonstructural Proteins. *Journal of Virology*, *87*(23), 12794–12804. https://doi.org/10.1128/JVI.01160-13

Katzelnick, L. C., Gresh, L., Halloran, M. E., Mercado, J. C., Kuan, G., Gordon, A., Balmaseda, A., & Harris, E. (2017). Antibody-dependent enhancement of severe dengue disease in humans. *Science*, *358*(6365), 929–932. https://doi.org/10.1126/science.aan6836

Katzelnick, L. C., Narvaez, C., Arguello, S., Lopez Mercado, B., Collado, D., Ampie, O., Elizondo, D., Miranda, T., Bustos Carillo, F., Mercado, J. C., Latta, K., Schiller, A., Segovia-Chumbez, B., Ojeda, S., Sanchez, N., Plazaola, M., Coloma, J., Halloran, M. E., Premkumar, L., … Harris, E. (2020). Zika virus infection enhances future risk of severe dengue disease. *Science*, *369*(6507), 1123–1128. https://doi.org/10.1126/science.abb6143

Kayser, M., Klein, H., Paasch, I., Pilaski, J., Blenk, H., & Heeg, K. (1985). Human antibody response to immunization with 17D yellow fever and inactivated TBE vaccine. *Journal of Medical Virology*, *17*(1), 35–45. https://doi.org/10.1002/jmv.1890170106

Kling, K., Domingo, C., Bogdan, C., Duffy, S., Harder, T., Howick, J., Kleijnen, J., McDermott, K., Wichmann, O., Wilder-Smith, A., & Wolff, R. (2022). Duration of protection after vaccination against yellow fever - systematic review and meta-analysis. *Clinical Infectious Diseases*, ciac580. https://doi.org/10.1093/cid/ciac580

Kohler, S., Bethke, N., Böthe, M., Sommerick, S., Frentsch, M., Romagnani, C., Niedrig, M., & Thiel, A. (2012). The early cellular signatures of protective immunity induced by live viral vaccination. *European Journal of Immunology*, *42*(9), 2363–2373. https://doi.org/10.1002/eji.201142306

Kotagiri, P., Mescia, F., Rae, W. M., Bergamaschi, L., Tuong, Z. K., Turner, L., Hunter, K., Gerber, P. P., Hosmillo, M., Hess, C., Clatworthy, M. R., Goodfellow, I. G., Matheson, N. J., McKinney, E. F., Wills, M. R., Gupta, R. K., Bradley, J. R., Bashford-Rogers, R. J. M., Lyons, P. A., & Smith, K. G. C. (2022). B cell receptor repertoire kinetics after SARS-CoV-2 infection and vaccination. *Cell Reports*, *38*(7), 110393. https://doi.org/10.1016/j.celrep.2022.110393

Kotliarov, Y., Sparks, R., Martins, A. J., Mulè, M. P., Lu, Y., Goswami, M., Kardava, L., Banchereau, R., Pascual, V., Biancotto, A., Chen, J., Schwartzberg, P. L., Bansal, N., Liu, C. C., Cheung, F., Moir, S., & Tsang, J. S. (2020). Broad immune activation underlies

shared set point signatures for vaccine responsiveness in healthy individuals and disease activity in patients with lupus. *Nature Medicine*, *26*(4), 618–629. https://doi.org/10.1038/s41591-020-0769-8

Kraemer, M. U. G., Sinka, M. E., Duda, K. A., Mylne, A. Q. N., Shearer, F. M., Barker, C. M., Moore, C. G., Carvalho, R. G., Coelho, G. E., Van Bortel, W., Hendrickx, G., Schaffner, F., Elyazar, I. R. F., Teng, H.-J., Brady, O. J., Messina, J. P., Pigott, D. M., Scott, T. W., Smith, D. L., … Hay, S. I. (2015). The global distribution of the arbovirus vectors Aedes aegypti and Ae. albopictus. *ELife*, *4*, e08347. https://doi.org/10.7554/eLife.08347

Li, X., Mukandavire, C., Cucunubá, Z. M., Echeverria Londono, S., Abbas, K., Clapham, H. E., Jit, M., Johnson, H. L., Papadopoulos, T., Vynnycky, E., Brisson, M., Carter, E. D., Clark, A., de Villiers, M. J., Eilertson, K., Ferrari, M. J., Gamkrelidze, I., Gaythorpe, K. A. M., Grassly, N. C., … Garske, T. (2021). Estimating the health impact of vaccination against ten pathogens in 98 low-income and middle-income countries from 2000 to 2030: a modelling study. *The Lancet*, *397*(10272), 398–408. https://doi.org/10.1016/S0140-6736(20)32657-X

Li, Y., Chen, Z., Wu, L., Dai, L., Qi, J., Chai, Y., Li, S., Wang, Q., Tong, Z., Ma, S., Duan, X., Ren, S., Song, R., Liang, M., Liu, W., Yan, J., & Gao, G. F. (2022). A neutralizing-protective supersite of human monoclonal antibodies for yellow fever virus. *The Innovation*, *3*(6). https://doi.org/10.1016/j.xinn.2022.100323

Lin, L., Finak, G., Ushey, K., Seshadri, C., Hawn, T. R., Frahm, N., Scriba, T. J., Mahomed, H., Hanekom, W., Bart, P.-A., Pantaleo, G., Tomaras, G. D., Rerks-Ngarm, S., Kaewkungwal, J., Nitayaphan, S., Pitisuttithum, P., Michael, N. L., Kim, J. H., Robb, M. L., … Gottardo, R. (2015). COMPASS identifies T-cell subsets correlated with clinical outcomes. *Nature Biotechnology*, *33*(6), 610–616. https://doi.org/10.1038/nbt.3187

Lobigs, M., Dalgarno, L., Schlesinger, J. J., & Weir, R. C. (1987). Location of a neutralization determinant in the E protein of yellow fever virus (17D vaccine strain). *Virology*, *161*(2), 474–478. https://doi.org/10.1016/0042-6822(87)90141-3

Lok, S. M., Kostyuchenko, V., Nybakken, G. E., Holdaway, H. A., Battisti, A. J., Sukupolvi-Petty, S., Sedlak, D., Fremont, D. H., Chipman, P. R., Roehrig, J. T., Diamond, M. S., Kuhn, R. J., & Rossmann, M. G. (2008). Binding of a neutralizing antibody to dengue virus alters the arrangement of surface glycoproteins. *Nature Structural and Molecular Biology*, *15*(3), 312–317. https://doi.org/10.1038/nsmb.1382

Lu, X., Xiao, H., Li, S., Pang, X., Song, J., Liu, S., Cheng, H., Li, Y., Wang, X., Huang, C., Guo, T., ter Meulen, J., Daffis, S., Yan, J., Dai, L., Rao, Z., Klenk, H. D., Qi, J., Shi, Y., & Gao, G. F. (2019). Double Lock of a Human Neutralizing and Protective Monoclonal Antibody Targeting the Yellow Fever Virus Envelope. *Cell Reports*, *26*(2), 438-446.e5. https://doi.org/10.1016/j.celrep.2018.12.065

Lücke, A.-C., vom Hemdt, A., Wieseler, J., Fischer, C., Feldmann, M., Rothenfusser, S., Drexler, J. F., & Kümmerer, B. M. (2022). High-Throughput Platform for Detection of

Neutralizing Antibodies Using Flavivirus Reporter Replicon Particles. In *Viruses* (Vol. 14, Issue 2). https://doi.org/10.3390/v14020346

Luppe, M. J., Verro, A. T., Barbosa, A. S., Nogueira, M. L., Undurraga, E. A., & da Silva, N. S. (2019). Yellow fever (YF) vaccination does not increase dengue severity: A retrospective study based on 11,448 dengue notifications in a YF and dengue endemic region. *Travel Medicine and Infectious Disease*, *30*, 25–31. https://doi.org/10.1016/j.tmaid.2019.05.002

Malafa, S., Medits, I., Aberle, J. H., Aberle, S. W., Haslwanter, D., Tsouchnikas, G., Wölfel, S., Huber, K. L., Percivalle, E., Cherpillod, P., Thaler, M., Roßbacher, L., Kundi, M., Heinz, F. X., & Stiasny, K. (2020). Impact of flavivirus vaccine-induced immunity on primary zika virus antibody response in humans. *PLoS Neglected Tropical Diseases*, *14*(2), 1–27. https://doi.org/10.1371/journal.pntd.0008034

Mathew, A., West, K., Kalayanarooj, S., Gibbons, R. V., Srikiatkhachorn, A., Green, S., Libraty, D., Jaiswal, S., & Rothman, A. L. (2011). B-Cell Responses During Primary and Secondary Dengue Virus Infections in Humans. *The Journal of Infectious Diseases*, *204*(10), 1514–1522. https://doi.org/10.1093/infdis/jir607

Matrajt, L., Halloran, M. E., & Antia, R. (2019). Successes and failures of the live-attenuated influenza vaccine: can we do better? *Clinical Infectious Diseases*. https://doi.org/10.1093/cid/ciz358

McKinstry, K. K., Strutt, T. M., Kuang, Y., Brown, D. M., Sell, S., Dutton, R. W., & Swain, S. L. (2012). Memory CD4+ T cells protect against influenza through multiple synergizing mechanisms. *The Journal of Clinical Investigation*, *122*(8), 2847–2856. https://doi.org/10.1172/JCI63689

McNamara, H. A., Idris, A. H., Sutton, H. J., Vistein, R., Flynn, B. J., Cai, Y., Wiehe, K., Lyke, K. E., Chatterjee, D., KC, N., Chakravarty, S., Lee Sim, B. K., Hoffman, S. L., Bonsignori, M., Seder, R. A., & Cockburn, I. A. (2020). Antibody Feedback Limits the Expansion of B Cell Responses to Malaria Vaccination but Drives Diversification of the Humoral Response. *Cell Host & Microbe*, *28*(4), 572-585.e7. https://doi.org/10.1016/j.chom.2020.07.001

Miller, J. D., van der Most, R. G., Akondy, R. S., Glidewell, J. T., Albott, S., Masopust, D., Murali-Krishna, K., Mahar, P. L., Edupuganti, S., Lalor, S., Germon, S., Del Rio, C., Mulligan, M. J., Staprans, S. I., Altman, J. D., Feinberg, M. B., & Ahmed, R. (2008). Human effector and memory CD8+ T cell responses to smallpox and yellow fever vaccines. *Immunity*, *28*(5), 710–722. https://doi.org/10.1016/j.immuni.2008.02.020

Mok, D. Z. L., & Chan, K. R. (2020). The effects of pre-existing antibodies on live-attenuated viral vaccines. *Viruses*, *12*(5). https://doi.org/10.3390/v12050520

Monath, T. P., & Vasconcelos, P. F. C. (2015). Yellow fever. *Journal of Clinical Virology : The Official Publication of the Pan American Society for Clinical Virology*, *64*, 160–173. https://doi.org/10.1016/j.jcv.2014.08.030

Morita, R., Schmitt, N., Bentebibel, S.-E., Ranganathan, R., Bourdery, L., Zurawski, G., Foucat, E., Dullaers, M., Oh, S., Sabzghabaei, N., Lavecchio, E. M., Punaro, M., Pascual, V., Banchereau, J., & Ueno, H. (2011). Human Blood CXCR5+CD4+ T Cells Are Counterparts of T Follicular Cells and Contain Specific Subsets that Differentially Support Antibody Secretion. *Immunity*, *34*(1), 108–121. https://doi.org/10.1016/j.immuni.2010.12.012

Morrone, S. R., Chew, V. S. Y., Lim, X.-N., Ng, T.-S., Kostyuchenko, V. A., Zhang, S., Wirawan, M., Chew, P.-L., Lee, J., Tan, J. L., Wang, J., Tan, T. Y., Shi, J., Screaton, G., Morais, M. C., & Lok, S.-M. (2020). High flavivirus structural plasticity demonstrated by a non-spherical morphological variant. *Nature Communications*, *11*(1), 3112. https://doi.org/10.1038/s41467-020-16925-y

Muecksch, F., Wang, Z., Cho, A., Gaebler, C., Ben Tanfous, T., DaSilva, J., Bednarski, E., Ramos, V., Zong, S., Johnson, B., Raspe, R., Schaefer-Babajew, D., Shimeliovich, I., Daga, M., Yao, K.-H., Schmidt, F., Millard, K. G., Turroja, M., Jankovic, M., … Nussenzweig, M. C. (2022). Increased memory B cell potency and breadth after a SARS-CoV-2 mRNA boost. *Nature*, *607*(7917), 128–134. https://doi.org/10.1038/s41586-022-04778-y

Mukhopadhyay, S., Kuhn, R. J., & Rossmann, M. G. (2005). A structural perspective of the flavivirus life cycle. *Nature Reviews Microbiology*, *3*(1), 13–22. https://doi.org/10.1038/nrmicro1067

Olkowski, S., Forshey, B. M., Morrison, A. C., Rocha, C., Vilcarromero, S., Halsey, E. S., Kochel, T. J., Scott, T. W., & Stoddard, S. T. (2013). Reduced Risk of Disease During Postsecondary Dengue Virus Infections. *The Journal of Infectious Diseases*, *208*(6), 1026–1033. https://doi.org/10.1093/infdis/jit273

Oyono, M. G., Kenmoe, S., Abanda, N. N., Takuissu, G. R., Ebogo-Belobo, J. T., Kenfack-Momo, R., Kengne-Nde, C., Mbaga, D. S., Tchatchouang, S., Kenfack-Zanguim, J., Lontuo Fogang, R., Zeuko'o Menkem, E., Ndzie Ondigui, J. L., Kame-Ngasse, G. I., Magoudjou-Pekam, J. N., Bowo-Ngandji, A., Nkie Esemu, S., & Ndip, L. (2022). Epidemiology of yellow fever virus in humans, arthropods, and non-human primates in sub-Saharan Africa: A systematic review and meta-analysis. *PLOS Neglected Tropical Diseases*, *16*(7), e0010610.

Painter, M. M., Johnston, T. S., Lundgreen, K. A., Santos, J. J. S., Qin, J. S., Goel, R. R., Apostolidis, S. A., Mathew, D., Fulmer, B., Williams, J. C., McKeague, M. L., Pattekar, A., Goode, A., Nasta, S., Baxter, A. E., Giles, J. R., Skelly, A. N., Felley, L. E., McLaughlin, M., … Wherry, E. J. (2023). Prior vaccination promotes early activation of memory T cells and enhances immune responses during SARS-CoV-2 breakthrough infection. *Nature Immunology*, *24*(10), 1711–1724. https://doi.org/10.1038/s41590-023-01613-y

Paprckova, D., Salyova, E., Michalik, J., & Stepanek, O. (2023). Bystander activation in memory and antigen-inexperienced memory-like CD8 T cells. *Current Opinion in Immunology*, *82*, 102299. https://doi.org/10.1016/j.coi.2023.102299

Parameswaran, P., Liu, Y., Roskin, K. M., Jackson, K. K. L., Dixit, V. P., Lee, J.-Y., Artiles, K. L., Zompi, S., Vargas, M. J., Simen, B. B., Hanczaruk, B., McGowan, K. R., Tariq, M. A., Pourmand, N., Koller, D., Balmaseda, A., Boyd, S. D., Harris, E., & Fire, A. Z. (2013). Convergent Antibody Signatures in Human Dengue. *Cell Host & Microbe*, *13*(6), 691–700. https://doi.org/10.1016/j.chom.2013.05.008

Pierson, T. C., & Diamond, M. S. (2012). Degrees of maturity: the complex structure and biology of flaviviruses. *Current Opinion in Virology*, *2*(2), 168–175. https://doi.org/10.1016/j.coviro.2012.02.011

Pierson, T. C., & Diamond, M. S. (2020). The continued threat of emerging flaviviruses. *Nature Microbiology*, *5*(6), 796–812. https://doi.org/10.1038/s41564-020-0714-0

Pierson, T. C., Xu, Q., Nelson, S., Oliphant, T., Nybakken, G. E., Fremont, D. H., & Diamond, M. S. (2007). The Stoichiometry of Antibody-Mediated Neutralization and Enhancement of West Nile Virus Infection. *Cell Host & Microbe*, *1*(2), 135–145. https://doi.org/10.1016/j.chom.2007.03.002

Poland, J. D., Calisher, C. H., Monath, T. P., Downs, W. G., & Murphy, K. (1981). Persistence of neutralizing antibody 30-35 years after immunization with 17D yellow fever vaccine. *Bulletin of the World Health Organization*, *59*(6), 895–900.

Pond, W. L., Ehrenkranz, N. J., Danauskas, J. X., & Carter, M. J. (1967). Heterotypic Serologic Responses after Yellow Fever Vaccination; Detection of Persons with Past St. Louis Encephalitis or Dengue. *The Journal of Immunology*, *98*(4), 673 LP – 682.

Priyamvada, L., Hudson, W., Ahmed, R., & Wrammert, J. (2017). Humoral cross-reactivity between Zika and dengue viruses: implications for protection and pathology. *Emerging Microbes & Infections*, *6*(1), 1–6. https://doi.org/10.1038/emi.2017.42

Pulendran, B. (2009). Learning immunology from the yellow fever vaccine: innate immunity to systems vaccinology. *Nature Reviews Immunology*, *9*(10), 741–747. https://doi.org/10.1038/nri2629

Quach, T. D., Rodriguez-Zhurbenko, N., Hopkins, T. J., Guo, X., Hernandez, A. M., Li, W., & Rothstein, T. L. (2016). Distinctions among Circulating Antibody-Secreting Cell Populations, Including B-1 Cells, in Human Adult Peripheral Blood. *Journal of Immunology (Baltimore, Md. : 1950)*, *196*(3), 1060–1069. https://doi.org/10.4049/jimmunol.1501843

Querec, T. D., Akondy, R. S., Lee, E. K., Cao, W., Nakaya, H. I., Teuwen, D., Pirani, A., Gernert, K., Deng, J., Marzolf, B., Kennedy, K., Wu, H., Bennouna, S., Oluoch, H., Miller, J., Vencio, R. Z., Mulligan, M., Aderem, A., Ahmed, R., & Pulendran, B. (2009). Systems biology approach predicts immunogenicity of the yellow fever vaccine in humans. *Nature Immunology*, *10*(1), 116–125. https://doi.org/10.1038/ni.1688

Rey, F. A., Stiasny, K., Vaney, M.-C., Dellarole, M., & Heinz, F. X. (2018). The bright and the dark side of human antibody responses to flaviviruses: lessons for vaccine design. *EMBO Reports*, *19*(2), 206–224. https://doi.org/10.15252/embr.201745302

Riccardo, F., Bella, A., Monaco, F., Ferraro, F., Petrone, D., Mateo-Urdiales, A., Andrianou, X. D., Del Manso, M., Venturi, G., Fortuna, C., Di Luca, M., Severini, F., Caporali, M. G., Morelli, D., Iapaolo, F., Pati, I., Lombardini, L., Bakonyi, T., Alexandra, O., … network, I. A. S. (2022). Rapid increase in neuroinvasive West Nile virus infections in humans, Italy, July 2022. *Eurosurveillance*, *27*(36). https://doi.org/10.2807/1560-7917.ES.2022.27.36.2200653

Riccò, M., Peruzzi, S., & Balzarini, F. (2021). Epidemiology of West Nile Virus Infections in Humans, Italy, 2012–2020: A Summary of Available Evidences. In *Tropical Medicine and Infectious Disease*. https://doi.org/10.3390/tropicalmed6020061

Rivera, L., Biswal, S., Sáez-Llorens, X., Reynales, H., López-Medina, E., Borja-Tabora, C., Bravo, L., Sirivichayakul, C., Kosalaraksa, P., Martinez Vargas, L., Yu, D., Watanaveeradej, V., Espinoza, F., Dietze, R., Fernando, L., Wickramasinghe, P., Duarte MoreiraJr, E., Fernando, A. D., Gunasekera, D., … Borkowski, A. (2022). Three-year Efficacy and Safety of Takeda's Dengue Vaccine Candidate (TAK-003). *Clinical Infectious Diseases*, *75*(1), 107–117. https://doi.org/10.1093/cid/ciab864

Robbiani, D. F., Bozzacco, L., Keeffe, J. R., Khouri, R., Olsen, P. C., Gazumyan, A., Schaefer-Babajew, D., Avila-Rios, S., Nogueira, L., Patel, R., Azzopardi, S. A., Uhl, L. F. K., Saeed, M., Sevilla-Reyes, E. E., Agudelo, M., Yao, K.-H., Golijanin, J., Gristick, H. B., Lee, Y. E., … Nussenzweig, M. C. (2017). Recurrent Potent Human Neutralizing Antibodies to Zika Virus in Brazil and Mexico. *Cell*, *169*(4), 597-609.e11. https://doi.org/10.1016/j.cell.2017.04.024

Rodenhuis-Zybert, I., Bastiaan, M., M., da S. V. J., Heidi, van der E.-M., S., D. M., Jan, W., & M., S. J. (2011). A Fusion-Loop Antibody Enhances the Infectious Properties of Immature Flavivirus Particles. *Journal of Virology*, *85*(22), 11800–11808. https://doi.org/10.1128/JVI.05237-11

Rogers, T. F., Goodwin, E. C., Briney, B., Sok, D., Beutler, N., Strubel, A., Nedellec, R., Le, K., Brown, M. E., Burton, D. R., & Walker, L. M. (2017). Zika virus activates de novo and cross-reactive memory B cell responses in dengue-experienced donors. *Science Immunology*, *2*(14). https://doi.org/10.1126/sciimmunol.aan6809

Rouvinski, A., Dejnirattisai, W., Guardado-calvo, P., Vaney, M., Supasa, P., Wongwiwat, W., Haouz, A., Sharma, A., Rey, A., & Screaton, G. R. (2017). *Covalently linked dengue virus envelope glycoprotein dimers reduce exposure of the immunodominant fusion loop epitope*. *May*. https://doi.org/10.1038/ncomms15411

Ryman, K. D., Ledger, T. N., Weir, R. C., Schlesinger, J. J., & Barrett, A. D. (1997). Yellow fever virus envelope protein has two discrete type-specific neutralizing epitopes. *Journal of General Virology*, *78*(6), 1353–1356. https://doi.org/10.1099/0022-1317-78-6-1353

Saito, Y., Moi, M. L., Takeshita, N., Lim, C.-K., Shiba, H., Hosono, K., Saijo, M., Kurane, I., & Takasaki, T. (2016). Japanese encephalitis vaccine-facilitated dengue virus infection-enhancement antibody in adults. *BMC Infectious Diseases*, *16*(1), 578. https://doi.org/10.1186/s12879-016-1873-8

Samokhina, M., Popov, A., Nazarov, V. I., Rumynskiy, E., & Zarodniuk, M. (2022). immunomind/immunarch: Immunarch 0.9.0 (0.9.0). *Zenodo*. https://immunarch.com/

Sandberg, J. T., Ols, S., Löfling, M., Varnaitė, R., Lindgren, G., Nilsson, O., Rombo, L., Kalén, M., Loré, K., Blom, K., & Ljunggren, H.-G. (2021). Activation and Kinetics of Circulating T Follicular Helper Cells, Specific Plasmablast Response, and Development of Neutralizing Antibodies following Yellow Fever Virus Vaccination. *The Journal of Immunology*, *207*(4), 1033–1043. https://doi.org/10.4049/jimmunol.2001381

Sanderson, R. D., Lalor, P., & Bernfield, M. (1989). B lymphocytes express and lose syndecan at specific stages of differentiation. *Cell Regulation*, *1*(1), 27–35. https://doi.org/10.1091/mbc.1.1.27

Santonja, I., Stiasny, K., Essl, A., Heinz, F. X., Kundi, M., & Holzmann, H. (2022). Tick-Borne Encephalitis in Vaccinated Patients: A Retrospective Case-Control Study and Analysis of Vaccination Field Effectiveness in Austria From 2000 to 2018. *The Journal of Infectious Diseases*, jiac075. https://doi.org/10.1093/infdis/jiac075

Santos-Peral, A., Luppa, F., Goresch, S., Nikolova, E., Zaucha, M., Lehmann, L., Dahlstroem, F., Karimzadeh, H., Kummerer, B. M., Thorn-Seshold, J., Winheim, E., Dobler, G., Hoelscher, M., Endres, S., Krug, A. B., Pritsch, M., Barba-Spaeth, G., & Rothenfusser, S. (2023). Prior flavivirus immunity skews the yellow fever vaccine response to expand cross-reactive antibodies with increased risk of antibody dependent enhancement of Zika and dengue virus infection. *BioRxiv*, 2023.05.07.539594. https://doi.org/10.1101/2023.05.07.539594

Schaefer-Babajew, D., Wang, Z., Muecksch, F., Cho, A., Loewe, M., Cipolla, M., Raspe, R., Johnson, B., Canis, M., DaSilva, J., Ramos, V., Turroja, M., Millard, K. G., Schmidt, F., Witte, L., Dizon, J., Shimeliovich, I., Yao, K.-H., Oliveira, T. Y., … Nussenzweig, M. C. (2023). Antibody feedback regulates immune memory after SARS-CoV-2 mRNA vaccination. *Nature*, *613*(7945), 735–742. https://doi.org/10.1038/s41586-022-05609-w

Scheck, M. K., Lehmann, L., Zaucha, M., Schwarzlmueller, P., Huber, K., Pritsch, M., Barba-Spaeth, G., Thorn-Seshold, O., Krug, A. B., Endres, S., Rothenfusser, S., & Thorn-Seshold, J. (2022). FluoRNT: A robust, efficient assay for the detection of neutralising antibodies against yellow fever virus 17D. *PLOS ONE*, *17*(2), e0262149. https://doi.org/10.1371/journal.pone.0262149

Schmid-Burgk, J. L., Schmidt, T., Gaidt, M. M., Pelka, K., Latz, E., Ebert, T. S., & Hornung, V. (2014). OutKnocker: a web tool for rapid and simple genotyping of designer nuclease edited cell lines. *Genome Research*, *24*(10), 1719–1723. https://doi.org/10.1101/gr.176701.114

Schultheiß, C., Paschold, L., Simnica, D., Mohme, M., Willscher, E., von Wenserski, L., Scholz, R., Wieters, I., Dahlke, C., Tolosa, E., Sedding, D. G., Ciesek, S., Addo, M., & Binder, M. (2020). Next-Generation Sequencing of T and B Cell Receptor Repertoires from COVID-19 Patients Showed Signatures Associated with Severity of Disease. *Immunity*, *53*(2), 442-455.e4. https://doi.org/10.1016/j.immuni.2020.06.024

Sevvana, M., & Kuhn, R. J. (2020). Mapping the diverse structural landscape of the flavivirus antibody repertoire. *Current Opinion in Virology*, *45*, 51–64. https://doi.org/10.1016/j.coviro.2020.07.006

Sharma, A., Zhang, X., Dejnirattisai, W., Dai, X., Gong, D., Wongwiwat, W., Duquerroy, S., Rouvinski, A., Vaney, M.-C., Guardado-Calvo, P., Haouz, A., England, P., Sun, R., Zhou, Z. H., Mongkolsapaya, J., Screaton, G. R., & Rey, F. A. (2021). The epitope arrangement on flavivirus particles contributes to Mab C10's extraordinary neutralization breadth across Zika and dengue viruses. *Cell*, *184*(25), 6052-6066.e18. https://doi.org/10.1016/j.cell.2021.11.010

Singanayagam, A., Zambon, M., Lalvani, A., & Barclay, W. (2018). Urgent challenges in implementing live attenuated influenza vaccine. *The Lancet Infectious Diseases*, *18*(1), e25–e32. https://doi.org/10.1016/S1473-3099(17)30360-2

Singh, T., Hwang, K.-K., Miller, A. S., Jones, R. L., Lopez, C. A., Dulson, S. J., Giuberti, C., Gladden, M. A., Miller, I., Webster, H. S., Eudailey, J. A., Luo, K., Von Holle, T., Edwards, R. J., Valencia, S., Burgomaster, K. E., Zhang, S., Mangold, J. F., Tu, J. J., … Bonsignori, M. (2022). A Zika virus-specific IgM elicited in pregnancy exhibits ultrapotent neutralization. *Cell*. https://doi.org/10.1016/j.cell.2022.10.023

Slon Campos, J. L., Mongkolsapaya, J., & Screaton, G. R. (2018). The immune response against flaviviruses. *Nature Immunology*, *19*(11), 1189–1198. https://doi.org/10.1038/s41590-018-0210-3

Slon-Campos, J. L., Dejnirattisai, W., Jagger, B. W., López-Camacho, C., Wongwiwat, W., Durnell, L. A., Winkler, E. S., Chen, R. E., Reyes-Sandoval, A., Rey, F. A., Diamond, M. S., Mongkolsapaya, J., & Screaton, G. R. (2019). A protective Zika virus E-dimer-based subunit vaccine engineered to abrogate antibody-dependent enhancement of dengue infection. *Nature Immunology*, *20*(10), 1291–1298. https://doi.org/10.1038/s41590-019-0477-z

Smith, S. A., de Alwis, A. R., Kose, N., Harris, E., Ibarra, K. D., Kahle, K. M., Pfaff, J. M., Xiang, X., Doranz, B. J., de Silva, A. M., Austin, S. K., Sukupolvi-Petty, S., Diamond, M. S., & Crowe, J. E. (2013). The Potent and Broadly Neutralizing Human Dengue Virus-Specific Monoclonal Antibody 1C19 Reveals a Unique Cross-Reactive Epitope on the bc Loop of Domain II of the Envelope Protein. *MBio*, *4*(6). https://doi.org/10.1128/mBio.00873-13

Sofou, E., Vlachonikola, E., Zaragoza-Infante, L., Brüggemann, M., Darzentas, N., Groenen, P. J. T. A., Hummel, M., Macintyre, E. A., Psomopoulos, F., Davi, F., Langerak, A. W., & Stamatopoulos, K. (2023). Clonotype definitions for immunogenetic studies:

proposals from the EuroClonality NGS Working Group. *Leukemia*, *37*(8), 1750–1752. https://doi.org/10.1038/s41375-023-01952-7

Souza, N. C. S. e, Félix, A. C., de Paula, A. V., Levi, J. E., Pannuti, C. S., & Romano, C. M. (2019). Evaluation of serological cross-reactivity between yellow fever and other flaviviruses. *International Journal of Infectious Diseases*, *81*, 4–5. https://doi.org/10.1016/j.ijid.2019.01.023

Stewart, A., Sinclair, E., Ng, J. C.-F., O'Hare, J. S., Page, A., Serangeli, I., Margreitter, C., Orsenigo, F., Longman, K., Frampas, C., Costa, C., Lewis, H.-M., Kasar, N., Wu, B., Kipling, D., Openshaw, P. J., Chiu, C., Baillie, J. K., Scott, J. T., … Dunn-Walters, D. K. (2022). Pandemic, Epidemic, Endemic: B Cell Repertoire Analysis Reveals Unique Anti-Viral Responses to SARS-CoV-2, Ebola and Respiratory Syncytial Virus. *Frontiers in Immunology*, *13*. https://doi.org/10.3389/fimmu.2022.807104

Stiasny, K., Aberle, J. H., Chmelik, V., Karrer, U., Holzmann, H., & Heinz, F. X. (2012). Quantitative determination of IgM antibodies reduces the pitfalls in the serodiagnosis of tick-borne encephalitis. *Journal of Clinical Virology*, *54*(2), 115–120. https://doi.org/10.1016/j.jcv.2012.02.016

Stiasny, K., Medits, I., Roßbacher, L., & Heinz, F. X. (2022). Impact of structural dynamics on biological functions of flaviviruses. *FEBS Journal*, 0–2. https://doi.org/10.1111/febs.16419

Stiasny, K., Medits, I., Roßbacher, L., & Heinz, F. X. (2023). Impact of structural dynamics on biological functions of flaviviruses. *The FEBS Journal*, *290*(8), 1973–1985. https://doi.org/10.1111/febs.16419

Svoboda, P., Haviernik, J., Bednar, P., Matkovic, M., Cervantes Rincón, T., Keeffe, J., Palus, M., Salat, J., Agudelo, M., Nussenzweig, M. C., Cavalli, A., Robbiani, D. F., & Ruzek, D. (2023). A combination of two resistance mechanisms is critical for tick-borne encephalitis virus escape from a broadly neutralizing human antibody. *Cell Reports*, *42*(9), 113149. https://doi.org/10.1016/j.celrep.2023.113149

Tan, J. L., & Lok, S. M. (2014). *Dengue Virus Purification and Sample Preparation for Cryo-Electron Microscopy BT - Dengue: Methods and Protocols* (R. Padmanabhan & S. G. Vasudevan, Eds.; pp. 41–52). Springer New York. https://doi.org/10.1007/978-1-4939-0348-1_4

Tannous, B. A. (2009). Gaussia luciferase reporter assay for monitoring biological processes in culture and in vivo. *Nature Protocols*, *4*(4), 582–591. https://doi.org/10.1038/nprot.2009.28

Tellier, J., & Nutt, S. L. (2017). Standing out from the crowd: How to identify plasma cells. *European Journal of Immunology*, *47*(8), 1276–1279. https://doi.org/10.1002/eji.201747168

Theiler, M., & Smith, H. H. (1937). The Effect of Prolongued Cultivation in vitro upon the Pathogenicity of Yellow Fever Virus. *The Journal of Experimental Medicine*, *65*(6), 767–786. https://doi.org/10.1084/jem.65.6.767

Throsby, M., Geuijen, C., Goudsmit, J., Bakker, A. Q., Korimbocus, J., Kramer, R. A., Clijsters-van der Horst, M., de Jong, M., Jongeneelen, M., Thijsse, S., Smit, R., Visser, T. J., Bijl, N., Marissen, W. E., Loeb, M., Kelvin, D. J., Preiser, W., ter Meulen, J., & de Kruif, J. (2006). Isolation and Characterization of Human Monoclonal Antibodies from Individuals Infected with West Nile Virus. *Journal of Virology*, *80*(14), 6982–6992. https://doi.org/10.1128/JVI.00551-06

Tough, D. F., Borrow, P., & Sprent, J. (1996). Induction of Bystander T Cell Proliferation by Viruses and Type I Interferon in Vivo. *Science*, *272*(5270), 1947–1950. https://doi.org/10.1126/science.272.5270.1947

Tsang, J. S., Schwartzberg, P. L., Kotliarov, Y., Biancotto, A., Xie, Z., Germain, R. N., Wang, E., Olnes, M. J., Narayanan, M., Golding, H., Moir, S., Dickler, H. B., Perl, S., Cheung, F., Obermoser, G., Chaussabel, D., Palucka, K., Chen, J., Fuchs, J. C., … Young, N. S. (2014). Global Analyses of Human Immune Variation Reveal Baseline Predictors of Postvaccination Responses. *Cell*, *157*(2), 499–513. https://doi.org/10.1016/j.cell.2014.03.031

Tsioris, K., Gupta, N. T., Ogunniyi, A. O., Zimnisky, R. M., Qian, F., Yao, Y., Wang, X., Stern, J. N. H., Chari, R., Briggs, A. W., Clouser, C. R., Vigneault, F., Church, G. M., Garcia, M. N., Murray, K. O., Montgomery, R. R., Kleinstein, S. H., & Love, J. C. (2015). Neutralizing antibodies against West Nile virus identified directly from human B cells by single-cell analysis and next generation sequencing. *Integrative Biology*, *7*(12), 1587–1597. https://doi.org/10.1039/C5IB00169B

Tsouchnikas, G., Zlatkovic, J., Jarmer, J., Strauß, J., Vratskikh, O., Kundi, M., Stiasny, K., & Heinz, F. X. (2015). Immunization with Immune Complexes Modulates the Fine Specificity of Antibody Responses to a Flavivirus Antigen. *Journal of Virology*, *89*(15), 7970–7978. https://doi.org/10.1128/JVI.00938-15

van Dongen, J. J. M., Langerak, A. W., Brüggemann, M., Evans, P. A. S., Hummel, M., Lavender, F. L., Delabesse, E., Davi, F., Schuuring, E., García-Sanz, R., van Krieken, J. H. J. M., Droese, J., González, D., Bastard, C., White, H. E., Spaargaren, M., González, M., Parreira, A., Smith, J. L., … Macintyre, E. A. (2003). Design and standardization of PCR primers and protocols for detection of clonal immunoglobulin and T-cell receptor gene recombinations in suspect lymphoproliferations: Report of the BIOMED-2 Concerted Action BMH4-CT98-3936. *Leukemia*, *17*(12), 2257–2317. https://doi.org/10.1038/sj.leu.2403202

Varnaitė, R., Blom, K., Lampen, M. H., Vene, S., Thunberg, S., Lindquist, L., Ljunggren, H.-G., Rombo, L., Askling, H. H., & Gredmark-Russ, S. (2020). Magnitude and Functional Profile of the Human CD4+ T Cell Response throughout Primary Immunization with Tick-Borne Encephalitis Virus Vaccine. *The Journal of Immunology*, *204*(4), 914–922. https://doi.org/10.4049/jimmunol.1901115

Vasilakis, N., Cardosa, J., Hanley, K. A., Holmes, E. C., & Weaver, S. C. (2011). Fever from the forest: prospects for the continued emergence of sylvatic dengue virus and its impact on public health. *Nature Reviews Microbiology*, *9*(7), 532–541. https://doi.org/10.1038/nrmicro2595

Vatti, A., Monsalve, D. M., Pacheco, Y., Chang, C., Anaya, J.-M., & Gershwin, M. E. (2017). Original antigenic sin: A comprehensive review. *Journal of Autoimmunity*, *83*, 12–21. https://doi.org/10.1016/j.jaut.2017.04.008

Viant, C., Weymar, G. H. J., Escolano, A., Chen, S., Hartweger, H., Cipolla, M., Gazumyan, A., & Nussenzweig, M. C. (2020). Antibody Affinity Shapes the Choice between Memory and Germinal Center B Cell Fates. *Cell*, *183*(5), 1298-1311.e11. https://doi.org/10.1016/j.cell.2020.09.063

Vratskikh, O., Stiasny, K., Zlatkovic, J., Tsouchnikas, G., Jarmer, J., Karrer, U., Roggendorf, M., Roggendorf, H., Allwinn, R., & Heinz, F. X. (2013). Dissection of antibody specificities induced by yellow fever vaccination. *PLoS Pathogens*, *9*(6), e1003458. https://doi.org/10.1371/journal.ppat.1003458

Waickman, A. T., Gromowski, G. D., Rutvisuttinunt, W., Li, T., Siegfried, H., Victor, K., Kuklis, C., Gomootsukavadee, M., McCracken, M. K., Gabriel, B., Mathew, A., Grinyo i Escuer, A., Fouch, M. E., Liang, J., Fernandez, S., Davidson, E., Doranz, B. J., Srikiatkhachorn, A., Endy, T., … Friberg, H. (2020). Transcriptional and clonal characterization of B cell plasmablast diversity following primary and secondary natural DENV infection. *EBioMedicine*, *54*, 102733. https://doi.org/10.1016/j.ebiom.2020.102733

Walker, P. J., Siddell, S. G., Lefkowitz, E. J., Mushegian, A. R., Adriaenssens, E. M., Alfenas-Zerbini, P., Dempsey, D. M., Dutilh, B. E., García, M. L., Curtis Hendrickson, R., Junglen, S., Krupovic, M., Kuhn, J. H., Lambert, A. J., Łobocka, M., Oksanen, H. M., Orton, R. J., Robertson, D. L., Rubino, L., … Zerbini, F. M. (2022). Recent changes to virus taxonomy ratified by the International Committee on Taxonomy of Viruses (2022). *Archives of Virology*, *167*(11), 2429–2440. https://doi.org/10.1007/s00705-022-05516-5

Watson, A. M., Lam, L. K. M., Klimstra, W. B., & Ryman, K. D. (2016). The 17D-204 Vaccine Strain-Induced Protection against Virulent Yellow Fever Virus Is Mediated by Humoral Immunity and CD4+ but not CD8+ T Cells. *PLOS Pathogens*, *12*(7), e1005786. https://doi.org/10.1371/journal.ppat.1005786

Wec, A. Z., Haslwanter, D., Abdiche, Y. N., Shehata, L., Pedreno-Lopez, N., Moyer, C. L., Bornholdt, Z. A., Lilov, A., Nett, J. H., Jangra, R. K., Brown, M., Watkins, D. I., Ahlm, C., Forsell, M. N., Rey, F. A., Barba-Spaeth, G., Chandran, K., & Walker, L. M. (2020). Longitudinal dynamics of the human B cell response to the yellow fever 17D vaccine. *Proceedings of the National Academy of Sciences of the United States of America*. https://doi.org/10.1073/pnas.1921388117

Weiskopf, D., Angelo, M. A., de Azeredo, E. L., Sidney, J., Greenbaum, J. A., Fernando, A. N., Broadwater, A., Kolla, R. V., De Silva, A. D., de Silva, A. M., Mattia, K. A., Doranz, B. J., Grey, H. M., Shresta, S., Peters, B., & Sette, A. (2013). Comprehensive analysis of

dengue virus-specific responses supports an HLA-linked protective role for CD8 + T cells. *Proceedings of the National Academy of Sciences*, *110*(22). https://doi.org/10.1073/pnas.1305227110

Wilkinson, T. M., Li, C. K. F., Chui, C. S. C., Huang, A. K. Y., Perkins, M., Liebner, J. C., Lambkin-Williams, R., Gilbert, A., Oxford, J., Nicholas, B., Staples, K. J., Dong, T., Douek, D. C., McMichael, A. J., & Xu, X.-N. (2012). Preexisting influenza-specific CD4+ T cells correlate with disease protection against influenza challenge in humans. *Nature Medicine*, *18*(2), 274–280. https://doi.org/10.1038/nm.2612

Wong, R., Belk, J. A., Govero, J., Uhrlaub, J. L., Reinartz, D., Zhao, H., Errico, J. M., D'Souza, L., Ripperger, T. J., Nikolich-Zugich, J., Shlomchik, M. J., Satpathy, A. T., Fremont, D. H., Diamond, M. S., & Bhattacharya, D. (2020). Affinity-Restricted Memory B Cells Dominate Recall Responses to Heterologous Flaviviruses. *Immunity*, *53*(5), 1078-1094.e7. https://doi.org/10.1016/j.immuni.2020.09.001

Xu, M., Hadinoto, V., Appanna, R., Joensson, K., Toh, Y. X., Balakrishnan, T., Ong, S. H., Warter, L., Leo, Y. S., Wang, C.-I., & Fink, K. (2012). Plasmablasts Generated during Repeated Dengue Infection Are Virus Glycoprotein–Specific and Bind to Multiple Virus Serotypes. *The Journal of Immunology*, *189*(12), 5877–5885. https://doi.org/10.4049/jimmunol.1201688

Zanini, F., Robinson, M. L., Croote, D., Sahoo, M. K., Sanz, A. M., Ortiz-Lasso, E., Albornoz, L. L., Rosso, F., Montoya, J. G., Goo, L., Pinsky, B. A., Quake, S. R., & Einav, S. (2018). Virus-inclusive single-cell RNA sequencing reveals the molecular signature of progression to severe dengue. *Proceedings of the National Academy of Sciences*, *115*(52). https://doi.org/10.1073/pnas.1813819115

Zhang, Y., Zhang, W., Ogata, S., Clements, D., Strauss, J. H., Baker, T. S., Kuhn, R. J., & Rossmann, M. G. (2004). Conformational Changes of the Flavivirus E Glycoprotein. *Structure*, *12*(9), 1607–1618. https://doi.org/10.1016/j.str.2004.06.019

Zhao, H., Xu, L., Bombardi, R., Nargi, R., Deng, Z., Errico, J. M., Nelson, C. A., Dowd, K. A., Pierson, T. C., Crowe, J. E., Diamond, M. S., & Fremont, D. H. (2020). Mechanism of differential Zika and dengue virus neutralization by a public antibody lineage targeting the DIII lateral ridge. *Journal of Experimental Medicine*, *217*(2). https://doi.org/10.1084/jem.20191792

Apendix A: Flow cytometry antibody table

			Marker	Titer	Clone
	T cells			1:	
UV 355 nm	BUV395		CD45RA	100	HI100
	Zombie UV		Viability	500	
	BUV496		CD16	100	3G8
	BUV563		CD127	100	HIL76M21
	BUV661		CCR6	100	11A9
	BUV737		PD1	100	EH12.1
	BUV805		ICOS	100	DX29
Violet 405 nm	Brilliant Violet™ 421		Tetramer	100	
	Pacific Blue™		CD57	400	HNK-1
	Brilliant Violet™ 480		CD56	200	NCAM16.2
	Brilliant Violet™ 510		CD4	200	SK3
	Brilliant Violet™ 570				
	Brilliant Violet™ 605		CXCR3	200	G025H7
	Brilliant Violet™ 650		Ki67	100	B56
	Brilliant Violet™ 711		KLRG1	100	2F1
	Brilliant Violet™ 750		CXCR5	100	J252D4
	Brilliant Violet™ 785		CCR7	80	G043H7
Blue 488 nm					
	FITC		Tbet	200	4B10
	Spark Blue™ 550		CD3	200	SK7
	BB700		CD25	100	BC96
Yellow/green 561nm	PE		TCF1	200	7F11A10
	PE/Dazzle 594		FoxP3	200	206D
	PE/Cyanine5.5		EOMES	400	WD1928
	PE/Cyanine7		CCR4	400	L291H4
Red 633 nm	APC		Tetramer		
	PE Fire 810		HLADR*	100	L243
	Alexa Fluor® 700		CD8	400	HIT8a
	APC/Fire™ 750		CD95	400	DX2
	APC Fire 810		CD38	100	HB-7

Table 2. T-cell panel for spectral flow cytometry

*Unless tetramer was used

		Marker	Titer	Clone
	B cell		1:	
UV 355 nm	BUV395	CD24	100	ML5
	Zombie UV	Viability	250	
	BUV496	CD21	80	1048
	BUV563	CD10	80	HI10a
	BUV661	CD71	80	M-A712
	BUV737	IgG	640	G18-145
	BUV805	IgM	100	UCH-B1
Violet 405 nm	Brilliant Violet™ 421	IL21R	50	2G1-K12
	Pacific Blue™	CXCR3	200	G025H7
	Brilliant Violet™ 570	CD19	100	HIB19
	Brilliant Violet™ 605	TACI	50	1A1-K21-M22
	Brilliant Violet™ 650	Ki67	100	B56
	Brilliant Violet™ 711	CD20	200	2H7
	Brilliant Violet™ 750	CXCR5	100	J252D4
Blue 488 nm	FITC	Tbet	200	4B10
	Spark Blue™ 550	CD3	200	SK7
	PerCP/Cyanine5.5	IgD	100	IA6-2
Yellow/green 561nm	PE	YFV/Se*		
	PE/Dazzle 594	BCMA	50	19F2
	PE/Cyanine5	CXCR4	400	12G5
	PE/Cyanine7	CD138	100	MI15
Red 633 nm	APC	YFV/Se*		
	Alexa Fluor® 700	CD27	80	O323
	APC Cy7	BAFF-R	400	11C1
	APC Fire 810	CD38	100	HIT2

Table 3. B cell panel for spectral flow cytometry

		Marker	Titer	Clone
	ICS			
Violet 405 nm	V450	IFNg	80	B27
	Brilliant Violet™ 510	CD45RA	160	HI100
	Brilliant Violet™ 605	CD27	80	O323
	Brilliant Violet™ 650	CD8	320	SK1
	Brilliant Violet™ 711	IL2	80	MQ1-17H12
	Brilliant Violet™ 785	CCR7	80	G043H7
Blue 488 nm	FITC	CD40L	50	24-31
	PerCP	CD3	80	SK7
Yellow/green 561nm	PE	IL21	40	3A3-N2
	PE/Dazzle 594	CD107a	200	H4A3
	PE/Cyanine7	CXCR5	80	J252D4
Red 633 nm	APC	TNFa	80	MAb11
	Alexa Fluor® 700	CD4	320	OKT4
	APC Cy7	Viability	3000	

Table 4. ICS panel for ex vivo restimulation assay
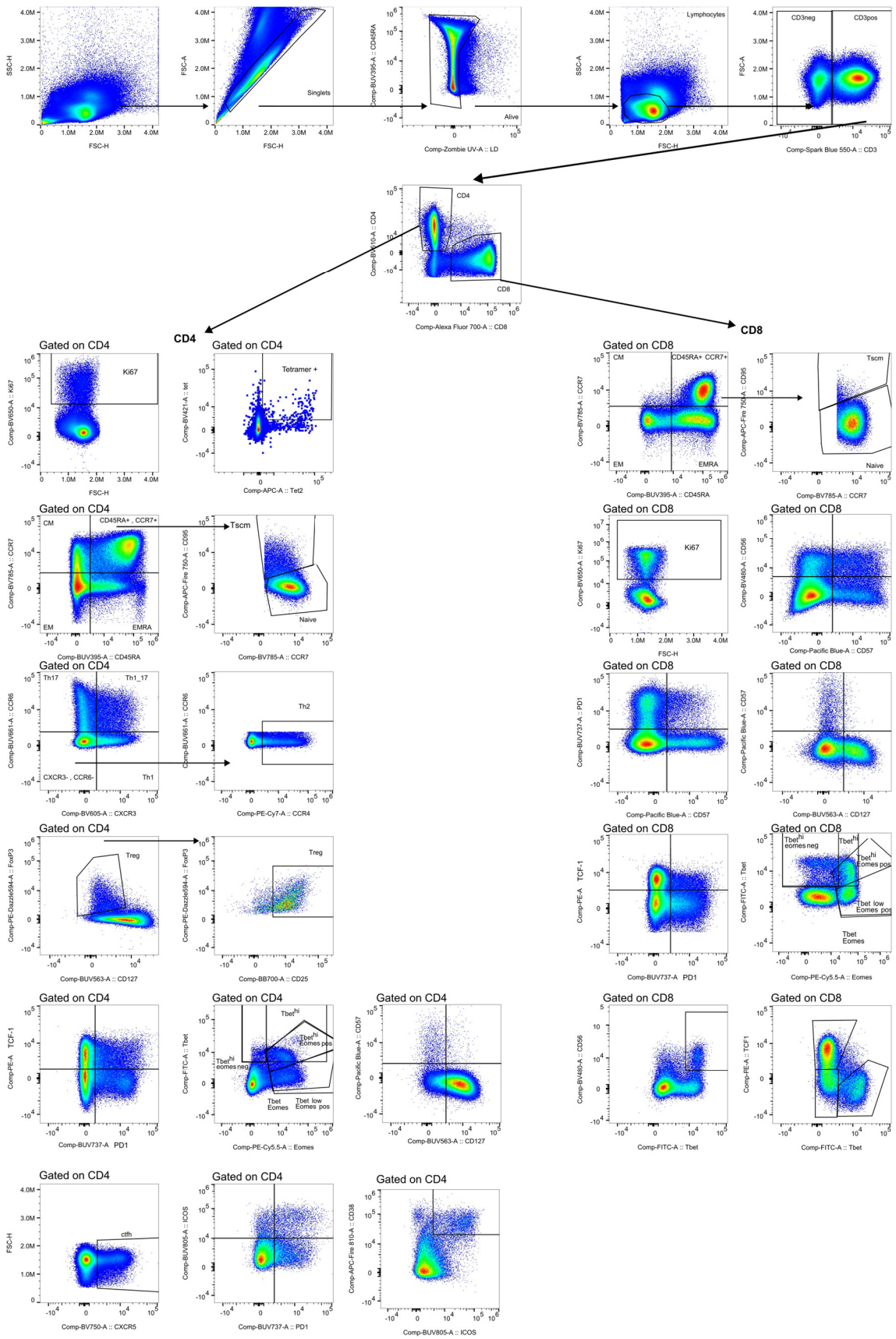
Appendix B: Gating strategy T cells

Figure 21. Gating strategy for T cell populations
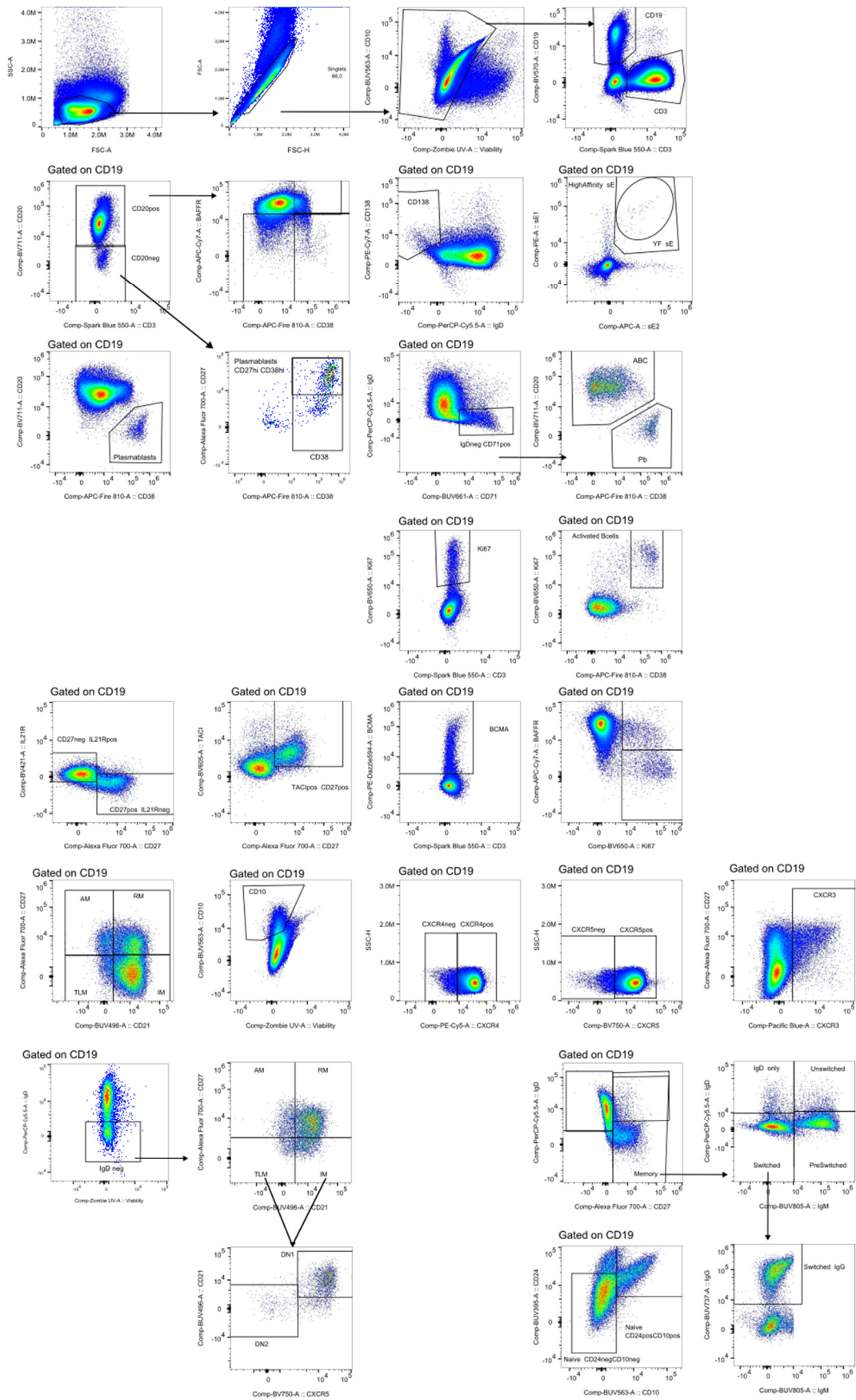
Appendix C: Gating strategy B

Figure 22. Gating strategy for B cell populations
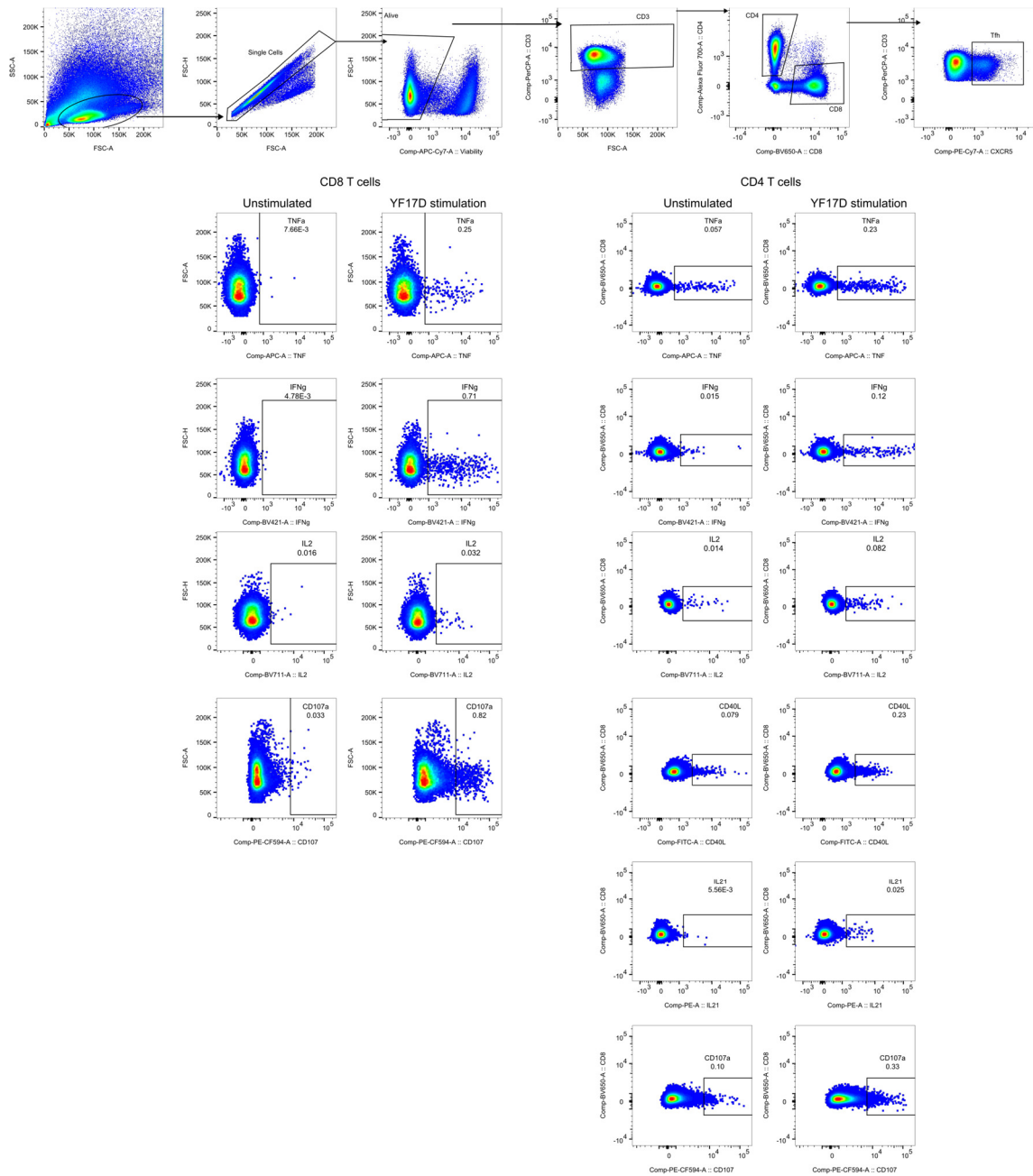
Apendix D: Gating strategy: ICS

Figure 23. Gating strategy for ex vivo restimulations and ICS

Apendix E: Immune populations identified in spectral flow cytometry

Cell Type	Gated population
CD4	CD4
CD4	CD4 Ki67
CD4	CD4 CCR4
CD4	CD4 CCR4 Ki67
CD4	CD4 CCR6
CD4	CD4 CCR6 Ki67
CD4	CD4 CD38
CD4	CD4 CD38 Ki67
CD4	CD4 CD45RA$^+$CCR7$^+$
CD4	CD4 CD45RA$^+$CCR7$^+$CD95$^-$ (Naïve)
CD4	CD4 Naive Ki67
CD4	CD4 CD45RA$^+$CCR7$^+$CD95$^+$ (Tscm)
CD4	CD4 Tscm Ki67
CD4	CD4 CD57$^+$CD127$^-$ senescent
CD4	CD4 CD57$^+$CD127$^-$ senescent Ki67
CD4	CD4 CD127$^+$CD57$^-$ Long-term
CD4	CD4 CD127$^+$CD57$^-$ Long-term Ki67
CD4	CD4 CD45RA$^-$CCR7$^+$ (CM)
CD4	CD4 CM Ki67
CD4	CD4 CXCR5$^+$ (ctfh)
CD4	CD4 ctfh CCR4
CD4	CD4 ctfh CCR4 Ki67
CD4	CD4 ctfh CCR6
CD4	CD4 ctfh CCR6 Ki67
CD4	CD4 ctfh CD38
CD4	CD4 ctfh CD38 Ki67
CD4	CD4 ctfh CXCR3
CD4	CD4 ctfh CXCR3 Ki67
CD4	CD4 ctfh CXCR3$^-$CCR6$^-$
CD4	CD4 ctfh ICOS CD38
CD4	CD4 ctfh ICOS CD38 Ki67
CD4	CD4 ctfh Ki67
CD4	CD4 ctfh PD1 CD38
CD4	CD4 ctfh PD1 CD38 Ki67
CD4	CD4 ctfh PD1$^+$ICOS$^-$
CD4	CD4 ctfh PD1$^+$ICOS$^-$ Ki67
CD4	CD4 ctfh PD1$^+$ICOS$^+$
CD4	CD4 ctfh PD1$^+$ICOS$^+$ Ki67
CD4	CD4 ctfh PD1$^-$ICOS$^+$
CD4	CD4 ctfh PD1$^-$ICOS$^+$ Ki67
CD4	CD4 ctfh PD1$^-$ICOS$^-$
CD4	CD4 ctfh Th1
CD4	CD4 ctfh Th1 CD38
CD4	CD4 ctfh Th1CD38 Ki67
CD4	CD4 ctfh Th1 Ki67
CD4	CD4 ctfh Th17
CD4	CD4 ctfh Th17 CD38
CD4	CD4 ctfh Th17 CD38 Ki67
CD4	CD4 ctfh Th17 Ki67
CD4	CD4 ctfh Th1 17
CD4	CD4 ctfh Th1 17 CD38
CD4	CD4 ctfh Th1 17 CD38 Ki67
CD4	CD4 ctfh Th1 17 Ki67
CD4	CD4 CXCR3
CD4	CD4 CXCR3 Ki67
CD4	CD4 CXCR3$^-$CCR6$^-$
CD4	CD4 CXCR3$^-$CCR6$^-$CCR4$^+$ (Th2)
CD4	CD4 Th2 Ki67
CD4	CD4 CD45RA$^-$CCR7$^-$ (EM)
CD4	CD4 EM Ki67
CD4	CD4 CD45RA$^+$CCR7$^-$ (EMRA)
CD4	CD4 EMRA Ki67
CD4	CD4 CD127$^+$CD57$^+$
CD4	CD4 CD127$^+$CD57$^+$ Ki67
CD4	CD4 CD127$^-$CD57$^-$
CD4	CD4 PD1$^-$TCF1$^+$
CD4	CD4 PD1$^-$TCF1$^+$ Ki67
CD4	CD4 PD1$^+$TCF1$^+$
CD4	CD4 PD1$^+$TCF1$^+$ Ki67
CD4	CD4 PD1$^+$TCF1$^-$
CD4	CD4 PD1$^-$TCF1$^-$
CD4	CD4 Tbet Eomes
CD4	CD4 Tbet Eomes Ki67
CD4	CD4 Tbet High
CD4	CD4 Tbet High Ki67
CD4	CD4 Tbet High Eomes$^-$
CD4	CD4 Tbet High Eomes$^+$
CD4	CD4 Tbet High Eomes$^+$ Ki67
CD4	CD4 Tbet Low Eomes$^+$
CD4	CD4 Tbet Low Eomes$^+$ Ki67
CD4	CD4 CXCR3$^+$CCR6$^-$ (Th1)
CD4	CD4 Th1 Ki67
CD4	CD4 CXCR3$^-$CCR6$^+$ (Th17)
CD4	CD4 Th17 Ki67
CD4	CD4 CXCR3$^+$CCR6$^+$ (Th1 17)
CD4	CD4 Th1 17 Ki67
CD4	CD4 Fosp3$^+$CD127$^-$CD25$^+$ (Treg)
CD4	CD4 Treg CCR4
CD4	CD4 Treg CCR4 Ki67
CD4	CD4 Treg CXCR3$^-$CCR6$^-$
CD4	CD4 Treg Ki67
CD4	CD4 Treg Th1
CD4	CD4 Treg Th1 Ki67
CD4	CD4 Treg Th17
CD4	CD4 Treg Th17 Ki67
CD4	CD4 Treg Th1 17
CD4	CD4 Treg Th1 17 Ki67
CD8	CD8
CD8	CD8 CD38
CD8	CD8 CD38 Ki67
CD8	CD8 CD45RA$^+$CCR7$^+$
CD8	CD8 CD45RA$^+$CCR7$^+$ Ki67
CD8	CD8 CD45RA$^+$CCR7$^+$ CD95$^-$ (Naive)
CD8	CD8 Naive Ki67
CD8	CD8 CD45RA$^+$CCR7$^+$ CD95$^+$ (Tscm)

CD8	CD8 Tscm Ki67
CD8	CD8 CD57$^+$CD56$^+$
CD8	CD8 CD57$^+$CD56$^+$ Ki67
CD8	CD8 CD57$^+$CD56$^-$
CD8	CD8 Ki67
CD8	CD8 CD57$^+$PD1$^+$
CD8	CD8 CD57$^+$PD1$^+$ Ki67
CD8	CD8 CD57$^+$PD1$^-$
CD8	CD8 CD57$^-$CD56$^+$
CD8	CD8 CD57$^-$CD56$^+$ Ki67
CD8	CD8 CD57$^-$PD1$^+$
CD8	CD8 CD57$^-$PD1$^+$ Ki67
CD8	CD8 CD57$^-$CD56$^-$
CD8	CD8 CD57$^-$PD1$^-$
CD8	CD8 CD57$^+$CD127$^-$ Senescent
CD8	CD8 CD57$^+$CD127$^-$ Senescent Ki67
CD8	CD8 CD127$^+$CD57$^-$ Longterm
CD8	CD8 CD127$^+$CD57$^-$ Longterm Ki67
CD8	CD8 CM
CD8	CD8 CM Ki67
CD8	CD8 EM
CD8	CD8 EM Ki67
CD8	CD8 EMRA
CD8	CD8 EMRA Ki67
CD8	CD8 PD1$^+$TCF1$^-$ Exhausted
CD8	CD8 PD1$^+$TCF1$^+$
CD8	CD8 PD1$^+$TCF1$^+$ Ki67
CD8	CD8 PD1$^+$CD56$^+$
CD8	CD8 PD1$^+$CD56$^+$ Ki67
CD8	CD8 PD1$^+$CD56$^-$
CD8	CD8 PD1$^-$TCF1$^+$
CD8	CD8 PD1$^-$TCF1$^+$ Ki67
CD8	CD8 PD1$^-$TCF1$^-$
CD8	CD8 PD1$^-$CD56$^+$
CD8	CD8 PD1$^-$CD56$^+$ Ki67
CD8	CD8 PD1$^-$CD56$^-$
CD8	CD8 CD127$^+$CD57$^+$
CD8	CD8 CD127$^+$CD57$^+$ Ki67
CD8	CD8 CD127$^-$CD57$^-$
CD8	CD8 Tbet Eomes
CD8	CD8 Tbet Eomes Ki67
CD8	CD8 Tbet High CD56
CD8	CD8 Tbet High CD56 Ki67
CD8	CD8 Tbet High
CD8	CD8 Tbet High Ki67
CD8	CD8 Tbet High Eomes$^-$
CD8	CD8 Tbet High Eomes$^+$
CD8	CD8 Tbet High Eomes$^+$ Ki67
CD8	CD8 Tbet Low Eomes$^+$
CD8	CD8 Tbet Low Eomes$^+$ Ki67
CD8	CD8 Tbet$^+$TCF1$^-$
CD8	CD8 TCF1$^-$CD57$^+$
CD8	CD8 TCF1$^-$CD57$^+$ Ki67
CD8	CD8 TCF1$^-$Tbet$^-$
CD8	CD8 TCF1$^+$
CD8	CD8 TCF1$^+$ Ki67
CD8	CD8 TCF1$^+$Tbet$^-$

CD4	CD4 ctfh HLADRCD38
CD4	CD4 ctfh Th1 HLADRCD38
CD4	CD4 HLADR CD38
CD8	CD8 HLADR CD38
B	CD38$^+$Ki67$^+$ Activated B cells
B	CD27$^+$CD21$^-$ (AM)
B	AM CD38
B	AM CD38 Ki67
B	AM Ki67
B	BAFFR$^-$ Ki67$^+$
B	BAFFR$^+$ Ki67$^+$
B	BCMA
B	CD10$^+$
B	CD20$^-$
B	CD20$^-$CD38$^+$
B	CD20$^-$Ki67$^+$
B	CD20$^+$
B	CD20$^+$BAFFR$^-$
B	CD20$^+$BAFFR$^+$
B	CD20$^+$CD38hi
B	CD20$^+$CD38hiCD27hi
B	CD20$^+$CD38$^+$BAFFR$^-$
B	CD20$^+$CD38$^+$BAFFR$^+$
B	CD20$^+$Ki67$^+$
B	CD20$^+$ CD38hi
B	CD27$^-$ IL21R$^+$
B	CD27$^+$ IL21R$^-$
B	CXCR3
B	CXCR3 Ki67$^+$
B	CXCR4$^-$
B	CXCR4$^-$ Ki67$^+$
B	CXCR4$^+$
B	CXCR4$^+$ Ki67$^+$
B	CXCR5$^-$
B	CXCR5$^-$ Ki67$^+$
B	CXCR5$^+$
B	CXCR5$^+$ Ki67$^+$
B	IgD$^-$
B	IgD$^-$
B	IgD$^-$ Ki67$^+$
B	IgD$^-$ IM
B	IgD$^-$ IM Ki67$^+$
B	IgD$^-$ RM
B	IgD$^-$ RM Ki67$^+$
B	IgD$^-$ TLM
B	IgD$^-$ TLM Ki67$^+$
B	IgD$^-$CD71$^+$
B	IgD$^-$CD71$^+$ CD38hi Plasmablasts
B	IgD$^-$CD71$^+$ CD71$^+$CD20$^+$ ABC
B	IgD$^+$CD27$^-$ Naive
B	IgD$^+$CD27$^-$ Naive CD24$^-$CD10$^-$
B	IgD$^+$CD27$^-$ Naive CD24$^+$CD10$^+$
B	IgD$^+$CD27$^-$ Naive CD38$^+$
B	IgD$^+$CD27$^-$ Naive Ki67$^+$
B	IgD$^+$CD27$^+$
B	IgD$^+$CD27$^+$ CD71$^+$ CD38$^+$
B	IgD$^+$CD27$^+$ IgD$^+$CD27$^+$ CD38$^+$

B	CD27$^-$CD21$^+$ (IM)
B	IM CD38 Ki67
B	IM Ki67
B	CD27$^+$ (Memory)
B	Memory CD38hi
B	Memory CD38 Ki67
B	Memory IgD only
B	Memory Ki67
B	Memory PreSwitched
B	Memory Switched
B	Memory Switched IgG
B	Memory CD38hi
B	Memory Ki67
B	Memory Switched IgG$^+$ Ki67
B	Memory Switched Ki67
B	Memory Unswitched
B	CD38$^+$CD20$^-$ (Plasmablast)
B	Plasmablast Ki67$^+$
B	CD27$^+$CD21$^+$ (RM)
B	RM CD38
B	RM CD38 Ki67
B	RM Ki67
B	TACI$^+$ CD27$^+$
B	CD27$^-$CD21$^-$ (TLM)
B	TLM CD38
B	TLM CD38 Ki67
B	TLM Ki67
B	CD138
B	CD138 CXCR4$^-$
B	CD138 CXCR4$^+$

B	CD138 CXCR5$^-$
B	CD138 CXCR5$^+$
B	CD138 IgG
B	CD138 IgM
B	CD138 Ki67
B	IgD$^-$ CD27$^-$ (DN)
B	DN CXCR4$^-$
B	DN CXCR4$^+$
B	DN CXCR5$^-$ (DN2)
B	DN CXCR5$^+$ (DN1)
B	DN DN1 CXCR4$^-$
B	DN DN1 CXCR4$^+$
B	DN DN1 IgG
B	DN DN1 IgM
B	DN DN1 Ki67
B	DN DN2 CXCR4$^-$
B	DN DN2 CXCR4$^+$
B	DN DN2 IgG
B	DN DN2 IgM
B	DN DN2 Ki67
B	DN IgG
B	DN IgM
B	Plasmablast CD138
B	Plasmablast CXCR4$^-$
B	Plasmablast CXCR4$^+$
B	Plasmablast CXCR5$^-$
B	Plasmablast CXCR5$^+$
B	Plasmablast IgG
B	Plasmablast IgM
B	Plasmablast Ki67$^+$

Acknowledgements

Affidavit

Affidavit

Santos del Peral, Antonio

Surname, first name

Zip code, town, country

I hereby declare, that the submitted thesis entitled:

"Effect of Prior Flavivirus Immunity on the Adaptive Response to the Yellow Fever 17D Vaccine"

is my own work. I have only used the sources indicated and have not made unauthorised use of services of a third party. Where the work of others has been quoted or reproduced, the source is always given.

I further declare that the dissertation presented here has not been submitted in the same or similar form to any other institution for the purpose of obtaining an academic degree.

Madrid, 25.04.2024   Antonio Santos del Peral

 place, date   Signature doctoral candidate

Confirmation of congruency

Confirmation of congruency between printed and electronic version of the doctoral thesis

Santos del Peral, Antonio

Surname, first name

Zip code, town, country

I hereby declare, that the submitted thesis entitled:

"Effect of Prior Flavivirus Immunity on the Adaptive Response to the Yellow Fever 17D

Vaccine" is congruent with the printed version both in content and format.

Madrid, 25.04.2024

place, date

Antonio Santos del Peral

Signature doctoral candidate